

THE ROLE OF RECEPTOR INTERACTING PROTEIN KINASES IN  
DIABETOGENIC BETA-CELL LOSS AND HYPERGLYCEMIA

Noyonika Mukherjee

Submitted to the faculty of the University Graduate School  
in partial fulfillment of the requirements  
for the degree  
Doctor of Philosophy  
in the Department of Biochemistry and Molecular Biology  
Indiana University

November 2024

Accepted by the Graduate Faculty of Indiana University, in partial fulfillment of the requirements for the degree of Doctor of Philosophy.

Doctoral Committee

Andrew T. Templin, PhD, Chair

X. Charlie Dong, PhD

September 6, 2024

Jeffrey S. Elmendorf, PhD

Carmella Evans-Molina, MD, PhD

Amelia K. Linnemann, PhD

© 2024

Noyonika Mukherjee

## DEDICATION

I dedicate this work to all those I have lost during my doctoral studies. Their love, support and trust inspired me to persevere and complete this journey.

*Late Dipali Roy Chowdhury*

*Late Runu Dugar*

*Late Sandhyarani Pal*

*Late Prababhati Das*

*Late Dr. Sukla Dutta*

*Late Jyoti and Santanu Bose*

*Late Narayan Chandra and Lilly Nag*

*Late Dr. Prabal Dasgupta*

*Late Dr. Amita Roy*

তুমি রবে নীরবে হৃদয়ে মম

নিবিড় নিভৃত পূর্ণিমানিশীথিনী-সম

- রবীন্দ্রনাথ ঠাকুর

(Thou shalt dwell in silence in my heart like the full moon in the summer night.)

- Rabindranath Tagore

## ACKNOWLEDGEMENT

This work is the result of immense dedication, effort, and intellect from a team of committed researchers. First and foremost, I would like to thank my mentor Dr. Andrew T. Templin. Andrew's mentorship has demonstrated how a doctoral journey can be rewarding, balancing hard work, mental and physical well-being, and committed family time. None of this work would have been possible without Andrew's support and guidance. Additionally, I would like to express my gratitude to my thesis committee members, Dr. X.C. Dong, Dr. Jeffrey S. Elmendorf, Dr. Carmella Evans-Molina and Dr. Amelia K. Linnemann. Their support, expertise, and guidance have been invaluable throughout my graduate school experience. I am also thankful to the investigators at the Center of Diabetes and Metabolic Diseases at IUSM, including Dr. Teresa Mastracci, Dr. Emily K. Sims and Dr. Jason Spaeth, for their valuable scientific insights. My fellow graduate students have been a source of encouragement and unwavering support. Special thanks to Kara Orr and Lata Udari at the Islet Physiology Core, Indiana University School of Medicine, for their outstanding expertise in islet isolations and animal physiology. I would also like to thank members of the Cellular Response Technologies Core and the Translational Core for their guidance and help with experimental design. Dr. Frederick Pavalko, a dear friend and guide, deserves special thanks for his support and trust in me.

All past and present members of the Templin lab have always offered a helping hand when needed. Our teamwork extended beyond experiments, and I have consistently found support from them. Special thanks go to Dr. Christopher J. Contreras and Dr. Renato C.S. Branco, postdoctoral fellows in the Templin lab, for their guidance and

helpful suggestions. Li Lin and Egan G. Mather's expertise in animal handling was critical for many of my studies. Jayden Pierce, Katy Atayde, and Rachel Schweiger were wonderful trainees, and I was fortunate to have the opportunity to train them. Kaitlyn Colglazier deserves a special thank you for her technical expertise in immunoblotting and immunofluorescence in many of my studies.

I would not have achieved what I did during my doctoral studies without the outstanding input and suggestions from Dr. Michael Kalwat and Dr. Erica P. Cai. Casual discussions about science and beyond at the Indiana Biosciences Research Institute (IBRI) often sparked some of the craziest scientific ideas. I am grateful to all my close friends and co-workers at IBRI. Special thanks to Dr. Isabella Iessi, Dr. Debjyoti Kundu, Dr. Nansa Amarikasan, Dr. Chialing Wu, Angela Hanskel, Karina Rodriguez, and Dr. Farrokh Shariffi for their crucial contributions throughout my doctoral studies. Dr. Jahnavi Aluri deserves special mention for helping me with her technical expertise in flow cytometry. My thanks extend to every member of IBRI; it has been an absolute pleasure working with each of you.

This work contains text, and figures published in multiple peer-reviewed journals, including *Metabolites*, *Molecular Metabolism*, and *Journal of Endocrinology*. I extend my gratitude to these journals for allowing me to use materials for my thesis from the published work.

Most importantly, I would like to thank my parents, Mr. Arjun Mukherjee and Mrs. Mou Mukherjee, and my in-laws, Mr. Gopal Pal and Mrs. Sabita Pal, for their constant support and encouragement. They have always shown me the light when I felt lost in the dark. I also thank all members of my family and friends back in India, who have been an

integral part of my journey. Lastly, my heartfelt thanks go to my husband, Soumiya Pal, for his loving encouragement, motivation, and support throughout my doctoral studies. None of this would have been possible without you.

Noyonika Mukherjee

THE ROLE OF RECEPTOR INTERACTING PROTEIN KINASES IN  
DIABETOGENIC BETA-CELL LOSS AND HYPERGLYCEMIA

Diabetes is characterized by pancreatic  $\beta$ -cell loss, insulin insufficiency, and hyperglycemia. Although major efforts have been made to manage diabetes using pharmacological agents that lower blood glucose levels, less effort has been focused on therapies to prevent the two major forms of diabetes, type 1 (T1D) and type 2 diabetes (T2D). Hence, there is a critical need to understand the mechanisms that underlie  $\beta$ -cell demise in these diseases, and to develop therapies targeting such mechanisms. Recent studies in non-islet cell types identified receptor interacting protein kinase 1 and 3 (RIPK1 and RIPK3) as mediators of inflammation and programmed cell death. RIPKs are being considered as potential therapeutic target in human diseases including renal, hepatic and neurodegenerative diseases. However, the role of RIPKs in  $\beta$ -cell loss in diabetes remains unknown. My thesis work evaluated the roles of RIPK1 and RIPK3 in mediating  $\beta$ -cell cytotoxicity and islet inflammation in diabetes pathogenesis. Through the studies, I examined the role of RIPK1 and RIPK3 in  $\beta$ -cell loss in response to known inducers of diabetogenic  $\beta$ -cell stress, including proinflammatory cytokines, endoplasmic reticulum (ER) stress and islet amyloid deposition. My work revealed roles of RIPK1 and RIPK3 in mediating both caspase-dependent and caspase-independent cell death, kinase activation and transcriptional responses *in vitro*. Furthermore, I found that RIPK1 and RIPK3 play important roles in regulating glucose homeostasis in mouse models *in vivo*.

The studies revealed a novel role of RIPKs in the pathogenesis of diabetes and suggests that RIPKs might be a potential target to treat or prevent the disease.

Andrew T. Templin, PhD, Chair

X. Charlie Dong, PhD

Jeffrey S. Elmendorf, PhD

Carmella Evans-Molina, MD, PhD

Amelia K. Linnemann, PhD

## TABLE OF CONTENTS

<b>List of Figures</b> .....	xi
<b>List of Abbreviations</b> .....	xii
<b>Chapter 1 – Introduction</b>	
Diabetes mellitus: a disease of $\beta$ -cell dysfunction and loss.....	1
The discovery of insulin.....	7
Overview of $\beta$ -cell biology .....	9
Classification of the different forms of diabetes.....	12
Contributors of $\beta$ -cell cytotoxicity in diabetes .....	18
Evidence for established and emerging forms of $\beta$ -cell demise .....	32
Summary.....	44
<b>Chapter 2 – Experimental Procedures</b>	
Materials and Methods .....	47
<b>Chapter 3 – RIPK1 and RIPK3 regulate TNF<math>\alpha</math>-induced <math>\beta</math>-cell death in concert with caspase activity</b>	
Introduction.....	58
Results.....	60
Discussion.....	76
<b>Chapter 4 – Investigating the role of RIPK1 in TNF<math>\alpha</math> and IFN<math>\gamma</math>-induced <math>\beta</math>-cell cytotoxicity</b>	
Introduction.....	87
Results.....	89
Discussion.....	96
<b>Chapter 5 – Investigating the role of caspase 3/7 activation and RIPK1 kinase activity in endoplasmic reticulum stress-induced <math>\beta</math>-cell death</b>	
Introduction.....	101
Results.....	103
Discussion.....	112
<b>Chapter 6 – RIPK3 promotes islet amyloid-induced <math>\beta</math>-cell loss and glucose intolerance in a humanized mouse model of T2D</b>	
Introduction.....	115
Results.....	117
Discussion.....	131
<b>Chapter 7 – Conclusion</b> .....	139
<b>References</b> .....	144
<b>Curriculum Vitae</b>	

## LIST OF FIGURES

Figure 1: Mechanism of glucose stimulated insulin secretion.....	13
Figure 2: Basic mechanism of necroptosis signaling.....	38
Figure 3: NIT-1 and INS-1 $\beta$ cells express components of TNF $\alpha$ pathway signaling.....	63
Figure 4: NIT-1 and INS-1 $\beta$ cells are susceptible to RIPK1- and cIAP-mediated TNF $\alpha$ -induced cell death.....	64
Figure 5: NIT-1 and INS-1 $\beta$ cells are susceptible to TNF $\alpha$ -induced cell death when caspases are inhibited.....	67
Figure 6: RIPK1 and cIAPs regulate TNF $\alpha$ -induced NIT-1 and INS-1 $\beta$ -cell death when caspases are inhibited.....	70
Figure 7: RIPK3 promotes TNF $\alpha$ -induced INS-1 cell death when caspases are inhibited.....	74
Figure 8: Mouse islets cells are susceptible to TNF $\alpha$ -induced cell death when cIAPs or caspases are inhibited.....	77
Figure 9: Ripk3 <sup>-/-</sup> mice are protected from STZ-induced hyperglycemia in vivo.....	79
Figure 10: RIPK1 is a T1D-relevant mediator of TNF $\alpha$ + IFN $\gamma$ signaling in $\beta$ cells.....	91
Figure 11: RIPK1 mediates TNF $\alpha$ - and IFN $\gamma$ -relevant kinase signaling in a mouse $\beta$ cells.....	92
Figure 12: RIPK1 mediates TNF $\alpha$ - and IFN $\gamma$ -relevant gene expression in a mouse $\beta$ cells.....	93
Figure 13: RIPK1 promotes TNF $\alpha$ +IFN $\gamma$ -induced cell death in mouse $\beta$ -cell lines.....	95
Figure 14: RIPK1 kinase inhibition alters NIT 1 $\beta$ -cell MHC I expression in vitro.....	97
Figure 15: NOD splenocyte-mediated killing of NIT-1 CTL and Ripk1 $\Delta$ cells in vivo.....	98
Figure 16: Inhibition of caspase activity does not prevent thapsigargin-induced $\beta$ -cell death.....	105
Figure 17: Inhibition of caspase activity does not prevent tunicamycin-induced $\beta$ -cell death.....	107
Figure 18: Ripk1 CRISPR-gene edited NIT-1 $\beta$ cells are resistant to ER stress-induced death independent of caspase activity.....	108
Figure 19: RIPK1 kinase inhibition fails to protect against thapsigargin-induced NIT-1 $\beta$ -cell death.....	110
Figure 20: RIPK1 kinase dead mice are not protected against ER stress-induced hyperglycemia in vivo.....	111
Figure 21: Real-time quantification of endogenous islet amyloid formation and islet cell death in vitro.....	119
Figure 22: Loss of RIPK3 protects from amyloid-induced islet cell death in vitro.....	122
Figure 23: RIPK3 promotes synthetic hIAPP-induced inflammatory gene expression in macrophages in vitro.....	125
Figure 24: Characterization of metabolic phenotypes in chow-fed WT, Ripk3 <sup>-/-</sup> , hIAPP and hIAPP;Ripk3 <sup>-/-</sup> mice.....	127
Figure 25: Loss of RIPK3 protects against amyloid-induced glucose intolerance in vivo.....	130
Figure 26: Loss of RIPK3 ameliorates amyloid-induced $\beta$ -cell loss in vivo.....	132

## LIST OF ABBREVIATIONS

AD	Alzheimer's disease
ADP	Adenosine diphosphate
AMP	Adenosine monophosphate
ASK	Apoptosis signal-regulating kinase
ATF6	Activating transcription factor 6
ATP	Adenosine triphosphate
BCA	Bicinchoninic acid assay
BCL-2	B-cell leukemia/lymphoma 2
BiP	Binding immunoglobulin protein
BMDM	Bone marrow derived macrophage
CCL2	C-C motif ligand 2
CD	Cluster of differentiation
CDK	Cyclin-dependent kinase
CFRD	Cystic fibrosis-related diabetes
CHOP	C/EBP homologous protein
cIAP1/2	Cellular inhibitor of apoptosis 1/2
CXCL1	C-X-C motif chemokine ligand 1
DAG	Diacylglycerol
DAMPs	Damage-associated molecular patterns
dAUC	Decremental area under the curve
DFO	Desferrioxamine
DNA	Deoxyribonucleic acid
EDTA	Ethylenediaminetetraacetic acid
EGTA	Ethyleneglycoltetraacetic acid
ELISA	Enzyme-linked immunosorbent assay
ENU	N-ethyl-N-nitrosourea
ER	Endoplasmic reticulum
FADD	Fas-associated death domain
FBS	Fetal bovine serum
FLICE	FADD [Fas-associated death domain]-like IL-1 $\beta$ -converting enzyme
GAD	Glutamic acid decarboxylase
GDM	Gestational diabetes mellitus
GIP	Gastric inhibitory polypeptide
GLP-1	Glucagon-like peptide-1
GLUT	Glucose transporter
GPX4	Glutathione peroxidase 4
GSDMD	Gasdermin D
GSH	Glutathione
HBSS	Hank's balanced salt solution
HFD	High-fat diet
HFN	Hepatocyte nuclear factor
hIAPP	Human islet amyloid polypeptide
HLA	Human leukocyte antigen
HMGB1	High mobility group box 1

HPAP .....	Human pancreas analysis program
HTRF .....	Homogeneous time resolved fluorescence
IA .....	Insulinoma antigen
IAA .....	Insulin autoantibody
IAPP .....	Islet amyloid polypeptide
iAUC .....	Incremental area under the curve
ICA .....	Islet cell cytoplasmic autoantigen
IFG .....	Impaired fasting glucose
IFN .....	Interferon
IFNGR .....	Interferon-gamma receptor
IKK .....	Inhibitor of nuclear factor- $\kappa$ B (I $\kappa$ B) kinase
IL .....	Interleukin
IPGTT .....	Intraperitoneal glucose tolerance test
IPITT .....	Intraperitoneal insulin tolerance test
iPSC .....	Induced pluripotent stem cells
IRP .....	Immediately releasable pool
ISG .....	Interferon-stimulated genes
IV .....	Intravenous
IVIS .....	In vivo imaging system
JNK .....	c-Jun N-terminal kinase
KRBH .....	Krebs-ringer bicarbonate HEPES buffer
LUBAC .....	Linear ubiquitin chain assembly complex
M-CSF1 .....	Macrophage colony-stimulating factor 1
MEF .....	Mouse embryonic fibroblast
MHC .....	Major histocompatibility complex
MIB-MS .....	Multiplexed kinase inhibitor-conjugated
.....	bead affinity chromatography and mass spectrometry
MLKL .....	Mixed lineage kinase domain like pseudokinase
MODY .....	Maturity-onset diabetes of the young
MTOR .....	Mammalian target of rapamycin
NF- $\kappa$ B .....	Nuclear factor kappa-light-chain-enhancer of activated B cells
NGT .....	Normal glucose tolerance
NK .....	Natural killer
NLRP3 .....	NOD-like receptor family, pyrin domain containing 3
NO .....	Nitric oxide
NOD .....	Non obese diabetes
NP-40 .....	Nonidet P-40
NSG .....	NOD scid gamma
PAMPs .....	Pathogen-associated molecular patterns
PBS .....	Phosphate-buffered saline
PC .....	Prohormone convertase
PCD .....	Programmed cell death
PCR .....	Polymerase chain reaction
PD-L1 .....	Programmed death-ligand 1
PERK .....	Protein kinase RNA-like ER kinase
PKA .....	Protein kinase A

PKC	Protein kinase C
PKR	Protein kinase R
PLC	Phospholipase C
PP	Polypeptide
PROTAC	Protein targeting chimera
PVDF	Polyvinylidene fluoride
qRT-PCR	Quantitative reverse transcriptase polymerase chain reaction
RER	Rough endoplasmic Reticulum
RHIM	Receptor-interacting protein homotypic interaction motif
rIAPP	Rodent islet amyloid polypeptide
RIPK	Receptor interacting protein kinase
RNA	Ribonucleic acid
RNA-seq	Ribonucleic acid sequencing
ROS	Reactive oxygen species
RP	Reserve pool
rRNA	Ribosomal ribonucleic acid
RRP	Readily releasable pool
SCID	Severe combined immunodeficiency
SDS	Sodium dodecyl sulphate
SDS-PAGE	Sodium dodecyl sulphate polyacrylamide gel electrophoresis
SEM	Smooth endoplasmic reticulum
SERCA2b	Sarco/endoplasmic reticulum Ca <sup>2+</sup> -ATPase 2b
SGLT2i	Sodium-glucose cotransporter 2 inhibitor
SMAC	Second mitochondria-derived activator of caspase
SNP	Single Nucleotide Polymorphism
SOCS-1	Suppressor of cytokine signaling 1
SOD	Superoxide dismutase
STAR	Spliced transcripts alignment to a reference
STAT-1	Signal transducer and activator of transcript-1
STZ	Streptozotocin
Thio S	Thioflavin S
TLR	Toll-like receptor
TNF $\alpha$	Tumor necrosis factor alpha
TNFR1	Tumor necrosis factor receptor 1
TRADD	Tumor necrosis factor receptor type 1-associated death domain
TRAILR	Targeting tumor necrosis factor-related apoptosis-inducing ligand receptor
TUDCA	Tauroursodeoxycholic acid
TUNEL	Terminal deoxynucleotidyl transferase dUTP nick-end labeling assay
TXNIP	Thioredoxin-interacting protein
TYK2	Tyrosine kinase 2
UPR	Unfolded protein response
WT	Wild type
XBP1	X-box binding protein 1

## **Chapter 1 – Introduction**

### **Diabetes mellitus: a disease of $\beta$ -cell dysfunction and loss**

Diabetes mellitus is a global epidemic affecting over 530 million people, about 10.5% of the global population <sup>1</sup>. This figure is projected to exceed 700 million by 2045 <sup>1</sup>. The worldwide direct health expenditure of the disease in 2019 was approximately \$760 billion <sup>2</sup>. Diabetes increases the risk of other conditions, including cardiovascular disease, chronic kidney disease, stroke, blindness, and amputation. In 2021, diabetes accounted for 6.7 million deaths. With around 44% of adults with diabetes undiagnosed, academics and healthcare providers must collaborate in diagnosing individuals and developing better treatment regimens to prevent and treat diabetes.

Diabetes is clinically defined by the presence of hyperglycemia, which is caused largely by insufficient insulin release from pancreatic  $\beta$  cells. Despite some uncertainties concerning the classification of diabetes, all forms have  $\beta$ -cell dysfunction, and most likely  $\beta$ -cell death, as a common pathophysiological component. Although  $\beta$ -cell dysfunction may be a prerequisite to this disease, the progressive nature of this dysfunction determines the progression of diabetes.

Some text and figures from the following portions are a part of published manuscripts that I have been an author on, used with permission from the journal. The publications have been mentioned in the references<sup>3,4</sup>.

#### **Observations of $\beta$ -cell loss in human diabetes**

Although the loss of insulin production was understood to be a factor in the development of diabetes by the early 1920s, it was at first not clearly established that a loss of functional  $\beta$  cells led to insufficient insulin release. Arriving at this conclusion

required a greater understanding of the divergent diabetic phenotypes observed clinically. It was known centuries ago that diabetes generally occurs in two distinct populations: 1) children and young adults with normal or low body weight, and 2) inactive, overweight adults. It was also recognized that diabetic phenotypes in these groups were similarly dichotomous, with hyperglycemia normally appearing as an acute and fatal affliction in children, but as a manageable chronic condition in adults. We now understand these divergent phenotypes to be separate diseases: type 1 diabetes (T1D, also known as insulin dependent diabetes and formerly as juvenile diabetes), which is associated with islet autoimmunity and near complete loss of insulin production, and type 2 diabetes (T2D, also known as insulin independent diabetes), which occurs in the setting of obesity, insulin resistance and relative insulin insufficiency.

To better understand the factors that contribute to loss of insulin production in diabetes, pathologists began studying pancreas sections from diabetic and non-diabetic individuals collected at autopsy well over one hundred years ago. Studies began to describe diabetes-associated  $\beta$ -cell loss in greater detail. Among these are the seminal studies conducted by Maclean and Ogilvie in the 1950's. Histological examination of pancreas sections, along with measurement of tissue mass, from young and old individuals (but primarily subjects over 40 years of age) revealed a significant reduction in  $\beta$ -cell mass in individuals with diabetes<sup>5</sup>. Among diabetic subjects,  $\beta$ -cell mass was observed to be lower in individuals diagnosed at less than 25 years of age and higher in individuals diagnosed later in life. When Maclean and Ogilvie analyzed pancreas tissue sections specifically from young subjects, they found diabetic individuals exhibit reduced islet number and mass, but no difference in islet size compared to non-diabetic

individuals <sup>6</sup>. They also observed that among young diabetic subjects, those with long-standing (chronic) disease has less islet mass than those with short-standing (acute) disease. When pancreas sections from young subjects with “juvenile diabetes” were analyzed by Doniach and Morgan in 1973, they were found to have an 85% reduction in the number of islets present <sup>7</sup>. Stefan and colleagues compared pancreas sections from 13 non-diabetic subjects and 2 insulin dependent diabetic subjects (T1D) and observed that the primary difference between these groups was the reduced number of insulin producing  $\beta$  cells <sup>8</sup>. When Klöppel et al. compared pancreas samples from recently diagnosed T1D individuals with age-matched controls in 1984, a 70-85% reduction  $\beta$ -cell abundance was again revealed <sup>9</sup>. These observations of reduced  $\beta$ -cell and islet abundance were among the first to demonstrate  $\beta$ -cell loss in what we now refer to as T1D.

In addition to observations of  $\beta$ -cell loss in T1D, evidence for  $\beta$ -cell loss in T2D has also existed for decades. In 1901, Eugene Opie observed the relationship between diabetes mellitus, islet cell loss and the presence of islet “hyaline deposits”, the last of which are now recognized as islet amyloid deposits (11,28). Notably, Maclean and Ogilvie excluded from their 1955 analyses pancreas samples that exhibited hyalinization of islets, which were observed in tissues specimens of individuals 40 years of age and older <sup>5</sup>. In contrast to their observations of extensive  $\beta$ -cell loss in T1D, Maclean and Ogilvie observed a less severe reduction in  $\beta$ -cell mass in individuals with T2D <sup>5</sup>. A more recent study estimates that a ~35% reduction in  $\beta$ -cell mass is present in T2D <sup>12</sup>.

Histological observation found increased islet size in a hyperglycemic individual <sup>13</sup>. Separately, Ogilvie found that islet size was increased in 19 obese individuals versus

controls, although none of these subjects had diabetes <sup>14</sup>. These observations likely reflect the presence of insulin resistance in obesity, leading to a compensatory increase in islet size. In 1985, Klöppel et al. noted that while T1D results from selective loss of  $\beta$  cells, these insulin producing cells are always present in T2D <sup>15</sup>, and Guiot et al. also questioned whether the reduced  $\beta$ -cell mass was responsible for insulin insufficiency in T2D <sup>16</sup>. A more recent study compared  $\beta$ -cell volume in explanted human pancreas tissue slices and found no significant reduction in  $\beta$ -cell volume in T2D versus control donors <sup>17</sup>.

On the other hand, several studies have observed significant reductions in  $\beta$ -cell abundance in adult diabetic compared to nondiabetic subjects. One differential volumetric analysis of pancreatic islets revealed a  $\beta$ -cell deficit in adults with diabetes that was associated with increased maximal blood glucose, suggesting that  $\beta$ -cell loss leads to reduced insulin production in T2D <sup>18</sup>. Examination of human pancreas from normoglycemic and T2D subjects following autopsy revealed a decrease in  $\beta$  cells in individuals with hyperglycemia <sup>5</sup>. In a cross-sectional analysis of pancreas sections, Sakuraba et al. observed a 30% reduction in  $\beta$ -cell mass in T2D subjects from Japan, along with increased amyloid deposition and oxidative stress compared to normoglycemic controls <sup>19</sup>. Butler and colleagues also sought to determine whether decreased  $\beta$ -cell mass underlies the hyperglycemia observed in T2D, when in 2003 they analyzed 124 pancreas tissue sections collected at autopsy. They found that individuals with impaired fasting glucose (IFG) or T2D exhibited 40% and 63% reductions in  $\beta$ -cell volume compared to non-diabetic individuals <sup>20</sup>. Jurgens et al. analyzed 68 pancreas tissue samples and again observed decreased  $\beta$ -cell area in tissue from individuals with

T2D<sup>21</sup>. Given the available data from individuals with T2D, it is now accepted that a relative deficit of  $\beta$ -cells exists in this disease. The recently appreciated heterogeneity of T2D phenotypes and human b-cell mass (39–42) may help explain the ongoing debate as to the role of b-cell loss in T2D pathogenesis.

#### Loss of $\beta$ -cell function in diabetes

As well as evidence for  $\beta$ -cell loss derived from histological measurements of pancreas tissue samples, the presence of  $\beta$ -cell loss in diabetes is supported by findings of reduced  $\beta$ -cell function in both major forms of diabetes. In general, these studies have defined impaired  $\beta$ -cell function as 1) impaired insulin synthesis leading to reduced insulin content in islets, 2) reduced plasma insulin (or C-peptide) in the fed or fasted state, or 3) reduced acute insulin release in response to a glucose bolus or mixed meal challenge (4,43). Using such measurements, numerous studies have identified loss of appropriate  $\beta$ -cell function as a primary factor underlying the hyperglycemia that characterizes T1D and T2D.

Given the use of insulin as a treatment for T1D, loss of insulin production in diabetes was widely recognized in the 1920's. In 1952, Wrenshall and colleagues showed that less extractable insulin was present in pancreases from individuals with diabetes compared to those without diabetes, and that among those with diabetes individuals diagnosed at less than 20 years of age possessed significantly less insulin than individuals diagnosed at 20 years of age or older<sup>28</sup>. Later, Cerasi and Luft used IV glucose infusion tests and computer modeling to identify an insufficient insulin response to glucose as a characteristic of diabetic individuals, concluding that this loss of insulin secretion was likely a “pre- requisite” for diabetes<sup>29</sup>. More recently, a large clinical study analyzed

fasting C-peptide data collected from 3668 subjects at the time of T1D diagnosis <sup>30</sup>.

Those diagnosed with T1D at a younger age exhibited lower fasting C-peptide and a greater decline in fasting C-peptide over time <sup>30</sup>.

Despite the clear loss of  $\beta$ -cell abundance and function in T1D, however, some functional  $\beta$  cells persist in individuals with the disease. The Medalist Study analyzed 1019 individuals with duration of T1D over 50 years <sup>31</sup>. Among these individuals, 32.4% had detectable C-peptide levels and 5.8% were able to double C-peptide in response to a mixed meal tolerance test <sup>31</sup>, despite their severe insulin insufficiency and hyperglycemia. A potential explanation for this residual insulin secretory function was uncovered when  $\beta$ -cell lineage tracing experiments identified dedifferentiation as an important driver of  $\beta$ -cell loss in  $\beta$ -cell specific FoxO1 knockout mice <sup>32</sup>. Later, a population of  $\beta$  cells that survive autoimmune attack was identified in mouse and human islets, with these cells expressing reduced  $\beta$ -cell identity genes and arising in response to insulinitis and inflammation <sup>33</sup>. These studies suggest that a subpopulation of  $\beta$  cells exist that, while not fully functional, are protected from cell death in the context of T1D.

Insufficient insulin secretion in T2D, and its relationship to obesity, insulin resistance and aging, are also well documented. In 1963, Karam and colleagues observed increased insulin responses in obese versus normal weight subjects following a glucose injection <sup>34</sup>. In 1967, Perley and Kipnis observed that in response to either oral or IV glucose, plasma insulin was higher in obese versus normal weight individuals without diabetes <sup>35</sup>. Later, Bonadonna and colleagues again found that insulin secretion was increased in obese versus control subjects and noted that obese individuals displayed decreased glucose uptake in response to specified insulin concentrations; that is, they were insulin

resistant<sup>36</sup>. Such observations established insulin resistance and hyperinsulinemia as characteristics of obese, non-diabetic individuals.

In contrast, Perley and Kipnis observed that obese diabetic subjects failed to increase insulin secretion to levels similar to their obese non-diabetic counterparts, displaying a “marked impairment in insulin secretion”<sup>35</sup>. More recently, Mitrakou et al. found that glucose intolerant individuals displayed reduced insulin secretion following glucose ingestion compared to age and weight matched controls subjects<sup>37</sup>. Of note, the reduced insulin secretion observed in T2D is not confined to obese individuals. Similar observations of insulin resistance and  $\beta$ -cell dysfunction have been made in aged individuals with normal body weight and glucose intolerance<sup>38</sup>. More recent observations have clearly defined the relationship between insulin resistance,  $\beta$ -cell function and T2D<sup>39</sup>. These studies demonstrate that obese, non-diabetic individuals increase insulin release to maintain normal blood glucose in the face of insulin resistance, and that this compensatory insulin response is lost in hyperglycemic diabetic individuals.

Together, these data provide evidence that loss of  $\beta$ -cell abundance and function are primary elements contributing to the insulin insufficiency and hyperglycemia that characterize both major forms of diabetes. Understanding the specific factors that underlie  $\beta$ -cell loss in these diseases may lead to new approaches to maintain insulin secretion and thereby treat or cure diabetes.

### **The discovery of insulin**

In 1889, Joseph von Mering and Oskar Minkowski discovered that removing the pancreas from dogs led to glycosuria<sup>40</sup>. Implanting a small piece of the pancreas under

the skin of these dogs prevented hyperglycemia until the implant was removed or degraded, demonstrating the importance of pancreatic secretion in glucose regulation. In 1920, physiologist Ernest Starling noted the unknown mechanism by which the pancreas influenced glucose production and utilization, hypothesizing a hormonal secretion into the bloodstream <sup>41</sup>. In 1921, Banting and Best injected pancreatic extracts into diabetic dogs, significantly reducing their blood glucose levels. James Collip later refined the extraction process, and the resulting substance was named insulin by MacLeod.

A landmark moment occurred on January 11, 1922, when insulin was first administered to Leonard Thompson, a 14-year-old boy with diabetes, dramatically improving his blood glucose levels. He lived another 13 years on insulin treatment. Similarly, Elisabeth Hughes Gossett, diagnosed with diabetes at age 11, received insulin in August 1922, leading to a long and relatively stable life until her death at 73.

The work of Banting and Best, in collaboration with Lilly Pharmaceutical Company in 1923, led to the development of the first commercially available insulin, Isletin. Insulin derived from cattle and pigs was used for many years but had issues like allergic reactions. In 1978, the first genetically engineered synthetic human insulin was produced using *Escherichia coli* bacteria, and Eli Lilly later marketed this biosynthetic human insulin as Humulin <sup>41</sup>.

Diabetes researchers have made it possible to develop insulin in many forms, allowing millions of individuals to choose from a variety of formulas and methods of using insulin that best suits their requirements and lifestyle. This ability comes from decades of research to appreciate the production of insulin and normal  $\beta$ -cell physiology in rodent and human models, as briefly described below.

## Overview of $\beta$ cell biology

The islets are a specialized mini-organ that produces multiple hormones to maintain glucose homeostasis. These pancreatic islets occupy approximately 1% of the entire pancreatic mass and obtain 10% of the pancreas blood flow to sense and appropriately respond to changes in blood glucose levels. The primary islet hormones include insulin and amylin ( $\beta$  cells; 60-85%), glucagon ( $\alpha$  cells; 15-20%), ghrelin ( $\epsilon$  cells, <1%), somatostatin ( $\delta$  cells; 3-10%) and pancreatic polypeptide (PP cells; 3-5%).

Insulin is a highly conserved 51 amino acid peptide hormone that permits glucose to be absorbed by cells throughout the body and be utilized for energy. Insulin also suppresses glucose output by the liver to maintain steady state blood glucose levels in the body.

Insulin is synthesized by  $\beta$  cells as a prohormone, subsequently proteolytically processed in the endoplasmic reticulum (ER), Golgi and secretory granules to the mature peptide, consisting of two polypeptide chains<sup>42</sup>. Insufficient insulin secretion or failure of insulin action is an underlying feature of both type 1 and type 2 diabetes<sup>43</sup>. Hence, approaches to preserve  $\beta$ -cell mass and function may lead to the development of new therapies for prevention or cure of diabetes.

### Insulin proprotein synthesis and granule maturation

Humans have one insulin gene while rodents and at least 3 fish species have two insulin (INS) genes<sup>44</sup>. The insulin gene contains 3 exons and 2 introns, and only <400 bp are needed for  $\beta$ -cell insulin synthesis and secretion. The final spliced insulin mRNA encodes preproinsulin. Glucose stimulation drives transcription of the insulin gene. However, this response takes approximately 1 h for pre-mRNA levels to increase and up to 48 h for mature transcripts to increase significantly<sup>45</sup>. On the contrary, studies in

rodent islets have shown that proinsulin translation, along with proIAPP and processing enzymes prohormone convertase 1/3 (PC 1/3) and PC2 rapidly increase in response to glucose<sup>46</sup>.  $\beta$  cells can achieve rapid glucose-induced pro-insulin synthesis by storing insulin mRNA in preassembled polysomes that are transported to the ER membrane and initiate translation in response to glucose within minutes<sup>47</sup>. The nascent preproinsulin mRNA associates with a signal recognition particle (SRP) in the cytosol. The SRP binds to its receptor, which facilitates translocation of preproinsulin into the RER lumen. Signal peptide cleavage allows conversion of preproinsulin to proinsulin. Formation of 3 intramolecular disulphide bonds by protein disulphide isomerases are critical for proper folding of proinsulin in the ER. Proinsulin is subjected to folding as it transits the Golgi, and after exit from the trans-Golgi network, it is sorted to the regulated secretory pathways<sup>48</sup>. As the secretory granules mature, the pH decreases and granule  $\text{Ca}^{2+}$  and  $\text{Zn}^{2+}$  concentrations increase through actions of vesicular  $\text{H}^{+}$ -ATPase<sup>49</sup> and Zinc transporter SLC30A8<sup>50</sup>. This increases prohormone convertase activity that initiates conversion of proinsulin to insulin and hexameric aggregation. Proteolytic processing to insulin in immature granules leaves C-peptide and requires acidification (pH 5)<sup>51</sup>. Not all proinsulin within a  $\beta$  cell will be ultimately secreted.  $\beta$ -cell proteostasis is maintained by (pro)insulin degradation by macroautophagy and selective autophagy<sup>52,53</sup>. Aged insulin granules are also degraded to make sure newer ones are preferentially released<sup>54</sup>. Disruption of proper insulin folding can lead to diabetes and misfolded proinsulin can be degraded via ER-coupled autophagy and ER-associated degradation pathways<sup>55</sup>. Altered autophagy of  $\beta$  cells have been observed in pancreas samples obtained from individuals with type 1 and type 2 diabetes<sup>56,57</sup>. Islet amyloid polypeptide (IAPP) is another  $\beta$ -cell

specific peptide which is normally produced and secreted in parallel with insulin <sup>58</sup>. The processing of proinsulin and pro-IAPP occurs simultaneously as described above.

#### Mechanism of glucose-stimulated insulin secretion (GSIS)

Insulin secretion by  $\beta$  cells is a tightly regulated mechanism that requires glucose stimulation. Under fed state, the digestive tract breaks down carbohydrates into glucose which is then released into the blood stream. Uptake of the glucose molecules into the  $\beta$  cell is facilitated by glucose transporter type 1/2 (GLUT1/2). GLUT1/2 is constitutively present at the  $\beta$  cell plasma membrane to facilitate glucose uptake <sup>59</sup>. Intracellular glucose is phosphorylated to glucose-6-phosphate by glucokinase. Glucokinase in  $\beta$  cells has a high  $K_m$  allowing controlled sensing of glucose levels in blood and acts as a rate limiting enzyme that regulates insulin secretion <sup>60</sup>. Metabolism upstream of mitochondrial metabolism releases ATP, but the additional ATP gained from mitochondrial metabolism leads to the net closure of ATP-sensitive potassium ( $K_{ATP}$ ) channels <sup>61</sup> (Figure 1). This phenomenon results in membrane depolarization and opening of voltage-operated calcium channels and  $Ca^{2+}$  influx. The subsequent increase in cytosolic  $Ca^{2+}$  causes insulin-containing vesicles to fuse to the  $\beta$ -cell plasma membrane <sup>62</sup>. Therefore, the  $\beta$  cell controls exocytosis of insulin in amounts appropriate to allow transport of glucose from blood into the cells of the body, particularly muscle and adipose tissue, and suppresses hepatic glucose output.

Insulin secretion by  $\beta$  cells is biphasic in nature. There are 3 granule pools that allow for biphasic insulin secretion, namely the immediately releasable pool (IRP), the readily releasable pool (RRP) and the reserve pool (RP) <sup>51</sup>. The IRP and RRP pools are primed by being physically located adjacent to the  $\beta$ -cell membrane and/or have been chemically

modified to allow for immediate release in the first phase of glucose stimulated insulin secretion. Most of these granules are in the immediate vicinity (~10 nm) of the L-type  $\text{Ca}^{2+}$  channels<sup>63</sup>. The RP granules are available for secretion with insulin already folded and readily available in the granules. However, these granules require trafficking to the plasma membrane along the microtubule network and primed before they can be released. Initial phase of GSIS is reflective of  $\text{Ca}^{2+}$  induced exocytosis of primed insulin granules. Extracellular messengers that modulate insulin secretion via the cAMP/PKA or PLC/DAG/PKC systems affect the priming phase<sup>64</sup>. Other extracellular modulators such as incretins (for example, GLP-1) mediate nutrient ingestion-induced priming phase. Docking to priming step requires ATP and sub- $\mu\text{M}$   $\text{Ca}^{2+}$ , while priming to fusion step requires  $\mu\text{M}$   $\text{Ca}^{2+}$ <sup>61</sup>. A secondary pathway involving  $\text{K}_{\text{ATP}}$ -channel independent secretion, known as the amplifying pathway, increases efficacy of  $\text{Ca}^{2+}$  on exocytosis of insulin granules, and is impaired in  $\beta$  cells of animal models of type 2 diabetes<sup>65</sup>.

### **Classification of the different forms of diabetes**

#### **Type 1 diabetes (T1D)**

The pathological feature of T1D is inflammatory lesion (insulinitis) of the pancreatic islet associated with  $\beta$ -cell loss, and a key role for autoreactive T cells, as observed in examinations of diabetic pancreata obtained at autopsy<sup>66</sup>. These studies of human pancreata observed that the degree of insulinitis is heterogenous, affects only 10-30% of islets and diffuse within an islet<sup>66-68</sup>. Studies also demonstrate that insulin-positive  $\beta$  cells may persist for many years after diagnosis, which suggests that alongside a reduction in  $\beta$ -cell mass,  $\beta$ -cell dysfunction must persist in individuals with T1D<sup>69</sup>. In T1D, autoreactive  $\text{CD4}^+$  and  $\text{CD8}^+$  T cells infiltrate the islet, leading to  $\beta$ -cell

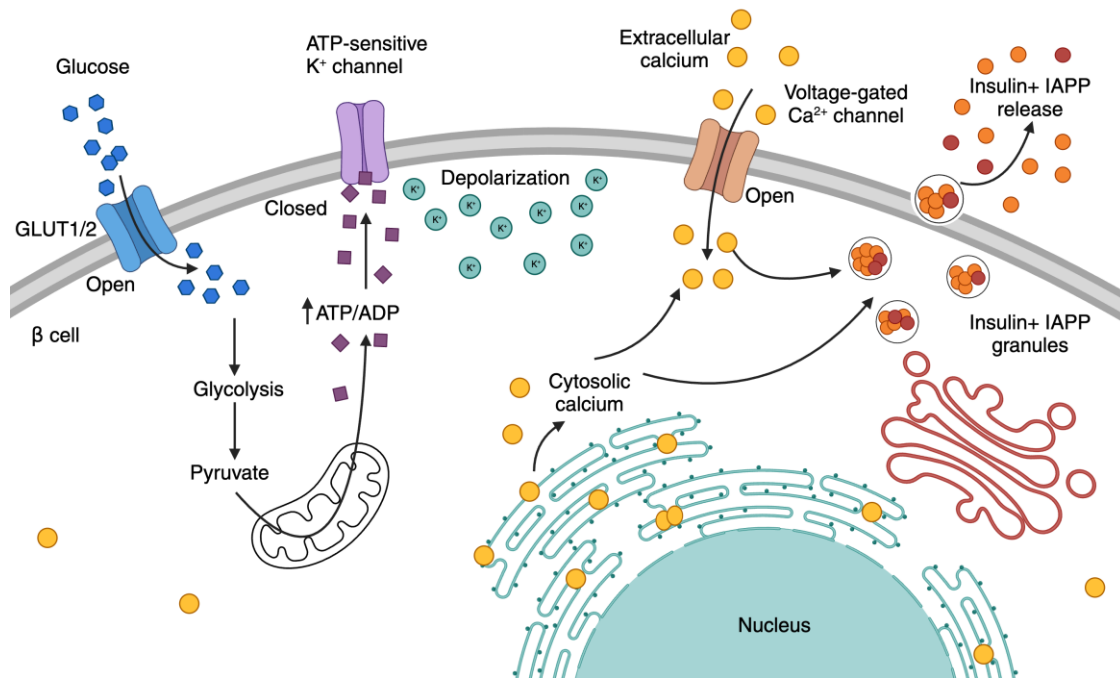


**Figure 1: Mechanism of glucose stimulated insulin secretion**

(From left to right) The canonical pathway of glucose stimulated insulin secretion (GSIS) requires glucose import into the  $\beta$  cell via GLUT1/2 transporter. Glucose is converted to pyruvate. Mitochondrial metabolism increases ATP/ADP ratio, that results in closure of ATP-dependent  $K^+$  channel. The resulting membrane depolarization leads to opening of voltage-gated  $Ca^{2+}$  channel, which allows calcium influx into the cell. Moreover, release of calcium from intracellular stores amplifies the increase in cytosolic calcium concentration. The rise in cytosolic calcium levels ultimately triggers the release and exocytosis of insulin and IAPP granules.

loss by cell-cell interactions and cytokine production by infiltrating immune cells. While this effect is likely aggravated by impaired function of regulatory T cells that should ideally provide immunological tolerance, the fact that  $\beta$  cells are a mere bystander of a rogue immune system is being challenged in recent studies <sup>70</sup>.  $\beta$  cells being professional secretory cells are predisposed to biosynthetic stress and have limited measures for self-defense. Immune interventions are capable of delaying onset of T1D, again suggesting a key role of  $\beta$ -cell stress can invoke an immune attack <sup>71</sup>.

Additionally,  $\beta$  cell dysfunction has been observed years before diagnosis of disease <sup>72</sup>. Hence, approaches to revitalize  $\beta$  cells alongside immunotherapy could provide a more effective treatment regimen for individuals with T1D <sup>70</sup>.

Genetic risk of developing T1D is largely derived from human leukocyte antigen (HLA) class II haplotypes and this is present in up to 80-90% of patients <sup>73</sup>. Additionally, more than 50 loci have been identified that confer risk for T1D. These include candidate genes associated with immune function and/or survival and function of the  $\beta$  cell <sup>74,75</sup>.

Apart from genetic predisposition, an environment trigger is observed to be necessary for development of T1D. The role of the environment is emphasized in a study that observed discordant incidence rate in monozygotic twins <sup>76</sup>. Furthermore, there seems to be differences in disease rates that is not simply explained by genetic differences <sup>77</sup>.

Environmental factors affecting development of autoimmunity in T1D include viral infection <sup>78</sup>, a role of gut microbiota <sup>79</sup> and dietary factors that trigger the immune system <sup>80</sup>.

### Type 2 diabetes (T2D)

T2D is characterized by hyperglycemia, insulin resistance and a reduction in  $\beta$ -cell number along with dysfunction of remaining  $\beta$  cells. Classically, T2D takes decades to develop and as the disease progresses, increasing doses of glucose lowering drugs is required to manage glucose homeostasis. Insulin administration might be necessary when  $\beta$  cells reach a condition of total “failure”.

Obesity, particularly visceral adiposity, is a key component driving pathogenesis of insulin resistance<sup>81</sup>. This results in insulin being less effective in stimulating glucose uptake by skeletal muscle, reduced inhibition of hepatic glucose production and adipose tissue lipolysis<sup>82</sup>. The development of insulin resistance stimulates  $\beta$ -cell compensation in the form of hypertrophy and proliferation to some extent to increase insulin production. This leads to development of hyperinsulinemia to maintain normal blood glucose (NGT). When  $\beta$ -cell compensation becomes inadequate, impaired glucose tolerance and impaired fasting glucose (IFG) is observed, ultimately leading to T2D development<sup>83</sup>.

While environmental factors, such as a sedentary lifestyle and excessive food intake leading to obesity play a key role in development of T2D, heritability is also a major determinant. Recent studies have identified more than 400 gene variants associated with T2D. These genetic variants are known to have effects on  $\beta$ -cell function, obesity/adiposity, insulin action and lipid metabolism<sup>84</sup>. Epigenetic changes such as DNA methylation, histone modification, miRNA and long non-coding RNA can possibly begin *in utero* and are additional factors that can influence T2D pathogenesis<sup>85,86</sup>.

Approximately 90% of individuals with T2D have islet amyloid deposits, and the degree of islet amyloid deposition is positively correlated with  $\beta$ -cell death in humans

<sup>87,88</sup>. Islet amyloid deposits are insoluble fibrillar structures that arise following aggregation of islet amyloid polypeptide (IAPP), a  $\beta$ -cell secretory product that is co-secreted with insulin <sup>58</sup>. While early studies found that prefibrillar oligomeric assemblies of human IAPP (hIAPP) directly disrupt cell membranes and elicit cytotoxicity <sup>89,90</sup>, more recent studies have shown that IAPP species can also bind receptors and induce receptor-mediated toxicity <sup>91,92</sup>. Separate from amyloid-induced  $\beta$ -cell death, recent research has identified islet amyloidosis as a major driver of islet inflammation. *In vivo* studies have observed that amyloid deposition is associated with increased cytokine (*Il1b*, *Tnf*, *Il6*) and chemokine (*Ccl2*, *Cxcl1*) expression, alongside increased immune cell infiltration <sup>93,94</sup>. It is well established that IAPP stimulates cytokine production from islet immune cells and leads to  $\beta$ -cell dysfunction and death <sup>3</sup>.

#### Maturity-onset diabetes of the young (MODY)

MODY was first described in 1974 when Tattersall et al. observed that in three families there was direct parent to child inheritance and although they diagnosis of diabetes occurred at teen or early 20s, the manifestation of diabetes was mild and does not progress to insulin dependence even over a period of 40 years <sup>95</sup>. MODY is a cluster of 11 different autosomal dominant forms of diabetes, mostly affecting transcriptional factors, resulting in impaired insulin production and release <sup>96</sup>. The 4 most common forms of MODY affect a) glucokinase (MODY 2), b) HFN-1 $\alpha$  (MODY 3) and less common HFN-4 $\alpha$  (MODY 1) and c) HNF-1 $\beta$  (MODY 5). In addition to these, several other gene are associated with MODY-like phenotypes, including *KLF1* (a regulator of Pdx1  $\beta$ -cell transcription factor), *PAX4*, and *preproinsulin*.

#### Neonatal diabetes

Neonatal diabetes is a form of monogenic diabetes that becomes apparent early in life and consists of homozygous mutations in certain MODY genes. This results in permanent neonatal diabetes and pancreas agenesis. Although it is characterized by defects in  $\beta$ -cell function, often neonatal diabetes is associated with defects in other organ systems <sup>96</sup>. About half of these cases are caused by mutations in gene encoding potassium channel (*KCNJ11* and *ABCC8*), resulting in impairment in GSIS that can be restored using sulfonylurea treatment <sup>97</sup>.

#### Cystic fibrosis-related diabetes (CFRD)

Mutation in the cystic fibrosis transmembrane conductance regulator gene (*CFTR*) results in cystic fibrosis, a common, lethal, autosomal recessive disorder <sup>98</sup>. CFRD has characteristic mild insulin resistance, reduced  $\beta$ -cell mass along with impaired  $\beta$ -cell function and glucagon release <sup>99</sup>. The  $\beta$ -cell dysfunction is associated with a marked inflammatory response, dysregulated chloride conductance in  $\beta$ -cell membrane and increased oxidative stress <sup>100,101</sup>. Surprisingly, islet amyloid has also been observed in patients with cystic fibrosis <sup>101</sup>. Unfortunately, some studies that have utilized CFTR modulators have failed to improve insulin secretion and glucose tolerance <sup>102</sup>.

#### Gestational diabetes mellitus (GDM)

Changes in metabolic demand during pregnancy can induce a state of insulin resistance in the body that requires  $\beta$ -cell compensation to restore euglycemic condition, similar to scenario observed during T2D <sup>103</sup>. However, in 10% of pregnancies, the  $\beta$  cells are unable to compensate appropriately, leading to insufficient release of insulin, glucose intolerance and eventually gestational diabetes <sup>104</sup>. Gestational diabetes during pregnancy poses the risk of development of diabetes during subsequent pregnancies due to added  $\beta$ -

cell stress and may contribute to development of T2D in the later stages of life <sup>105</sup>. Recent studies have observed autoimmune and genetic factors, such as presence of anti-insulin antibodies during pathogenesis of GDM, which leading to risk of latent T1D development <sup>106</sup>. Studies focusing on single nucleotide polymorphisms (SNPs) in genes that affect impaired first phase of insulin secretion, such as cyclin-dependent kinase 5 (CDK5) regulatory subunit associated protein1-like1 gene (CKDAL1) in T2D and GDM may hold hope for new treatment strategies <sup>107</sup>.

In summary,  $\beta$ -cell stress, dysfunction and death is observed in all forms of diabetes, even though difference in pathophysiology of the disease exist. My studies majorly focus on understanding the underlying mechanisms of  $\beta$ -cell dysfunction and loss in pathogenesis of diabetes.

### **Contributors of $\beta$ -cell cytotoxicity in diabetes**

#### **Autoimmune-associated $\beta$ -cell death in T1D**

Upon examination of pancreas section from 42 individuals with T1D and 14 non-diabetic controls, Meier and colleagues observed that  $\beta$ -cell death was twice as frequent in individuals with T1D (49). They also observed that this increased cell death was accompanied by increased infiltration of macrophages and T lymphocytes in islets, suggestive of autoimmune-mediated destruction of  $\beta$  cells in T1D (49). Coppieters et al. identified islet-autoreactive CD8+ T cells in insulitic lesions that were specific to T1D patients and were not observed in cases of T2D or gestational diabetes (71). Research conducted at the level of individual islets suggests  $\beta$ -cell killing is mediated by direct CD8+ T cell contact with  $\beta$  cells, and that M1 polarization of islet resident macrophages by CD4+ T cells contribute to this process (71,72). Such findings have added to previous

observations of autoimmune-associated destruction of  $\beta$  cells in T1D (20,44,73) and led to studies of the mechanisms that promote this process.

T1D is thought to result primarily from destruction of healthy  $\beta$  cells by self-reactive T cells that occurs by mistake, a view adopted following identification of islet-reactive CD4<sup>+</sup> and CD8<sup>+</sup> T cells in individuals with T1D (71,74–76). In line with this understanding, numerous immunotherapy trials have been conducted in individuals with recent-onset T1D in hopes of preserving  $\beta$ -cell mass and function. Teplizumab and oteelixizumab, anti-CD3 monoclonal antibodies that target T cells, have been shown to improve C-peptide responses and reduce exogenous insulin requirements in individuals with recent-onset T1D (77–79). In addition, teplizumab has been shown to delay onset of T1D in relatives at risk for T1D (80). Abatacept, a molecule used to modulate T cell co-stimulation, has also been shown to transiently preserve  $\beta$ -cell function in T1D patients (81). Studies in animal models of diabetes further support the role of T cells in T1D. In 1985, Miyazaki et al. reported on the prominence of CD4<sup>+</sup> and CD8<sup>+</sup> T cells in the insulinitic lesion observed in the NOD mouse model of T1D (82). In 1993, Christianson and colleagues observed that while NOD background mice lacking T and B cells (NOD/SCID) did not develop diabetes, diabetes could be induced in these mice by adoptively transferring T cells from diabetic NOD mice (83). Also around this time, Posselt and associates observed that autoimmune diabetes in spontaneously diabetic BioBreeding rats could be prevented by intrathymic islet transplantation, possibly due to modulation of the T cell repertoire upon exposure to the transplanted islets (84). In sum, these studies provide strong evidence for T cell-associated  $\beta$  cell-death in T1D.

In 1974, autoantibodies against islet cell proteins were first detected in the sera of T1D patients (73). Autoantibodies observed in individuals with T1D include those against islet cell cytoplasmic protein (ICA), insulin (IAAs), glutamic acid decarboxylase (GAD65), insulinoma antigen 2 protein (IA-2), and zinc transporter 8 (ZnT8) (85). Presence of at least one of these autoantibodies is present in >95% of individuals diagnosed with T1D (85). The most well-known  $\beta$ -cell-specific-antigens are insulin and pro-insulin, with insulin autoantibodies (IAAs) detected in >59% patients with late pre-clinical or early-onset T1D (86). Despite the strong association between islet autoantibodies and T1D, it is debated whether autoantibodies drive  $\beta$ -cell death or whether they arise because of islet destruction. However, it's largely accepted that presence of islet autoantibodies is associated with increased risk of developing T1D (87). Rituximab, an anti-CD20 monoclonal antibody that depletes B lymphocytes was observed to delay, but not prevent, loss of  $\beta$ -cell function in subjects with recently diagnosed T1D (88). Mariño et al. observed that B lymphocytes depletion delays diabetes onset and reduced diabetes incidence in NOD mice, again indicating a role for B cells in T1D pathogenesis (89).

Given that islet autoimmunity is a key feature of T1D, it is important to identify the factors that initiate this immune-associated  $\beta$ -cell destruction. Counter to the traditional hypothesis that the immune system errantly identifies  $\beta$  cells for removal, another hypothesis has more recently been put forward: that the  $\beta$  cell itself prompts the autoimmune assault observed in T1D. In their recent review, Roep and colleagues suggest that  $\beta$  cells are an “active participant” in interactions with the immune system in T1D rather than a “non-provoking victim of an autoimmune attack” (90).

Several observations support the concept that  $\beta$  cells contribute to the pathophysiology of T1D. Studies performed in NOD mice have shown that  $\beta$  cell-death precedes the appearance of insulinitis (58) and promotes  $\beta$ -cell autoantigen presentation (91). NOD mouse islets exhibit increased endoplasmic reticulum (ER) stress markers and alterations in ER structure prior to insulinitis and hyperglycemia, suggesting that  $\beta$ -cell stress contributes to development of T1D in this model (92). Indeed, treatment of prediabetic NOD mice with an ER stress mitigating agent (TUDCA) was shown to reduce diabetes incidence (93).  $\beta$  cell-stress may lead to the production of antigenic products such as “hybrid insulin peptides” which are composed of proinsulin and other secretory peptides and have been identified as targets of CD4<sup>+</sup> T cells found in NOD mice and individuals with T1D (94). Also supporting a role of the  $\beta$  cell in T1D pathogenesis, the immunosuppression therapies targeting T and B cells (discussed above) exhibit a lack of durable effects, with these interventions delaying, but not preventing, development of T1D (77,78,81,88).

These observations suggest that unfounded islet immune responses may not be the inciting event in  $\beta$ -cell death in T1D. Together, they have led the field to question whether  $\beta$  cells, the target tissue of immune attack, may participate in their own demise and carry more blame in T1D pathogenesis than originally thought. Additional studies are needed to better understand how  $\beta$ -cell stress or death may initiate the islet immune responses that have long characterized T1D.

#### Islet amyloid-induced $\beta$ -cell death in T2D

In 1901, Eugene Opie first reported a form of islet “hyaline degeneration” that occurs in association with diabetes mellitus and that we now recognized as islet amyloid deposition

(10). More recent studies have confirmed the relationship between islet amyloid deposition and hyperglycemia in T2D, with these works demonstrating that islet amyloid deposition is associated with reduced  $\beta$ -cell abundance and increased  $\beta$ -cell death in humans (35,52). Islet amyloid formation is accepted to be a contributor to the pathogenesis of T2D, but studies have suggested that it may also contribute to  $\beta$ -cell loss in T1D (95–97) and following islet transplantation (98,99). Islet amyloid deposits are insoluble fibrillar structures composed primarily of islet amyloid polypeptide (IAPP, also known as amylin), a  $\beta$ -cell secretory product (100,101). Although monomeric IAPP has physiological functions on satiety and gastric emptying (102,103), human IAPP (hIAPP) is amyloidogenic and can aggregate into larger structures including oligomers, protofibrils and eventually full amyloid fibrils (104). Significant effort has been expended to identify the mechanisms that underlie amyloid-associated  $\beta$ -cell death in diabetes. Early observations of the mechanisms of hIAPP-induced  $\beta$ -cell death focused on direct actions of hIAPP to induce cytotoxicity (105,106). Studies of hIAPP have found that oligomeric peptide species can directly elicit  $\beta$ -cell cytotoxicity in cell lines and primary islet cells (107–109). This cytotoxic effect has been linked to both receptor-mediated signaling events (110–113) and cytotoxic interaction with cell membranes (114–116). In addition to the direct action of hIAPP on  $\beta$  cells, it has been demonstrated that hIAPP also directly induces cytokine production from macrophages and dendritic cells via activation of the NLRP3 inflammasome (117). Work to define the structure of these cytotoxic hIAPP species is ongoing (118–120). A better understanding of the mechanisms of direct hIAPP-induced cytotoxicity may provide strategies to reduce  $\beta$ -cell death elicited by hIAPP.

In contrast to hIAPP, rodent IAPP is not amyloidogenic or cytotoxic due to several amino acid substitutions in the amyloidogenic region of the peptide in rodent compared to human IAPP (104). Thus, rodent models that express hIAPP in the  $\beta$  cell have been created (121–124). These animal models develop *in situ* islet amyloid deposits,  $\beta$ -cell loss and  $\beta$ -cell death similar to that observed in humans with T2D, thereby facilitating study of the process of islet amyloid-induced and  $\beta$ -cell destruction (119–121). Given that IAPP is a  $\beta$ -cell secretory peptide, insulin resistance and high secretory demand were postulated to promote to islet amyloid formation in T2D. Indeed, genetic loss of  $\beta$ -cell secretory function reduces islet amyloid formation (125), while elevated glucose concentrations increase amyloid deposition (126). More recent studies of these animal models have led to a series of observations that identified amyloid formation as a driver of islet inflammation (127–130). *In vivo* studies using these models showed that islet amyloid deposition is associated with increased cytokine (*Il1 $\beta$* , *Tnf*, *Il6*) chemokine (*Ccl2*, *Cxcl1*) and immune cell marker (*Emr1*, *Itgax*) expression (128,129), with several studies identifying IL-1 $\beta$  as an important mediator of amyloid-induced  $\beta$ -cell death (127,128,130–132). Studies in other models of islet amyloidosis have identified ER stress as an important contributor to amyloid-induced  $\beta$ -cell death (133,134).

Several strategies to ameliorate hIAPP-induced  $\beta$ -cell death have been evaluated. Various small molecule chemical inhibitors have been shown to effectively block hIAPP aggregation and its associated cytotoxicity (135–137), with the same being true of certain endogenous proteins (138,139). Interestingly, the structure of amyloid aggregates is similar between divergent amyloidogenic peptides such as hIAPP and amyloid  $\beta$  (140), suggesting that a single amyloid-inhibiting molecule may be used to prevent amyloidosis

in multiple tissues such as the islet and brain (120). In addition to these approaches, vaccination against hIAPP has been shown to effectively prevent amyloid-associated  $\beta$ -cell loss in some (109,141), but not all (142), studies. Other work has focused on preventing islet amyloid associated inflammation, with blockade of IL-1 $\beta$  and toll-like receptor signaling both shown to be effective in preventing  $\beta$ -cell loss (131,132).

#### Mechanisms of proinflammatory cytokine-induced $\beta$ -cell death

As discussed previously, proinflammatory cytokines from islet resident or infiltrating immune cells contribute to  $\beta$ -cell loss in both T1D and T2D. A series of investigations have focused on understanding the role of proinflammatory cytokines on  $\beta$ -cell dysfunction and death. These studies have used single cytokines or combinations of cytokines meant to approximate the inflammatory environment that  $\beta$  cells are exposed to in the pathogenesis of diabetes.  $\beta$  cells express cytokine receptors that, when activated, initiate complex signaling cascades that can impact insulin secretion (143,144), ER stress (92,145), oxidative stress (146–148), and eventually cell death (149–152). Treatment with a combination of IL-1 $\beta$ , TNF $\alpha$  and IFN $\gamma$  are commonly used to study mechanisms of cytokine-induced  $\beta$ -cell cytotoxicity. These studies have characterized cytokine-stimulated signaling pathways in  $\beta$  cells and evaluated the impact of these on  $\beta$ -cell cytotoxicity in the pathogenesis of diabetes.

Treatment of primary  $\beta$  cells with interleukin 1 $\beta$  (IL1 $\beta$ ) for 24 to 48 hours was found to elicit cell death, and these effects could be prevented by inhibition of nitric oxide synthase, suggesting that IL1 $\beta$  mediates its cytotoxic effect through NO production (146,148,153). IL1 $\beta$  has also been shown to induce ER Ca<sup>2+</sup> release and activate ER stress pathways. Cotreatment of immortalized and primary rat  $\beta$  cells with a combination

of IL1 $\beta$  and IFN $\gamma$  has been shown to downregulate SERCA2b, a Ca<sup>2+</sup> pump important for ER homeostasis, activate ER stress and induce  $\beta$ -cell death, with these effects again being dependent on NO production (145). IL1 $\beta$  has also been shown to cause  $\beta$ -cell death via activation of JNK pathway signaling in rat and mouse  $\beta$  cell lines resulting in cell death (154,155). Anakinra, a clinically approved IL-1 receptor antagonist (IL-1RA), has been shown to prevent cytokine-mediated NO production, mitochondrial dysfunction and cell death in cultured rat islets (156). Overexpression of dominant negative MyD88, an IL-1R interacting protein, was found to decrease nuclear NF- $\kappa$ B localization, NO production and cell death in an IL-1 $\beta$  treated mouse  $\beta$ -cell line (157).

Tumor necrosis factor  $\alpha$  (TNF $\alpha$ ) has been recognized as a cell death stimulus since the 1970s (158,159). In 1999, Ishizuka and colleagues showed that TNF receptor 1 (TNFR1) and its signaling components TRADD, FADD and FLICE are expressed in the MIN6 mouse  $\beta$ -cell line, and that TNF $\alpha$  elicits death in a time- and dose-dependent manner in these cells (160). To test the role of TNF $\alpha$  in autoimmune diabetes, Green et al. developed an NOD mouse with transgenic expression of TNF $\alpha$  in  $\beta$  cells and observed accelerated diabetes onset, with  $\beta$ -cell death preceding hyperglycemia and immune cell infiltration in this model (161). TNFR1 deficient NOD mice develop insulinitis similar to control NOD mice, yet they failed to develop diabetes (162). When TNFR1 deficient mice were subjected to adoptive transfer of spleen cells from diabetic control NOD donor mice, diabetes was significantly delayed, indicating a role for  $\beta$ -cell TNFR1 signaling in autoimmune-mediated  $\beta$ -cell death (162). TNF $\alpha$  is considered an important  $\beta$ -cell death effector. However, while TNF $\alpha$  alone is capable of eliciting cell death in immortalized  $\beta$ -cell lines, it has been observed that primary  $\beta$ -cell death requires treatment with a

combination TNF $\alpha$  and IFN $\gamma$  (163). Recently, a human monoclonal antibody targeting TNF $\alpha$ , golimumab, was shown to improve endogenous insulin production and reduce exogenous insulin requirement in individuals with recent onset T1D (164). This landmark study was the first to directly target TNF $\alpha$  for preservation of  $\beta$ -cell function in human T1D.

Studies in non-islet cell types have found that TNF $\alpha$  can induce both apoptotic and non-apoptotic cell death signaling pathways, thereby influencing inflammatory microenvironment in diseases conditions. I investigate TNF $\alpha$  signaling in greater details in the following portions of this thesis.

In 1985, Campbell and associates cultured mouse islets in the presence of interferon  $\gamma$  (IFN $\gamma$ ) and observed a 10-fold increase in major histocompatibility complex (MHC) class I antigen expression on  $\beta$  cells (165). They also observed that IFN $\gamma$  directly inhibits  $\beta$ -cell growth and insulin synthesis in RIN-m5F  $\beta$  cells (166). This marked increase in MHC expression suggested that IFN $\gamma$  may contribute to  $\beta$  cell-directed autoimmunity in T1D. However, Thomas et al. found that while loss of functional IFN $\gamma$  receptors prevented upregulation of  $\beta$ -cell MHC class I expression, it did not prevent diabetes in NOD mice (167). Gysemans and colleagues found that loss of signal transducer and activator of transcript-1 (STAT-1), a transcription factor activated by IFN $\gamma$  and IFN $\alpha$ , prevents  $\beta$ -cell death in response to IFN $\gamma$  and IL-1 $\beta$  *in vitro*, and were protected from STZ-induced hyperglycemia *in vivo* (168).

Individuals at genetic risk for developing T1D exhibit a type 1 interferon signature in peripheral blood mononuclear cells that precedes development of islet autoantibodies (169). IFN $\alpha$ , a type 1 interferon, induces HLA class I expression, ER stress markers and

inflammation in human  $\beta$  cells, and acts in coordination with IL-1 $\beta$  to elicit  $\beta$ -cell death (170). Polymorphisms in TYK2, a type I interferon receptor signaling molecule, confer risk for development of diabetes (171). Mice carrying a mutant Tyk2 fail to respond to type I interferon appropriately, leading to a failed  $\beta$ -cell antiviral response and sensitization to virus-induced diabetes (172). Loss of TYK2 in human  $\beta$  cells has been shown to reduce IFN $\alpha$ -induced MHC class I upregulation and diminish cell death (173). Thus, IFN $\alpha$ -TYK2 mediated inflammation and cell death may be required for effective  $\beta$ -cell defense against viral infection.

Cytokine exposure can also contribute to  $\beta$ -cell reactive oxygen species (ROS) generation.  $\beta$  cells are particularly vulnerable to oxidative stress because they have low levels of antioxidant defenses, making strategies that inhibit ROS formation, like targeting 12-lipoxygenase, crucial for protection. IL1 $\beta$  alone or in combination with TNF $\alpha$  has been shown to elicit NO production from primary islet cells and  $\beta$  cell lines, resulting in DNA cleavage, nuclear shrinkage, chromatin condensation and formation of apoptotic bodies, indicative of apoptosis (197). Thioredoxin-interacting protein (TXNIP) is a redox regulatory protein that is upregulated in  $\beta$  cells in response to glucose and IFN $\gamma$  (198–200) and has been shown to promote  $\beta$ -cell death (198,201,202).

#### Endoplasmic reticulum stress-induced $\beta$ -cell death

In the setting of insulin resistance and hyperglycemia, high insulin secretory demand is placed on the  $\beta$  cell. This elevated insulin demand has been described as the  $\beta$  cell's Achilles' heel; it's innate physiological function of glucose stimulated insulin secretion makes it vulnerable to chronic ER stress (174). Although  $\beta$  cells initially activate the unfolded protein response (UPR) to balance the demand for insulin synthesis with the

capacity of the ER to process insulin properly (93,175,176), changes in insulin molecule sequence (177), ER Ca<sup>2+</sup> homeostasis (178,179) or insulin demand (180,181), can favor insulin misfolding that leads to chronic ER stress, and eventually,  $\beta$ -cell death (67,152,155,182). It has been proposed that ER-stress mediated protein misfolding may lead to  $\beta$ -cell autoantigen production and adaptive immune responses in T1D (90,183) and contribute to hIAPP aggregation and islet amyloid deposition in T2D (133,134). The basic molecular mechanisms that govern the UPR and ER stress signaling have been reviewed elsewhere (182,184,185).

Several studies have observed that markers of ER stress are elevated in  $\beta$  cells of humans with T2D and animal models thereof. BiP and CHOP, two ER stress markers, were found to be increased in  $\beta$  cells from pancreas sections collected from patients with T2D compared to non-diabetic subjects (186). When Marchetti and colleagues evaluated pancreas sections from subjects with T2D they observed increased  $\beta$ -cell ER volume and  $\beta$ -cell death compared to non-diabetic subjects (187). They also observed increased expression of ER stress markers BiP and XBP1 when islets from donors with T2D were cultured in high glucose, although this increase was not observed in islets isolated from non-diabetic donors (187). Huang and associates reported increased CHOP expression in  $\beta$  cells of obese individuals, and increased nuclear localization of CHOP was observed in  $\beta$  cells of obese diabetic compared to obese non-diabetic subjects (133). In the early 2000s, it was observed that chemical chaperones (which aid protein folding) could reduce ER stress, decrease blood glucose concentrations and restore insulin sensitivity in an animal model of T2D (180,188). The importance of  $\beta$ -cell ER stress in this process was highlighted by studies of CHOP, an ER stress-induced transcription factor and key

effector of cell death (189,190). In 2002, CHOP deficiency was found to delay the onset of diabetes in Akita mice that exhibit insulin misfolding and  $\beta$ -cell ER stress (191). In response to genetic and diet-induced insulin resistance, loss of CHOP resulted in improved blood glucose homeostasis, increased  $\beta$ -cell mass and decreased  $\beta$ -cell death compared to control mice (192). The improved metabolic profiles observed in this model of CHOP deficiency were associated with increased expression of islet UPR and oxidative stress response genes (192).

Although ER stress-induced  $\beta$ -cell death was initially thought to pertain mostly to T2D, ER stress has since become considered a likely contributor to  $\beta$ -cell destruction in T1D as well. As noted previously, cytokines were found to alter ER  $\text{Ca}^{2+}$  homeostasis and induce ER stress *in vitro* (143). This observation led to *in vivo* studies on the role of ER stress in T1D. In 2012, Tersey and colleagues observed increased expression of ER stress markers in islets of prediabetic NOD mice compared to non-diabetic control mice, noting that this stress signature preceded insulinitis (92). Using a mouse  $\beta$ -cell line and primary mouse islets, they also observed that proinflammatory cytokine treatment altered ribosomal occupancy of RNA, consistent with translational repression and ER stress (90). Around the same time, Engin et al., observed that ATF6 and XBP1 expression was deficient in islets from humans with T1D and mouse models of autoimmune diabetes (93). They also showed that treatment of prediabetic mice with a chemical inhibitor of ER stress increased expression of UPR markers, decreased  $\beta$ -cell death and reduced T1D incidence (93). More recently, proinflammatory cytokines have been shown to induce ER stress and cell death in induced pluripotent stem cell-derived  $\beta$ -like cells (152).

Additional evidence for involvement of ER stress in insulin-dependent diabetes comes from individuals with Wolcott-Rallison syndrome. Here, mutations in eukaryotic translation initiation factor 2-alpha kinase 3 (also known as PERK), which plays a major role in remediating ER stress, are linked to insulin-dependent diabetes that occurs neonatally or in early infancy (193). These studies and others indicate a clear importance of maintaining ER homeostasis in  $\beta$ -cell health and the ability for chronic ER stress to induce  $\beta$ -cell death.

#### Other stress-inducers of $\beta$ -cell death

##### Oxidative stress

Studies have shown that  $\beta$  cells are significantly more sensitive to oxidative damage than other cell types, such as liver or kidney cells. The deficiency in antioxidant enzymes like superoxide dismutase (SOD), glutathione peroxidase, and catalase, which are present at about 30% of the levels found in the liver, contributes to this heightened sensitivity <sup>108</sup>.

Various factors contribute to the exposure of  $\beta$  cells to reactive oxygen species (ROS), such as glucose-stimulated insulin secretion (GSIS) and cytokine exposure <sup>109,110</sup>. The production of ROS is a by-product of mitochondrial respiration, essential for ATP synthesis in  $\beta$  cells <sup>111</sup>. High insulin demand can lead to elevated ROS levels, which can cause cell damage and death. Additionally, cytokines like IL1 $\beta$  can induce nitric oxide (NO) production in  $\beta$  cells by upregulating inducible nitric oxide synthase (iNOS), leading to DNA damage and apoptosis <sup>112</sup>.

To mitigate oxidative damage, strategies have been developed to inhibit free radical formation. One such approach involves the inhibition of 12-lipoxygenase (12-LO), an enzyme involved in the oxidation of arachidonic acid to proinflammatory intermediates

<sup>113</sup>. Research has shown that the loss or chemical inhibition of 12-LO can increase the expression of antioxidant enzymes Sod1 and Gpx1, reduce ROS production, and protect  $\beta$  cells from oxidative stress <sup>114</sup>.

### Glucotoxicity and lipotoxicity

The toxic effects of glucose and lipids on  $\beta$  cells, known as glucotoxicity and lipotoxicity respectively, have been researched for decades. When these effects occur simultaneously, the phenomenon is termed glucolipotoxicity. In 1996, Prentki and Corkey suggested that molecules regulating fatty acid synthesis act as fuel sensors in diabetes-relevant tissues <sup>115</sup>. They noted that when excess glucose and lipids are present, a metabolic abnormality called glucolipoxia becomes evident <sup>115</sup>. Despite the importance of this research, the relevance of in vitro lipotoxicity studies to in vivo  $\beta$ -cell dysfunction in diabetes is debated <sup>116</sup>. High glucose levels decrease insulin gene transcription, a condition reversible by culturing in low glucose media. Glucose-associated oxidative stress was found to reduce the expression of transcription factors Pdx1 and MafA, contributing to diminished insulin synthesis. Reducing  $\beta$ -cell insulin demand has been shown to restore insulin content and GSIS <sup>117</sup>.

Early 1990s studies showed that prolonged exposure of rat islets to FFAs reduces insulin synthesis and GSIS while increasing basal insulin release <sup>118</sup>. FFAs also induce  $\beta$ -cell apoptosis through caspase and ceramide-dependent pathways <sup>119</sup>. LDL-induced  $\beta$ -cell death follows cellular uptake and oxidation. Studies found that FFA-induced  $\beta$ -cell death is exacerbated by high glucose levels, implicating oxidative stress <sup>120</sup>. FFA-mediated cell death in rat  $\beta$  cells was shown to involve an NF-kB and NO-independent form of ER stress, while palmitate exposure in a mouse  $\beta$ -cell line indicated ER stress-induced cell

death via changes in Ca<sup>2+</sup> dynamics and increased CHOP expression <sup>121</sup>. Despite clear evidence of FFA-induced  $\beta$ -cell death in vitro, its applicability to in vivo diabetes remains debated.

### **Evidence for established and emerging mechanisms of $\beta$ -cell demise**

#### Apoptosis

Apoptosis is the most well-known and well-characterized form of PCD. It is tightly regulated by cell-intrinsic and -extrinsic signaling mechanisms <sup>122</sup>, and it is required for several physiological processes including development, tumor suppression, and removal of damaged or unwanted cells during normal cellular turnover <sup>123–125</sup>. Apoptotic programs are critically dependent on caspases, a family of cysteine-aspartic proteases that are activated in response to specific stimuli <sup>126</sup>. With respect to apoptosis signaling, caspases can be categorized as initiator caspases (caspase 2, 8, 9, and 10) or executioner caspases (caspase 3, 6 and 7). Upon appropriate stimulation, initiator caspases are activated by autoproteolysis, these initiator caspases activate executioner caspases via proteolysis, and executioner caspases then initiate apoptotic programs via proteolysis of key structural, cell cycle, and signal transduction proteins <sup>127</sup>. Cells undergoing apoptosis exhibit cytoplasmic shrinkage, chromatin condensation, DNA fragmentation, and plasma membrane blebbing <sup>122</sup>. These membrane blebs encompass cellular contents to form apoptotic bodies that are then taken up by phagocytes through efferocytosis; this feature of apoptosis is critical in that it allows apoptotic cells to be removed in a non-inflammatory manner <sup>128</sup>.

There is a great deal of evidence that  $\beta$ -cells undergo apoptosis in response to diabetes-relevant cell death stimuli <sup>129–131</sup>. Studies performed by Yamada et al. in 1999

found that Fas signaling in  $\beta$ -cells results in cell death that is characterized by chromatin condensation, nucleolar disintegration, DNA fragmentation, and annexin V positivity, hallmarks of apoptosis<sup>132</sup>. In 2005, Liadis and colleagues found that caspase 3 deficient mice were protected from hyperglycemia following multiple low dose streptozotocin (STZ) treatment, and this was related to reduced  $\beta$ -cell loss<sup>133</sup>. Similarly, a study utilizing caspase 3 deficient islets or a small molecule caspase 3 inhibitor found that caspase 3 activity mediates amyloid-induced  $\beta$ -cell death<sup>134</sup>. Studies of proinflammatory cytokine-induced  $\beta$ -cell death have also identified apoptosis as a key mediator of  $\beta$ -cell cytotoxicity, with studies finding that a cytokine cocktail (IL1 $\beta$  + IFN $\gamma$  + TNF $\alpha$ ) elicits  $\beta$ -cell death in association with caspase 3 activation<sup>135</sup>, and that suppressor of cytokine signaling-1 (SOCS-1) mediates IL1 $\beta$  + IFN $\gamma$  + TNF $\alpha$ -induced  $\beta$ -cell death in a caspase 3 dependent fashion<sup>136</sup>. In a study of  $\beta$ -cell specific loss of caspase 8, islets were protected from Fas ligand and ceramide-induced cell death *in vitro*, and mice were protected from STZ-induced hyperglycemia *in vivo*<sup>137</sup>. Notably, this study also showed that loss of caspase 8 in  $\beta$ -cells results in elevated rates of islet cell death and glucose intolerance in aged chow-fed mice *in vivo*, indicating distinct roles for  $\beta$ -cell caspase 8 under these conditions<sup>137</sup>.

Apoptosis has also been identified as a key contributor to  $\beta$ -cell demise in the context of islet transplantation<sup>138–140</sup>. For example, treatment of isolated mouse islets with a small molecule pan-caspase inhibitor (zVAD) prior to transplantation combined with 5 days of zVAD treatment after transplant resulted in significantly improved rates of euglycemia following islet transplantation, and the glycemic benefit of zVAD-FMK treatment remained 1 year after islet transplantation<sup>138</sup>. Similarly, Pepper and colleagues

cultured human islets with a pan-caspase inhibitor (F573) for 24 hours prior to transplantation, then administered F573 for 5 days post-transplantation in immunodeficient mice. This approach resulted in improved blood glucose during an intraperitoneal glucose tolerance test (IPGTT) for up to 100 days post-transplant and was accompanied by preservation of  $\beta$ -cell mass and viability<sup>140</sup>. Other studies using small molecule caspase inhibitors to protect transplanted islets have observed similar results<sup>141,142</sup>. In addition, several studies found that blockade of IL1 $\beta$  and TNF $\alpha$ , classical apoptotic stimuli, significantly improves islet transplant outcomes<sup>143–145</sup>.

These and other studies demonstrate that  $\beta$ -cells undergo apoptosis in response to diabetes-relevant cell death stimuli.

### Necrosis

$\beta$ -cells are also susceptible to non-apoptotic forms of cell death such as necrosis<sup>146,147</sup>. Necrosis was first described by Rudolf Virchow in 1858 and is considered distinct from mechanisms of regulated cell death or PCD<sup>148</sup>. Necrosis is typically understood as a form of unprogrammed or accidental cell death that results from cellular damage, infection, or trauma<sup>149</sup>. In contrast to apoptosis, necrosis is characterized by lytic loss of membrane integrity that leads to unregulated release of cell contents<sup>148,149</sup>. Given that these cell contents are not packaged in apoptotic bodies or membrane blebs, this release of cell contents is inflammatory in nature<sup>150,151</sup>. Thus, necrosis can be characterized by the release of cellular factors such as high mobility group box 1 (HMGB1), a nuclear-localized protein that is normally associated with chromatin<sup>152</sup>. In addition, morphological hallmarks of necrotic cell death such as karyolysis, karyorrhexis and pyknosis, all of which relate to altered morphology of nuclear DNA within the dying cell

body, can be used to identify necrotic cells <sup>153</sup>. Such changes are not observed in apoptosis, where proteases and nucleases break down nuclear contents into apoptotic bodies <sup>153</sup>.

Several studies have found that necrosis contributes to  $\beta$ -cell loss in diabetes. Notably, studies from Fehsel et al. examined STZ-treated mouse islets *in vitro* and prediabetic diabetes-prone BB rat pancreas sections *ex vivo* using electron microscopy, quantification of DNA damage, and annexin V staining <sup>146</sup>. These studies identified only a small number of cells expressing markers of apoptosis, but  $\beta$  cells with characteristics of necrosis were significantly more abundant <sup>146</sup>. When evaluating mechanisms of IL1 $\beta$ -mediated cell death in rat  $\beta$  cells, Steer and colleagues found evidence of necrosis including loss of viability, a lack of caspase 3 activity, annexin V positivity, and robust HMGB1 release, whereas the apoptosis inducer camptothecin strongly induced caspase 3 activity and annexin V positivity, but not HMGB1 release <sup>110</sup>. In addition, two studies using a rat  $\beta$ -cell line and rat islets found that IL1 $\beta$  + IFN $\gamma$ -induced  $\beta$ -cell cytotoxicity was not associated with increased caspase 3 activity or annexin V positivity <sup>154,155</sup>. Similarly, TNF $\alpha$  + IFN $\gamma$  treatment was observed to induce mouse islet cell death in a caspase 3-independent manner <sup>156</sup>, and IFN $\gamma$  + synthetic double stranded RNA (poly I:C) induces NO-dependent necrosis of rat islet cells <sup>157</sup>. Necrosis has also been identified as a mediator of  $\beta$ -cell cytotoxicity in islet transplantation, with studies observing characteristics of islet cell necrosis such as pyknotic nuclei and HMGB1 release following islet graft failure <sup>158-160</sup>.

Together, these studies provide evidence that  $\beta$  cells undergo necrosis in response to diabetogenic cell death stimuli.

## Necroptosis

Although necrosis has traditionally been viewed as an unregulated, accidental form of cell death, many of the studies described above identified programmed  $\beta$ -cell death that is morphologically consistent with necrosis. How might this occur when all mechanisms of PCD have customarily been considered apoptosis<sup>122,161</sup>? An explanation has surfaced from studies that identified and characterized mechanisms of regulated necrosis which occur downstream of programmed signaling events, are distinct from apoptosis, and constitute novel forms of PCD<sup>162–165</sup>. These discoveries have been aided by improved definitions of distinct cell death signaling pathways<sup>166</sup> and have led to renewed interest in understanding molecular mechanisms of PCD and their roles in human disease, including diabetes<sup>167–170</sup>. We propose that novel mechanisms of PCD such as necroptosis, ferroptosis, and pyroptosis may contribute to T1D pathogenesis, not only as end-stage mechanisms of  $\beta$ -cell loss, but potentially as early-stage mechanisms of islet inflammation and  $\beta$ -cell autoimmunity.

Necroptosis is a regulated form of necrotic cell death that is mediated by receptor interacting protein kinase 1 (RIPK1), receptor interacting protein kinase 3 (RIPK3), and mixed lineage kinase domain like pseudokinase (MLKL)<sup>164</sup> (Figure 2). Necroptosis was first identified as a form of cell death that occurs downstream of tumor necrosis factor receptor 1 (TNFR1) signaling when caspase activity is inhibited<sup>171,172</sup>, and the pathway is most well-defined in this context. In canonical necroptosis signaling, TNF $\alpha$  binds to TNFR1 and molecules including TNFR-associated death domain (TRADD), TNFR-associated factor 2 (TRAF2), cellular inhibitors of apoptosis proteins (cIAP1/2), linear ubiquitin chain assembly complex (LUBAC) and RIPK1 are recruited to form complex I

<sup>173</sup>. RIPK1 undergoes extensive ubiquitination and deubiquitination in complex I, and this process regulates its pro-survival and pro-death functions <sup>163,174,175</sup>. In its pro-survival role, linear ubiquitination of RIPK1 in complex I is crucial for NF-κB activation, leading to the upregulation of pro-survival gene expression <sup>162,176</sup>. Deubiquitination of RIPK1 facilitates the formation of complex II with caspase-8 and Fas-associated death domain (FADD)<sup>175</sup>. When caspases are active, caspase 8 in complex IIa or IIb inactivates RIPK1<sup>177</sup> and RIPK3<sup>178</sup>, eliciting caspase 3/7 activation and apoptosis<sup>175</sup>. When caspases are inactive, however, complex IIc, (the necrosome) forms via phosphorylation and interaction of RIPK1 and RIPK3, leading to the recruitment and phosphorylation of MLKL, the terminal effector of necroptosis<sup>179,180</sup>. This RIPK1-RIPK3-MLKL phosphorylation cascade leads to a conformational change in MLKL that exposes its four helix bundle domain and leads to its oligomerization, membrane translocation, and loss of cell membrane integrity<sup>181</sup>. Although the precise mechanisms of necroptosis execution downstream of MLKL oligomerization are not fully established, membrane-localized MLKL pore formation results in cell swelling and lysis<sup>180</sup>. This lysis releases cell contents including danger-associated molecular patterns (DAMPs) and pathogen-associated molecular patterns (PAMPs) that promote inflammation and immune responses<sup>182,183</sup>. In addition to TNFR1, several other receptors including interferon gamma receptor (IFNGR), toll-like receptors (TLRs), Fas receptor, and TNF-related apoptosis-inducing ligand receptor (TRAILR) have been implicated in necroptosis signaling and are thought to converge at the level of necrosome formation<sup>162,164,184-186</sup>. Stimuli known to induce necroptosis have previously been observed to elicit caspase-independent β-cell death. For example, TNFα + IFNγ<sup>156</sup>, IL1β + IFNγ<sup>154,155</sup>, and IFNγ +

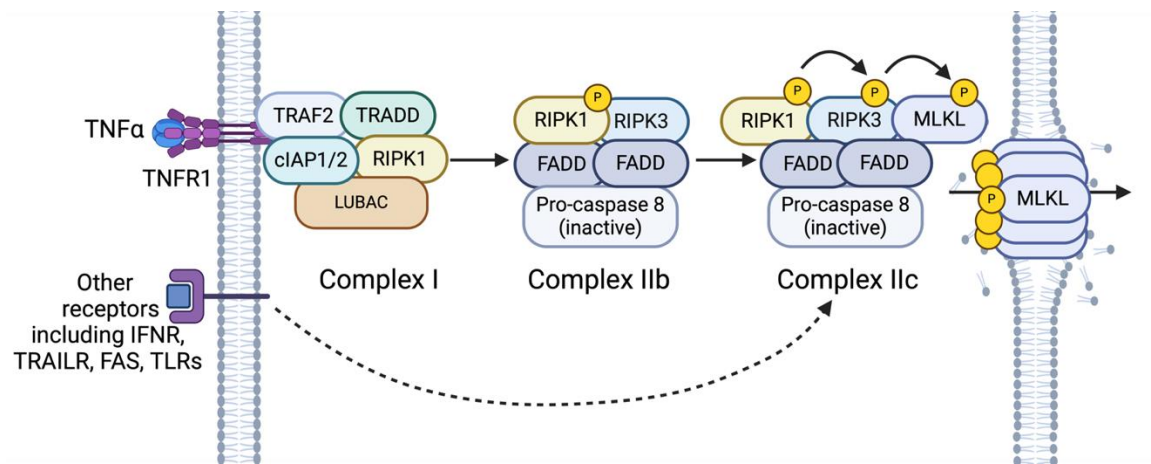


**Figure 2: Basic mechanism of necroptosis signaling.**

Binding of TNF $\alpha$  to TNFR1 initiates recruitment of TRAF2, TRADD, RIPK1, cIAP1/2, and LUBAC to form complex I at the receptor. Under appropriate stimulation, RIPK1 associates with pro-caspase 8, FADD and RIPK3 to form complex IIb. When pro-caspase 8 is inactive, RIPK1 activates RIPK3 via phosphorylation, and activated RIPK3 recruits and phosphorylates MLKL in complex IIc (the necrosome). Phosphorylation of MLKL leads to its conformational change, oligomer formation, membrane translocation and disruption of membrane integrity, resulting in cell lysis. Other receptors including IFNR, TRAILR, FAS and TLRs have also been found to contribute to necrosome formation and necroptosis.

double-stranded RNA <sup>157</sup> have been found to induce  $\beta$ -cell death with necrotic morphology in the absence of caspase activation, consistent with regulated necrosis. Although these studies did not examine whether such mechanisms of  $\beta$ -cell death are biochemically consistent with necroptosis, they provide early evidence that diabetes-relevant stimuli can trigger programmed  $\beta$ -cell death distinct from caspase-mediated apoptosis.

RIPK1 is a key upstream regulator of necroptosis. It is a multifunctional protein with an N-terminal kinase domain, a C-terminal death domain, and a receptor interacting protein (RIP) homotypic interaction motif (RHIM) that mediates interactions with RIPK3 and other RHIM-containing molecules <sup>187</sup>. Human Pancreas Analysis Program (HPAP) data indicates that *Ripk1* gene expression is increased 2.7 fold in  $\beta$  cells from individuals with T1D compared to those without diabetes <sup>188</sup>, and several studies have investigated the role of RIPK1 kinase function in  $\beta$ -cell cytotoxicity using small molecule RIPK1 kinase inhibitors. One study evaluated the effects of necrostatin-1 (Nec-1) on human islets cultured in low-nutrient and low-oxygen conditions, finding that Nec-1 treatment reduced dsDNA and uric acid release from human islets, indicative of decreased lytic cell death <sup>189</sup>. Another study in rodent  $\beta$ -cell lines and mouse islets found that inhibition of RIPK1 kinase function with Nec-1 protects from NO donor-induced  $\beta$ -cell cytotoxicity *in vitro* <sup>190</sup>. In a study of young porcine islets, Nec-1 was found to improve islet viability in response to NO or hypoxia in a dose dependent manner *in vitro* <sup>191</sup> and another recent study found that Nec-1 treatment prevented  $\beta$ -cell loss in a zebrafish model of overnutrition and insulin resistance <sup>169</sup>. In the contrary, mice harboring a *Ripk1*<sup>S25D/S25D</sup> mutation that mimics inhibitory phosphorylation of RIPK1 were not protected mice from

hyperglycemia following STZ or HFD<sup>192</sup>. Considering that RIPK1 has several inhibitory and activating phosphorylation sites as well as actions in multiple tissues<sup>187</sup>, studies evaluating Ripk1 kinase dead (Ripk1<sup>D138N/D138N</sup>) or Ripk1 tissue specific knockout (Ripk1<sup>flox/flox</sup>) mice may shed additional light on the role of RIPK1 kinase activity in diabetogenic  $\beta$ -cell decline *in vivo*.

RIPK3 is a major downstream phosphorylation target of RIPK1 that is known to promote inflammation and cell death signaling in non-islet cell types<sup>193–195</sup>. In comparison to RIPK1, RIPK3 retains an N-terminal kinase domain and a RIP homotypic interaction motif (RHIM) but does not contain a death domain<sup>196</sup>. HPAP data indicates that Ripk3 gene expression is increased 2.2 fold in  $\beta$ -cells from individuals with T1D compared to those without<sup>188</sup>, and recent studies have begun to decipher the roles of RIPK3 in  $\beta$ -cell inflammation and cell death signaling.

RIPK3 also promotes inflammation in a cell death-independent manner in non-islet cell types<sup>195</sup>, and a recent study found that RIPK3 contributes to inflammation in zebrafish, mouse and human  $\beta$  cells<sup>169</sup>. This work found that endoplasmic reticulum (ER) stress activates RIPK3 to elicit NF- $\kappa$ B-mediated proinflammatory gene expression in cultured  $\beta$  cells, and that RIPK3 kinase inhibition protects mouse islets from palmitate-induced  $\beta$ -cell dysfunction *in vitro*<sup>169</sup>. Islet inflammation,  $\beta$ -cell dysfunction, and  $\beta$ -cell loss were found to occur in a RIPK3-dependent manner in a zebrafish model of  $\beta$ -cell cytotoxicity, and human islets grafted in hyperglycemic mice underwent a marked increase in RIPK3 and NF- $\kappa$ B activation that was accompanied by increased islet macrophage infiltration<sup>169</sup>. Although further investigation is needed to clarify the

specific roles of RIPK3 in islet inflammation and  $\beta$ -cell death, therapies targeting RIPK3 could protect  $\beta$  cells from diabetes-relevant cytotoxic stimuli.

Necroptosis has also been identified as a mediator of graft failure following transplantation, including in the setting of heart, kidney, and lung transplant<sup>197-199</sup>. In a study of islet transplantation, porcine islets treated with the RIPK1 kinase inhibitor Nec-1 were found to exhibit increased insulin content and insulin secretion following glucose stimulation *in vitro*, and treatment of islets with Nec-1 prior to transplantation in diabetic athymic mice resulted in shorter times to normoglycemia and higher plasma insulin levels *in vivo*<sup>200</sup>. In contrast, a study evaluating transplantation of RIPK3 deficient mouse islets found them to be normally susceptible to CD4+ T cell-mediated destruction *in vivo*<sup>201</sup>. Additional studies are warranted to understand the role of necroptosis in islet graft failure.

My studies in the following sections of this thesis investigate the roles of RIPK1 and RIPK3 in regulating  $\beta$ -cell fate.

#### Other emerging mechanisms of $\beta$ -cell demise

While my research primarily explores the role of necroptosis signaling molecules in  $\beta$ -cell cytotoxicity, recent studies suggest that other forms of PCD, such as ferroptosis and pyroptosis, may also contribute to  $\beta$ -cell loss. Below, I provide an overview of these PCD forms and their relevance to  $\beta$  cells.

#### Ferroptosis

Ferroptosis is a non-apoptotic form of PCD characterized by iron-dependent lipid peroxidation, leading to cell death with intact nucleus, reduced mitochondrial volume, increased lipid bilayer membrane density and membrane rupture<sup>202</sup>. Identified in 2012,

ferroptosis results from the inhibition of cystine import, leading to decreased glutathione (GSH) levels and reduced activity of glutathione peroxidase 4 (GPX4), which normally scavenges lipid peroxides<sup>203,204</sup>. This process generates reactive oxygen species (ROS) that damages cell membranes<sup>170</sup>.

Recent studies suggest ferroptosis plays a role in  $\beta$ -cell death, relevant to diabetes.  $\beta$  cells naturally have a low antioxidant defense, making them susceptible to oxidative stress<sup>205,206</sup>. Experiments show that human islets treated with ferroptosis inducers like erastin exhibit impaired insulin secretion and cell viability<sup>170</sup>, whereas treatment with ferroptosis inhibitors like ferrostatin-1 (Fer-1) can mitigate these effects. Investigations into ferroptosis inducers, such as high glucose and proinflammatory cytokines, reveal increased ROS, lipid peroxidation and iron levels, alongside decreased GPX4 expression in  $\beta$  cells. Notably, Fer-1 can rescue  $\beta$  cells from certain stress-induced deaths but not those caused by cytokines<sup>207</sup>. Iron homeostasis is crucial in ferroptosis, with transferrin transporting iron, which, if unregulated, leads to harmful reactions producing hydroxyl radicals<sup>202</sup>. Studies in mice show that excess iron correlates with  $\beta$ -cell damage and reduced insulin expression<sup>208</sup>. Iron chelation with agents like desferrioxamine (DFO) has shown potential in protecting  $\beta$ -cell function and enhancing islet transplantation outcomes<sup>209</sup>. Although the susceptibility of  $\beta$  cells to ferroptosis is clear, its role in diabetes pathogenesis requires further research.

### Pyroptosis

Pyroptosis is an inflammatory form of PCD that occurs in response to infections, triggering immune responses<sup>210</sup>. The process is primarily driven by gasdermin D (GSDMD), a protein with a pore-forming N-terminal domain<sup>211</sup>. Upon activation by

inflammatory caspases GSDMD is cleaved, releasing the N-terminal fragment that forms pores in the cell membrane<sup>212-214</sup>. The pyroptosis pathway begins with the recognition of pathogen-associated molecular patterns (PAMPs) and damage-associated molecular patterns (DAMPs) by pattern-recognition receptors such as TLRs. This activation leads to the upregulation of components like NLRP3 inflammasome, which plays a critical role in the maturation and release of pro-inflammatory cytokines<sup>215</sup>. Caspase 1, also known as IL1 $\beta$  converting enzyme, is essential for this process, as it facilitates the cleavage of GSDMD<sup>216</sup>. Research has shown that pyroptosis is distinct from apoptosis, although both involve DNA damage and chromatin condensation<sup>210</sup>. Pyroptosis uniquely features cell lysis, membrane rupture and an inflammatory response<sup>217,218</sup>.

Recent studies have explored the role of pyroptosis in  $\beta$ -cell death. HPAP data suggest that GSDMD expression is 2.2 fold increased in  $\beta$  cells from individuals with T1D<sup>188</sup>. Additionally, inflammatory cytokines have been found to upregulate GSDMD in  $\beta$  cells, leading to increased cell death<sup>219</sup>. Certain molecules have shown potential in modulating pyroptosis-related pathways in  $\beta$  cells. For example, the microRNA miR-17-5p has been observed to improve glucose homeostasis and reduce markers of pyroptosis in C57B/L6 mice subjected to HFD and STZ *in vivo*<sup>220</sup>. Similarly, irisin, a hormone linked to exercise benefits, has been found to decrease pyroptosis markers, providing protective effects against cell death<sup>221</sup>. Moreover, natural compounds such as salidroside and emodin<sup>222,223</sup>, as well as sodium/glucose cotransporter 2 inhibitor (SGLT2i) empagliflozin, have demonstrated the ability to lower GSDMD and inflammasome expression, suggesting potential therapeutic avenues for protecting  $\beta$  cells from pyroptosis-induced damage<sup>224</sup>. Overall, understanding the mechanisms of pyroptosis in  $\beta$

cells is crucial for developing new therapeutic strategies for diabetes. Continued research in physiologically relevant models will help clarify the role of pyroptosis in  $\beta$ -cell loss and diabetes progression.

### **Summary**

Interest in understanding and targeting the mechanisms of  $\beta$ -cell death to combat diabetes comes from extensive research linking  $\beta$ -cell cytotoxicity to insulin insufficiency and hyperglycemia. Although reduced insulin-producing  $\beta$  cells were noted as early as the 1950s, it wasn't until decades later that this was connected to increased  $\beta$ -cell death. Techniques developed in the 1990s, such as TUNEL, annexin V staining, and propidium iodide staining allowed for detection and quantification of dead cells in pancreatic tissues<sup>20,88</sup>. While these studies highlight the link between increased  $\beta$ -cell death,  $\beta$ -cell loss and insulin insufficiency, they also raised questions about the role of  $\beta$ -cell death in the disease pathogenesis. Evaluating  $\beta$ -cell death requires considering that pancreas samples are often donated long after diagnosis of disease, which leads to possible underestimation of the rate of cell death during active  $\beta$ -cell demise. The loss of  $\beta$  cells likely starts years before clinical symptoms appear. At diagnosis,  $\beta$ -cell loss may obscure ongoing cell death, and remaining  $\beta$  cells might be more resistant to cytotoxic damage. Therefore, understanding the role of  $\beta$ -cell death requires capturing the active period of cell demise and how this death affects  $\beta$ -cell mass over time.

Furthermore, while one may assume that a cell death stimulus elicits a single mode of cell death, evidence indicate that cell death responses are heterogeneous within a cell population. In various studies, glutamate induced early necrosis in neurons followed by

apoptosis, while acetaminophen overdose in mouse hepatocytes showed features of both necrosis and apoptosis<sup>225</sup>. Tanshinone IIA, a natural product of *Salvia miltiorrhiza*, was found to simultaneously elicit apoptosis and necroptosis in HepG2 cells, and this apoptosis could be converted to necroptosis via treatment with a small molecule pan caspase inhibitor<sup>226</sup>. Preedy and colleagues recently observed heterogeneity in TNF $\alpha$ /TNFR1 signaling within a population of mouse fibroblasts, leading them to advocate for the use of novel live-cell imaging techniques to understand cell fate at the level of single cells<sup>227</sup>. Such heterogeneity in cell death responses may be influenced by different transcriptional or mitochondrial states of single cells at the time of exposure to a cell death stimulus.

Heterogeneity of cell death responses has also been observed in  $\beta$  cells. For example,  $\beta$ -cells isolated from Wistar rats were found to undergo both necrosis and apoptosis following oleate and palmitate treatment, as determined by neutral red and PI staining<sup>228</sup>. Saldeen and colleagues showed that treatment with IL1 $\beta$ , IFN $\gamma$ , and TNF $\alpha$  increased both necrosis (17% of cells) and apoptosis (5% of cells) in isolated rat islets via a Bcl-2-inhibitable pathway<sup>229</sup>. Moreover, IFN $\gamma$  and double stranded RNA (Poly I:C) treatment was found to stimulate a five-fold increase in necrosis and a seven-fold increase in apoptosis after 48 hours in Sprague-Dawley rat islets, as determined by acridine orange and ethidium bromide staining<sup>157</sup>. Although transcriptional and functional heterogeneity within  $\beta$ -cell populations is well recognized, these findings indicate that heterogeneity in the context of  $\beta$ -cell death deserves further consideration.

The **primary goal** of the studies in this thesis is to better understand the mechanisms of  $\beta$ -cell demise. We believe that understanding  $\beta$ -cell death pathways is crucial for both

our basic understanding of  $\beta$ -cell biology and for identifying novel targets to prevent or cure diabetes. Receptor interacting protein kinases (RIPKs) are being considered crucial mediators of cell death and inflammation, with potential as therapeutic targets for several human diseases, including osteoarthritis, chronic kidney disease (CKD), and Alzheimer's disease. However, the role of RIPKs in diabetogenic  $\beta$ -cell loss and islet inflammation has not yet been extensively investigated. Therefore, I aimed to explore the role of RIPKs (RIPK1 and RIPK3), which recent research has shown to mediate cell death in concert with caspase activation and to be involved in kinase signaling and gene regulatory effects in non-islet cell types. I focus on RIPK1- and RIPK3-mediated  $\beta$ -cell cytotoxicity and islet inflammation, downstream of known inducers of  $\beta$ -cell stress, including proinflammatory cytokines, endoplasmic reticulum (ER) stress, and islet amyloid deposition. I hypothesize that RIPK1 and RIPK3 are key components of  $\beta$ -cell stress responses and islet inflammation, thus playing crucial roles in mediating diabetes pathogenesis.

For the first time, I employ techniques like live cell imaging and analysis to monitor cell death, caspase 3/7 activation, and amyloid deposition in real-time. I combine this novel technique with the use of small molecule inhibitors, unique mouse models, and CRISPR gene-edited  $\beta$ -cell lines to investigate the role of RIPK1 and RIPK3 in  $\beta$ -cell demise *in vitro*. Additionally, I examine transcriptional and post-translational changes related to  $\beta$ -cell cytotoxicity influenced by the modulation of RIPK1 and RIPK3. Furthermore, I characterize glucose homeostasis in these mouse models to monitor the diabetic phenotype *in vivo*.

## Chapter 2 – Experimental Procedures

### Materials and Methods

#### A. Animals and islet isolations

Mice used for the studies were maintained with ad libitum access to food and water under protocols approved by the Indiana University Institutional Animal Care and Use Committee. Whole body *Ripk3* mutant mice ((*Ripk3*<sup>-/-</sup>, 025738, Jax, Bar Harbor, ME) were maintained as heterozygotes on a C57BL/6J;DBA/2J background with wild type littermates used as controls. The *Ripk3*<sup>-/-</sup> mice used in these studies have an ENU-induced mutation in the donor splice site of intron 2 of the *Ripk3* gene that results in retention of intron 2 and introduction of an in-frame stop codon in the *Ripk3* RNA message. Heterozygous RIPK1 kinase dead mice (*Ripk1*<sup>D138N/+</sup>) on a C57BL/6J background were previously obtained from Dr. Michelle Kelliher at the University of Massachusetts. *Ripk1*<sup>D138N/+</sup> mice are bred to obtain littermate *Ripk1*<sup>+/+</sup> and *Ripk1*<sup>D138N/D138N</sup> mice needed for studies. Akita mice on C57BL/6J background (C57BL/6-*Ins2*<sup>Akita</sup>/J, 003548, Jax, Bar Harbour, ME) were obtained from The Jackson Laboratory and bred with *Ripk1*<sup>D138N/+</sup> mice to obtain Akita mice with RIPK1 kinase dead mutation and littermate controls. Mice carrying the hIAPP transgene were previously generated at the University of Washington<sup>230</sup>. Hemizygous hIAPP mice (*hIAPP*<sup>+0</sup>) that express hIAPP under control of the rat insulin II promoter and were maintained on a C57BL/6 x DBA/2J background. Whole body *Ripk3* null mice and DBA/2J mice (000671, Jax) were obtained from Jackson Laboratories and backcrossed to obtain *Ripk3*<sup>-/-</sup> mice on a C57BL/6 x DBA/2J background. *Ripk3*<sup>-/-</sup> mice on a C57BL/6 x DBA/2J background were bred with hIAPP mice to obtain hIAPP;*Ripk3*<sup>+/-</sup> mice on a

C57BL/6 x DBA/2J background. hIAPP;Ripk3<sup>+/-</sup> mice were then crossed with Ripk3<sup>+/-</sup> mice to generate hIAPP;Ripk3<sup>-/-</sup> mice and littermate controls for use in studies. For high fat diet (HFD) studies, 8-10 weeks male mice were fed a 45% kcal from fat HFD (D12451, Research Diets, New Brunswick, NJ) for the 12-month HFD study period.

Islets were isolated from 8–12-week-old male and female mice by the Indiana University Center for Diabetes and Metabolic Diseases Islet and Physiology Core (IU CDMD), hand-picked, and allowed to recover overnight in RPMI 1640 media with 11.1 mM glucose, 10% fetal bovine serum (FBS), 1% sodium pyruvate and 1% penicillin-streptomycin prior to experimentation.

#### B. Cell line and islet culture

INS-1 832/13 cells were obtained from the IU CDMD and the University of Washington Diabetes Research Center Metabolic and Cellular Phenotyping Core (UW DRC). NIT-1 cells were obtained from Dr. Erica Cai (Indiana Biosciences Research Institute). NIH-3T3 cells were obtained from Dr. Michael Kalwat (Indiana Biosciences Research Institute). NIT-1 2055 (CRL-2055, ATCC) cells were obtained from ATCC. INS-1 and islet cells were cultured in 11.1 mM glucose RPMI 1640 media while all NIT-1 and NIH-3T3 cells were cultured in 25mM DMEM plus 10% FBS, 1% sodium pyruvate and 1% penicillin-streptomycin in a 37°C incubator with 5% CO<sub>2</sub>. RIPK3 overexpressing INS-1 cell lines were generated via transfection with empty pcDNA3 or pcDNA3 expressing mouse Ripk3 (pcDNA3-mRIPK3), followed by selection with G418 (10131027, ThermoFisher). Ripk1-deficient NIT-1 cells (NIT-1 RIPK1Δ) were generated as previously described<sup>231</sup> using guide RNAs (gRNAs) targeting exons 2-3 of the Ripk1 gene (5'-GAGAAGACAGACCTAGACAG-3' and 5'-CCAAATGGTCTGATAGATAT-

3'). Ripk3-deficient NIT-1 cells (NIT-1 RIPK3 $\Delta$ ) were generated using gRNAs targeting exon 6 of the Ripk3 gene (5'-ATGTTATCCCCCAACTCCAG-3' and 5'-GGAGTCTCAGGGCTACCTGG-3'). Non-targeting control gRNA (5'-TAAAAACGCTGGCGGCCTAG-3') was used to generate NIT-1 control cells (NIT-1 CTL). Briefly, lenti-multi-CRISPR plasmid (85402, Addgene, Watertown, MA) was used to express gRNA cassettes, followed by cloning into lentiCRISPR v2 vector (52961, Addgene). Lentivirus containing non-targeting, Ripk1 or Ripk3 gRNA was used to establish NIT-1 CTL, RIPK1 $\Delta$  and RIPK3 $\Delta$  cell lines, respectively. Editing of *Ripk1* or *Ripk3* was verified by PCR of genomic DNA. Mouse islet cells were dispersed in trypsin-EDTA (0.25%, ThermoFisher, Waltham, MA) for 30 minutes at 37°C, collected by centrifugation, resuspended in culture media, plated, and allowed to recover prior to analysis. The following reagents were used during cell culture treatment: zVAD-fmk (50  $\mu$ M, G7232, Promega, Madison, WI), TNF $\alpha$  (40 ng/ml, mouse: CYT-252, Prospec, Rehovot, Israel), IFN $\gamma$  (100ng/ml, mouse CYT358, Prospec, Rehovot, Israel), BV6 (5  $\mu$ M, HY-16701, MedChemExpress, Monmouth Junction, NJ), GSK'872 (5  $\mu$ M, HY-101872, MedChemExpress).

Bone marrow derived macrophages cells were cultured in MEM media (10-010, Corning), 10% FBS, 1% penicillin-streptomycin, 10 ng/ml M-CSF1 (416-ML, R&D Systems, Minneapolis, MN). Briefly, femur and tibia were isolated, washed in 70% ethanol, then placed in HBSS + 2% FBS (isolation buffer). Bone marrow was flushed into a petri dish containing isolation buffer, the cell suspension was filtered through a 40 mm cell strainer, and cells were counted. Media was changed on day 3 after plating and every 2 days thereafter. Cells obtained on day 7 were used as BMDMs, with BMDMs

obtained from one mouse considered a single replicate. Cells and islets were maintained in a 37°C incubator with 5% CO<sub>2</sub>. The following reagents were applied to BMDM cultures: synthetic hIAPP (20 mM, AS-60254-1, Anaspec, Fremont, CA), synthetic rIAPP (20 mM, AS-60253-1, Anaspec). For islet macrophage depletion, islets were isolated from 8- to 12-week-old male and female mice, cultured in 11.1 mM glucose RPMI, then treated with either 1 mg/ml clodronate-containing liposomes (C-0010, Liposoma, Amsterdam, Netherlands) or 1 mg/ml PBS-containing liposomes (P-010, Liposoma) for 48 h.

#### C. Caspase activity and DNA laddering assays

Caspase activity assays were conducted on NIT-1 cells, INS-1 cells, or dispersed mouse islet cells. Cells were cultured in 96-well plates and treated for the indicated times, then a luminogenic caspase substrate specific for caspase 3 and caspase 7 (G8090, Promega, Madison, WI) was added for 1 hour and luminescence was quantified using a microplate reader (BioTek Synergy H1, Agilent, Santa Clara, CA). DNA laddering assays were conducted on NIT-1 CTL cells following culture in 6-well plates and treatment for the indicated times as previously described<sup>232</sup>. Briefly, cells were lysed and proteins were removed using phenol-chloroform-isoamyl alcohol, then genomic DNA was precipitated from solution with isopropanol, spun at 14k g for 10 min, then resuspended in water. 4 µg of DNA per condition was loaded on 1.5% agarose gels and visualized using ethidium bromide.

#### D. Real-time islet amyloid formation, cell death and caspase 3/7 activity assays

Islet amyloid formation and cell death were quantified in real time using a Sartorius Incucyte S3 live-cell imaging and analysis instrument (Sartorius, Göttingen, Germany).

To quantify amyloid formation, single intact islets were added to each well of a 96-well round-bottom plate (7007, Corning, Corning, NY) containing 16.7 mM glucose and Thioflavin S (5 nM, T1892, MilliporeSigma, Burlington, MA). Amyloid deposition was quantified every 2 hours for 96 h and reported as Thio S positive area normalized to islet brightfield area for each condition and replicate. To quantify cell death, single intact islets were added to each well of a 96-well round-bottom plate (7007, Corning) containing 16.7 mM glucose and Sytox green (100 nM, S7020, ThermoFisher Scientific, Waltham, MA). Cell death was quantified every 2 h for 96 h and reported as Sytox green positive area normalized to islet brightfield area for each condition and replicate. To quantify islet caspase 3/7 activity in real time, single intact islets were added to each well of a 96-well round-bottom plate (7007, Corning) containing 16.7 mM glucose and Incucyte Caspase 3/7 dye (5 mM, 4440, Sartorius). Caspase 3/7 activity was quantified every 2 hours for 96 h and reported as caspase 3/7 positive area normalized to islet brightfield area for each condition and replicate. Alternatively, caspase 3/7 activity was quantified using a luminogenic caspase 3/7 substrate (G8090, Promega, Madison, WI). Briefly, following culture islets were lysed, caspase 3/7 substrate was added for 1 h, then luminescence was quantified using a microplate reader (BioTek Synergy H1, Agilent, Santa Clara, CA) and data were reported relative to control islets for each replicate.

#### E. Quantitative real-time reverse transcription polymerase chain reaction (qRT-PCR)

Total RNA was recovered from NIT-1 cells, INS-1 cells or islets using the RNeasy Mini Kit (74104, Qiagen, Roche, Basel, Switzerland), reverse transcribed with the QuantiTect Reverse Transcription Kit (205411, Qiagen) and subjected to qRT-PCR. Data were normalized to *18S* rRNA levels and expressed as  $\Delta$ CT of the gene of interest. All qRT-

PCR data points represent means of triplicate technical determinations. The following Taqman probes (ThermoFisher Scientific, Waltham, MA) were used to quantify mRNA expression: *Tnfrsf1a* (rat: Rn01492348\_m1; mouse: Mm Mm00441883\_g1); *Ripk1* (rat: Rn01757369\_m1; mouse: Mm00436354\_m1); *Casp8* (rat: For: 5'CCTCTGACCTCCGGTGTTTTA-3', Rev: 5'-ATGTGGTCCAAGCACAGGAA-3', SYBR green chemistry; mouse: Mm00802247\_m1); *Ripk3* (Mm00444947\_m1); *Mkl1* (rat: Rn01432489\_m1, mouse: Mm01244222\_m1); and *18S* rRNA (HS99999901\_s1), *Emr1* (Mm00802529\_m1), *Tnf* (Mm00443258\_m1), *Il1b* (Mm00434228\_m1), *Nos2* (Mm00440502\_m1), *Ppib* (Mm00478295\_m1) ); and *18S* rRNA (HS99999901\_s1).

#### F. Immunoblot analysis

Islet cell lysates were prepared in lysis buffer containing 1% SDS, 0.1% NP-40, 0.2% sarkosyl, 10% glycerol, 1 mM dithiothreitol, 1 mM EDTA, 10 mM NaF, 50 mM Tris, and protease and phosphatase inhibitors (04693116001 and 0490683700; MilliporeSigma). BMDM cell lysates were prepared in lysis buffer containing 0.2% Triton X-100, 10 mM EDTA, 2 mM EGTA, 10 mM NaF, 50 mM Tris, and protease and phosphatase inhibitors (04693116001 and 0490683700; MilliporeSigma). Cell lysates were centrifuged at 10,000 x g for 10 minutes, supernatants collected, and protein concentrations determined by BCA assay (23227, ThermoFisher Scientific). Equal amounts of protein were separated on SDS-PAGE gels (4561093, BioRad, Hercules, CA) and transferred to PVDF membranes (IPVH00010, MilliporeSigma). Proteins were visualized using the following primary antibodies: RIPK3 (1:1000, ab62344, Abcam, Cambridge, UK), phospho-MLKL (1:500, ab196436, Abcam),  $\beta$ -ACTIN (1:2000, ab8226, Abcam). Primary antibodies were detected with goat anti-mouse 800 (1:5000,

926-32210, LI-COR) or donkey anti-rabbit 680 (1:5000, 926-68071, LI-COR) IRDye secondary antibodies (LI-COR, Lincoln, NE), and visualized with a LI-COR CLx imaging system. Representative immunoblot images are shown.

#### G. RNAseq analysis

RNAseq was performed at the Indiana University School of Medicine Center for Medical Genomics as described previously<sup>233</sup>. Briefly, RNA was isolated from INS-1 cells with the RNeasy Mini Kit (74104, Qiagen), then used to prepare cDNA libraries with the KAPA mRNA HyperPrep kit (08098093702, Roche, Indianapolis, IN). Libraries were sequenced with a 100 bp paired-end configuration using a NovaSeq 6000 Sequencing System (Illumina, San Diego, CA). Sequence reads were mapped to the reference genome using the STAR (Spliced Transcripts Alignment to a Reference) RNAseq aligner<sup>234</sup>. Differential gene expression analysis was performed with edgeR<sup>235</sup>. Statistical information is described below.

#### H. Immunoprecipitation

INS-1 cells overexpressing RIPK3 were grown in T75 flasks, treated with TNF $\alpha$ +zVAD for 24 hours, and lysed in buffer containing 20mM Tris HCl, 137mM NaCl, 1% Nonidet P-40 (NP-40) and 2mM EDTA. Protein concentrations from each sample were determined by Bradford assay (5000201, BioRad) and 2.5% of the protein lysate was saved as input. Protein A/G coupled Sepharose beads (ab193262, Abcam) were washed with lysis buffer, then equal amounts of protein were incubated with protein A/G beads and either anti-IgG (ab124055, Abcam), anti-RIPK3 (ab62344, Abcam) or anti-MLKL (ab243142, Abcam) primary antibodies overnight at 4°C with shaking. Protein complexes

were collected by centrifugation at 8000 x g for 3 minutes at 4°C, washed, and subjected to immunoblot analysis.

#### I. Kinome profiling

Active kinases were identified with kinome profiling experiments performed by Dr. Steve Angus at Indiana University School of Medicine. Briefly, cells were treated as mentioned and collected in protein lysis buffer (see above for composition). Activated kinases in solution are identified using multiplexed kinase inhibitor-conjugated bead affinity chromatography and mass spectrometry (MIB-MS), as described previously<sup>236</sup>.

#### J. Blood glucose, streptozotocin administration, intraperitoneal glucose tolerance and insulin tolerance tests

Prior to HFD feeding and every 4 weeks thereafter, non-fasting blood glucose was measured using a handheld glucometer (Contour Next, Bayer, Leverkusen, Germany). Mice were subjected to intraperitoneal administration of low dose streptozotocin (STZ, 50 mg/kg body weight) on 5 consecutive days. Fasting blood glucose measurements were collected after overnight fast using a handheld glucometer. Intraperitoneal glucose tolerance tests (IPGTTs) were performed following an overnight fast. Briefly, glucose was administered intraperitoneally at a dose of 2 g/kg body weight, then blood glucose was measured via tail vein at 0 (before glucose injection), 10, 20, 30, 60, 90 and 120 minutes after glucose injection using a handheld glucometer (Contour Next, Bayer). Intraperitoneal insulin tolerance tests (IPITTs) were performed following a 2 h fast. Briefly, insulin was administered intraperitoneally at a dose of 0.75 U/kg body weight, then blood glucose was measured at 0 (before insulin injection), 15, 30, 45, and 60 minutes after insulin injection using the handheld glucometer.

### K. Insulin secretion assays

For *in vitro* GSIS, islets were isolated from 8- to 12-week-old male and female mice and cultured overnight in 11.1 mM glucose RPMI media. Briefly, 20 islets per condition were washed with Krebs-Ringer Bicarbonate HEPES buffer (KRBH: 134 mM NaCl, 4.8 mM KCl, 1 mM CaCl<sub>2</sub>, 1.2 mM MgSO<sub>4</sub>, 1.2 mM KH<sub>2</sub>PO<sub>4</sub>, 5 mM NaHCO<sub>3</sub>, 10 mM HEPES, 0.1% BSA), preincubated in 2.8 mM glucose KRBH, then cultured in KRBH containing either 2.8 mM or 16.7 mM glucose for 1 h. For secreted insulin, supernatants were collected, centrifuged, transferred to fresh tubes and stored at -80°C. For insulin content, islets were lysed, sonicated and stored at -80°C. Secreted insulin was assayed with an insulin ultra-sensitive homogeneous time resolved fluorescence (HTRF) kit (62IN2PEG, Cisbio, Codolet, France) and insulin content was assayed with an insulin high range HTRF kit (62IN1PEG, Cisbio). For *in vivo* GSIS, mice were fasted overnight then intraperitoneal glucose was administered at a dose of 2 mg/kg body weight. Blood samples were collected from the tail vein 0 (before glucose injection), 2 and 10 mins after glucose injection, and serum was obtained. Serum insulin measurements were performed by the IU CDMD Translational Core using insulin ELISA assays (10-1247-01, Merckodia, Uppsala, Sweden).

### L. Immunohistochemistry and quantitative microscopy

Pancreases were extracted and fixed in 10% neutral buffered formalin (SF100-4, ThermoFisher Scientific). Fixed pancreas samples were embedded in paraffin, processed, 4 mm sections were cut, then sections were stained as previously described<sup>237</sup>. Briefly,  $\beta$  cells were stained using mouse monoclonal anti-insulin antibody (I2018; MilliporeSigma) followed by goat anti-mouse Cy3 (115-165-146; Jackson

ImmunoResearch, West Grove, PA). Amyloid fibrils were stained in Thioflavin S (5 mM) for 2 minutes followed by 10 dips in 70% ethanol and a 5 min wash in water at RT. Sections were then mounted with polyvinyl alcohol with 0.2% Hoechst and images were captured on a Zeiss LSM710 confocal microscope (Zeiss, Oberkochen, Germany). Islet area,  $\beta$ -cell area, and amyloid severity were quantified using a computer-based quantitative method described previously<sup>88,238,239</sup>. Briefly, areas of insulin and nuclei positivity consistent with islet morphology were identified and islet regions of interest were defined using Zen Blue 2.1 image analysis software (Zeiss). This software was then used to quantify islet areas as well as insulin-positive and amyloid-positive areas within islet regions of interest. Average islet area was quantified as  $(\Sigma \text{islet area})/\text{number of islets}$  quantified per mouse,  $\beta$ -cell area was quantified as  $(\Sigma \text{insulin positive area})/(\Sigma \text{islet area}) \times 100\%$  for each mouse and amyloid severity was quantified as  $(\Sigma \text{amyloid positive area})/(\Sigma \text{islet area}) \times 100\%$  for each mouse. An average of  $24 \pm 4$  islets were analyzed per mouse by an observer blinded to pancreas sample genotype<sup>240</sup>. Representative islet images are shown.

#### M. In vivo transplantation model of autoimmune-mediated $\beta$ -cell killing

NIT-1 CTL or Ripk1 $\Delta$  cells expressing firefly luciferase (Luc2) was transplanted on opposite flanks of 8-week-old female non-diabetic NSG mice lacking T-, B- and NK immune cells. Following  $\beta$ -cell transplantation, quantified *in vivo* graft luminescence by IVIS imaging (Perkin Elmer) after administration of splenocytes isolated from diabetic NOD mice.

#### N. Statistical analyses

Two-tailed Student's t-tests were used to analyze data sets with two groups, and one-way analysis of variance (ANOVA) tests were used to analyze data sets with more than two groups. Significant ANOVA results were followed with Holm-Sidák post-tests to analyze differences between groups of interest. For islet amyloid deposition, non-parametric Mann-Whitney tests were used to analyze data sets with two groups, and non-parametric Kruskal-Wallis tests were used to analyze data sets with more than two groups. Significant Kruskal-Wallis tests were followed by Dunn's post-tests to analyze differences between groups of interest. Correlation analysis was performed by simple linear regression. Statistical tests were performed with GraphPad Prism 10 software (GraphPad, San Diego, CA). Data are presented as mean  $\pm$  SEM. A value of  $p < 0.05$  was considered significant.

## **Chapter 3 – RIPK1 and RIPK3 regulate TNF $\alpha$ -induced $\beta$ -cell death in concert with caspase activity**

### **Introduction**

These studies aim to characterize the mechanisms of  $\beta$ -cell TNF receptor signaling. It is well established that in non-islet cell types, following TNFR1 stimulation, RIPK1 and RIPK3 play crucial roles in defining cell fate. I aim to first evaluate the roles of RIPK1, RIPK3, and caspase activation in TNF $\alpha$ -induced  $\beta$ -cell cytotoxicity, and whether  $\beta$  cells are susceptible to caspase-independent cell death. CRISPR gene-edited  $\beta$ -cell lines used in this study were generated by Dr. Erica P. Cai's lab at Indiana Biosciences Research Institute.

TNF $\alpha$  is a proinflammatory cytokine associated with  $\beta$ -cell loss, insulin insufficiency and hyperglycemia in the pathogenesis of type 1 diabetes (T1D) <sup>241–245</sup>. Previous studies found that TNF $\alpha$  elicits  $\beta$ -cell death in NIT-1 and MIN6  $\beta$ -cell lines *in vitro*, with Fas-associated death domain (FADD) promoting this process <sup>246</sup> and NF $\kappa$ B signaling inhibiting it <sup>247</sup>. Other studies failed to observe TNF $\alpha$ -induced  $\beta$ -cell death <sup>248</sup> or observed it only in the presence of cycloheximide <sup>249</sup>. Although primary islet  $\beta$  cells are less prone to TNF $\alpha$ -induced cell death *in vitro*, TNF $\alpha$  and IFN $\gamma$  cotreatment strongly elicits primary  $\beta$ -cell death, which Irawaty and colleagues found to be caspase-independent <sup>246,250</sup>. *In vivo*, overexpression of TNF $\alpha$  in  $\beta$  cells accelerates the onset of hyperglycemia in the non-obese diabetic (NOD) mouse model of T1D <sup>243</sup>, while either loss of TNF receptor 1 (TNFR1) <sup>244</sup> or treatment with an anti-TNF $\alpha$  antibody <sup>251</sup> protects NOD mice from hyperglycemia. In humans, etanercept, a TNF $\alpha$  neutralizing antibody

was shown to promote glucose homeostasis and  $\beta$ -cell function in a pilot study of 18 individuals with newly diagnosed T1D <sup>252</sup>, and more recently, golimumab, an anti-TNF $\alpha$  monoclonal antibody, was shown to preserve  $\beta$ -cell function in a cohort of 84 children and young adults with new-onset T1D <sup>245</sup>, revealing the importance of this pathway in human disease. Although these studies established that TNF $\alpha$  promotes hyperglycemia in T1D, the role of TNF $\alpha$ -mediated  $\beta$ -cell loss in this process remains poorly understood. As such, studies to characterize the mechanisms of  $\beta$ -cell TNF receptor signaling may lead to novel approaches to protect  $\beta$  cells and diminish hyperglycemia in T1D.

Although studies of TNF $\alpha$ -induced  $\beta$ -cell death have focused on apoptosis <sup>242,253</sup>, in other cell types TNF $\alpha$  can elicit a distinct mechanism of caspase-independent programmed cell death termed necroptosis <sup>254,255</sup>. In contrast to apoptosis, necroptosis is an inflammatory and immunogenic form of lytic cell death that occurs when caspases are inactivated <sup>256,257</sup>, leading to release of damage-associated molecular patterns and immune responses <sup>183,257</sup>. Following stimulation of TNFR1, activation of receptor interacting protein kinase 1 (RIPK1) and caspase 8 promote apoptosis in diverse cell types <sup>258–260</sup>. However, when caspase 8 activity is inhibited genetically or pharmacologically <sup>261–263</sup>, RIPK1 signals via receptor interacting protein kinase 3 (RIPK3) and mixed lineage kinase domain like pseudokinase (MLKL) to execute necroptosis <sup>255,256,264</sup>. Thus, RIPK1 and caspase 8 function as critical regulators of TNFR1 signaling that can direct either caspase-dependent apoptosis or RIPK3-mediated necroptosis depending on caspase activation state (Figure 1A) <sup>265</sup>. Interestingly,  $\beta$ -cell specific caspase 8 knockout mice display hyperglycemia and loss of islet area with age <sup>137</sup>, and caspase 8 mutations have been linked to hyperglycemia in humans <sup>266</sup>. However,

the roles of RIPK1 and RIPK3 in TNF $\alpha$ -induced  $\beta$ -cell loss have not been clearly described.

We hypothesized that  $\beta$  cells are susceptible to TNF $\alpha$ -induced cell death and that RIPK1 and RIPK3 regulate this process in concert with caspase activity. To test this hypothesis, we quantified TNF $\alpha$ -induced cell death and caspase activity in immortalized NIT-1 and INS-1  $\beta$ -cell lines and primary mouse islet cells *in vitro*. We utilized real-time, high-content measurements of cell death, Ripk1 and Ripk3 deficient  $\beta$  cells, a synthetic pan-caspase inhibitor (zVAD-fmk), a small molecule RIPK3 inhibitor (GSK'872), RIPK3 overexpressing  $\beta$  cells, and Ripk3<sup>-/-</sup> islets to characterize the roles of RIPK1 and RIPK3 in TNF $\alpha$ -induced  $\beta$ -cell loss. We also evaluated the susceptibility of Ripk3<sup>-/-</sup> mice to hyperglycemia following exposure to the  $\beta$ -cell toxin streptozotocin (STZ). To our knowledge, this study is the first to systematically evaluate the roles of RIPK1, RIPK3, and caspase activity in TNF $\alpha$ -induced  $\beta$ -cell death, and to determine the susceptibility of  $\beta$  cells to caspase-independent programmed cell death.

## **Results**

### **A. NIT-1 and INS-1 $\beta$ cells express components of TNF $\alpha$ pathway signaling and are susceptible to RIPK1- and cIAP-mediated TNF $\alpha$ -induced cell death.**

TNF $\alpha$  is known to elicit apoptosis and necroptosis via RIPK1 and RIPK3 in non-islet cell types<sup>260,267-270</sup>, but these signaling pathways have not been well characterized in  $\beta$  cells (Figure 1A). Like necroptosis-prone NIH-3T3 cells<sup>271</sup>, mouse NIT-1 and rat INS-1  $\beta$ -cell lines express TNF pathway signaling components including TNFR1, RIPK1, CASP8, RIPK3 and MLKL at the mRNA and protein levels (Figure 3B,C). We first generated

NIT-1 control (NIT-1 CTL) and NIT-1 RIPK1 deficient cells (NIT-1 RIPK1 $\Delta$ ) containing a 1262 base pair deletion extending from exon 2 to exon 3 of the Ripk1 gene. Using a high-content live-cell imaging and analysis system, we quantified NIT-1 and INS-1 cell death in response to TNF $\alpha$  in real-time each hour. We found that TNF $\alpha$  (shown in blue) significantly increased death in NIT-1 control cells (NIT-1 CTL, shown in circles, Figure 2A,B,C) after 24 h, and that RIPK1 deficient NIT-1 cells (NIT-1 RIPK1 $\Delta$ , shown in triangles) were protected from TNF $\alpha$ -induced death (Figure 4A,B). Similarly, TNF $\alpha$  treatment increased caspase 3/7 activity in NIT-1 CTL cells, and this was abrogated in NIT-1 RIPK1 $\Delta$  cells (Figure 4D). Cellular inhibitor of apoptosis proteins (cIAPs) are endogenous inhibitors of cell death that interact with TNF receptor signaling molecules<sup>272</sup>. Treatment with BV6, a small molecule cIAP inhibitor and second mitochondria-derived activator of caspases (SMAC) mimetic<sup>273,274</sup>, significantly increased TNF $\alpha$ -induced NIT-1 cell death after 4 h (Figure 4E,F,G), and this effect was diminished in NIT-1 RIPK1 $\Delta$  cells (Figure 4E,F). The reduced cell death observed in NIT-1 RIPK1 $\Delta$  versus CTL cells following TNF $\alpha$ - or TNF $\alpha$ +BV6-treatment was associated with reduced caspase 3/7 activity (Figure 4H). Following treatment of NIT-1 CTL cells with TNF $\alpha$ +BV6 for 4 h, we also identified genomic DNA laddering (Figure 4I) characteristic of apoptosis<sup>232</sup>. INS-1 cells were also observed to be susceptible to TNF $\alpha$ -induced cell death which was amplified by BV6 cotreatment (Figure 4J,K,L). Representative cell death images are shown in Figure 4M. These data show that NIT-1 and INS-1  $\beta$  cells are susceptible to TNF $\alpha$ -induced cell death, which is regulated by cIAPs and RIPK1, and that this process occurs in association with increased caspase 3/7 activity.

B. NIT-1 and INS-1  $\beta$  cells are susceptible to TNF $\alpha$ -induced cell death when caspases are inhibited.

We next utilized the synthetic pan-caspase inhibitor zVAD-fmk (zVAD) to determine whether increased caspase activity is required for TNF $\alpha$ -induced  $\beta$ -cell death. TNF $\alpha$  treatment strongly induced NIT-1 cell death after 48 hours, and cell death was unaltered by zVAD alone (Figure 5A,B,C). TNF $\alpha$ +zVAD treatment (shown in green) significantly increased NIT-1 cell death after 48 hours, although to a lesser extent than TNF $\alpha$  alone (shown in blue) (Figure 5A,B,C). As expected, TNF $\alpha$ -induced cell death was associated with increased caspase 3/7 activity, while zVAD or TNF $\alpha$ +zVAD treatment significantly reduced caspase 3/7 activity (Figure 5D). In INS-1 cells, we again found that either TNF $\alpha$  alone or TNF $\alpha$ +zVAD treatment increased cell death, although the magnitude was less than that observed in NIT-1 cells (Figure 5E,F,G). TNF $\alpha$ -induced INS-1 cell death occurred with increased caspase 3/7 activity, and TNF $\alpha$ +zVAD-induced cell death occurred with decreased caspase 3/7 activity (Figure 5H). Representative cell death images are shown in Figure 5I. These data indicate that caspase activation is not required for TNF $\alpha$ -induced cell death in NIT-1 or INS-1  $\beta$ -cells.

We next determined whether distinct gene expression profiles accompany cell death induced by TNF $\alpha$  versus TNF $\alpha$ +zVAD. Using RNA sequencing of INS-1 cell lysates, we identified genes with high differential expression in response to TNF $\alpha$  or TNF $\alpha$ +zVAD versus vehicle treatment (Figure 5J), with focus on genes expressed differentially between TNF $\alpha$  and TNF $\alpha$ +zVAD conditions. 2932 genes were down-regulated commonly by TNF $\alpha$  or TNF $\alpha$ +zVAD treatment, with 1558 genes down-

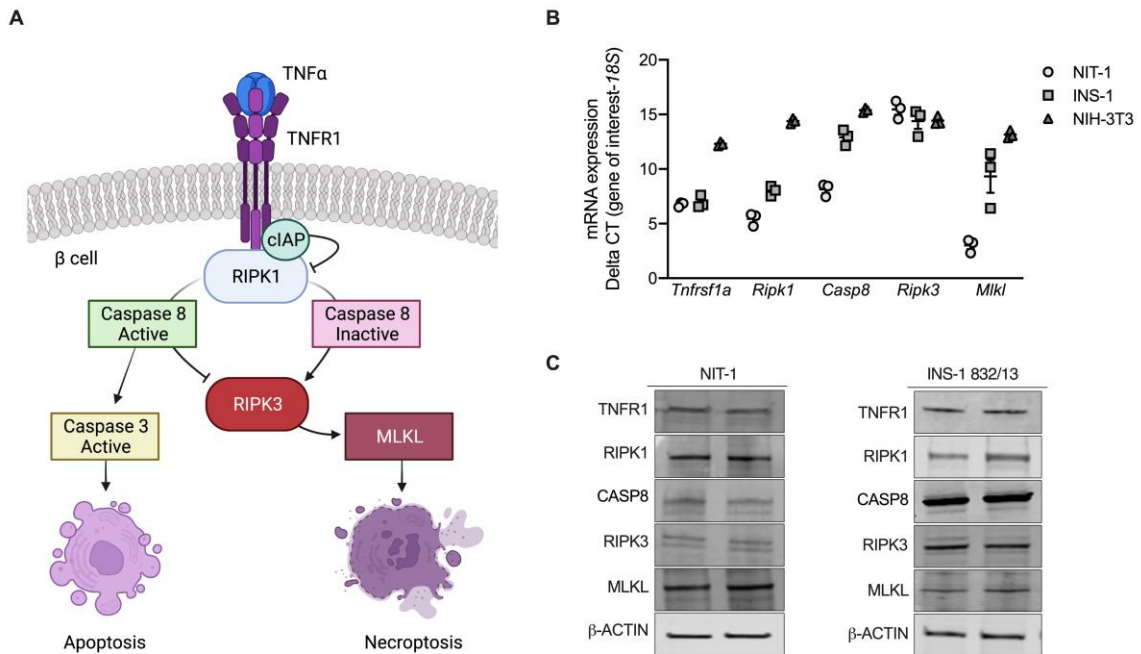


**Figure 3: NIT-1 and INS-1 β cells express components of TNF $\alpha$  pathway signaling.**

**A)** Schematic of TNF $\alpha$  death signaling pathways as described in non-islet cell types. **B)** *Tnfrsf1a*, *Ripk1*, *Casp8*, *Ripk3* and *Mkl1* RNA expression were quantified in NIT-1 (circles), INS-1 (squares), and NIH-3T3 (triangles) cells, normalized to *18S* rRNA levels, and expressed as  $\Delta$ CT of the gene of interest (n=3). **C)** NIT-1 and INS-1 β cells express TNFR1, RIPK1, CASP8, RIPK3 and MLKL protein, as visualized by duplicate immunoblot analysis of 20 mg of protein from total cell lysates.

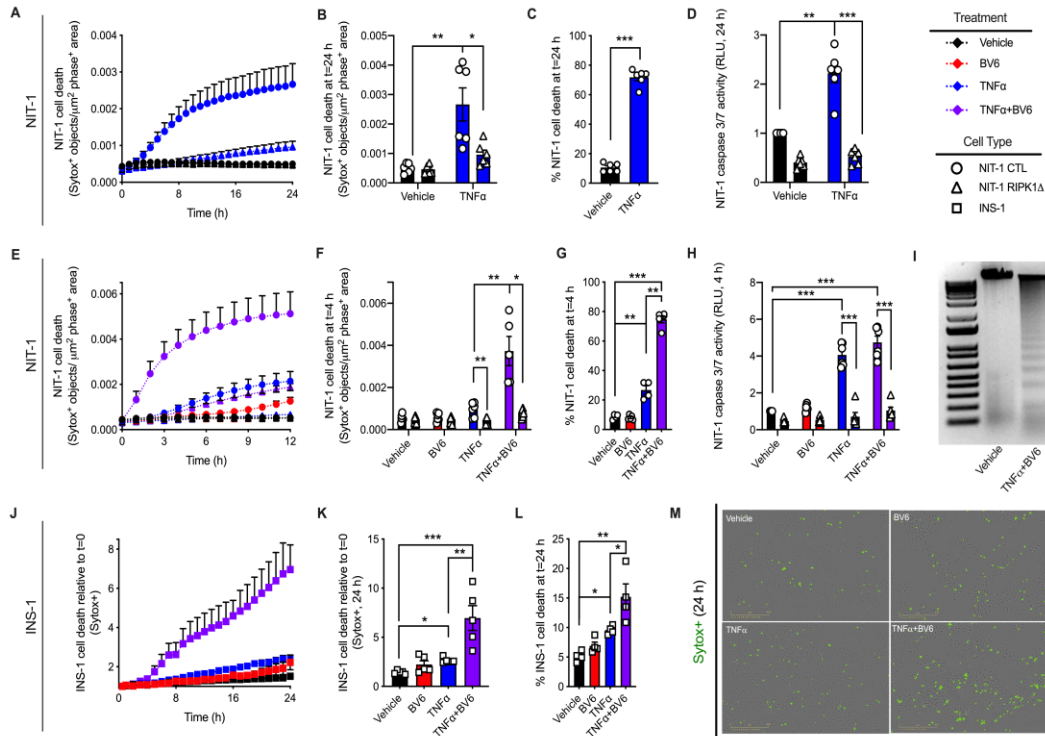


**Figure 4: NIT-1 and INS-1  $\beta$  cells are susceptible to RIPK1- and cIAP-mediated TNF $\alpha$ -induced cell death.**

A Sartorius IncuCyte S3 live cell imaging and analysis instrument was used to monitor cell death via quantification of Sytox green positive cells. Cell culture treatment conditions are indicated by color (black: vehicle, blue: 40 ng/mL TNF $\alpha$ , red: 5 mM BV6, purple: TNF $\alpha$ +BV6) and  $\beta$ -cell lines are indicated by shapes (NIT-1 CTL: circles, NIT-1 RIPK1 $\Delta$ : triangles, INS-1: squares). A) Cell death was monitored for 24 h in NIT-1 CTL and NIT-1 RIPK1 $\Delta$  cells following TNF $\alpha$  treatment, and B) cell death was quantified 24 h post treatment (n=6). C) Percent NIT-1 CTL cell death was quantified 24 h after treatment with vehicle or TNF $\alpha$  using the Sartorius IncuCyte S3 advanced label-free classification analysis software module, as described (n=6). D) NIT-1 CTL and NIT-1

RIPK1 $\Delta$  cell caspase 3/7 activity was quantified 24 h after treatment and expressed relative to vehicle treated NIT-1 CTL cells (n=6). E) NIT-1 CTL and NIT-1 RIPK1 $\Delta$  cells were treated with BV6, TNF $\alpha$  or a combination thereof, then F) cell death was quantified 4 h post treatment (n=5-6). For comparisons between cell lines, cell death was reported as Sytox green positive cell objects normalized to phase positive cell area for each time point. G) Percent NIT-1 CTL cell death was quantified 4 h after treatment with BV6, TNF $\alpha$  or a combination thereof using the Sartorius IncuCyte S3 advanced label-free classification analysis software module (n=4-5). H) NIT-1 CTL and NIT-1 RIPK1 $\Delta$  cell caspase 3/7 activity was quantified 4 h after treatment and expressed relative to vehicle treated NIT-1 CTL cells (n=4-6). I) Genomic DNA was isolated from NIT-1 CTL cells following treatment with vehicle or TNF $\alpha$ +BV6 for 4 h, then visualized on an agarose gel. J) For INS-1 cells, cell death was monitored for 24 h following treatment with BV6, TNF $\alpha$  or a combination thereof, then K) cell death was quantified 24 h post treatment (n=5). For comparisons within a cell line, cell death was reported as Sytox green positive cell objects relative to time t=0. L) Percent INS-1 cell death was quantified 24 h after treatment using the Sartorius IncuCyte S3 advanced label-free classification analysis software module, as described (n=4). M) Representative IncuCyte images illustrate Sytox green positive INS-1 cells 24 h post treatment. Data are presented as mean  $\pm$  SEM and were analyzed by one-way ANOVA followed by Sidák post-test and multiple comparisons correction. \* $p$  < 0.05; \*\* $p$  < 0.01; \*\*\* $p$  < 0.001 as indicated.

regulated specifically by TNF $\alpha$  and 2188 down-regulated specifically by TNF $\alpha$ +zVAD treatment (Figure 5J,K). 301 genes were up-regulated commonly by TNF $\alpha$  and TNF $\alpha$ +zVAD treatment, including *Nfkb2* (nuclear factor kappa B subunit 2) and its transcriptional target *Birc3* (baculoviral IAP Repeat containing 3, also known as cIAP2) (Figure 5J,K). 435 genes were up-regulated specifically by TNF $\alpha$  while 225 were up-regulated specifically by TNF $\alpha$ +zVAD treatment (Figure 5J,K). Among the genes up-regulated specifically by TNF $\alpha$ +zVAD are lymphocyte expansion molecule (*Lexm*) and lymphocyte activation gene 3 (*Lag3*). These data show that distinct transcriptional profiles characterize TNF $\alpha$ - versus TNF $\alpha$ +zVAD-induced cell death in INS-1 cells.

C. RIPK1 and cIAPs regulate TNF $\alpha$ -induced NIT-1 and INS-1  $\beta$ -cell death when caspases are inhibited.

To examine whether caspase-independent TNF $\alpha$ -induced  $\beta$ -cell death is regulated downstream of TNF receptor signaling, we next treated NIT-1 CTL and RIPK1 $\Delta$  cells with TNF $\alpha$ +zVAD (shown in green) or TNF $\alpha$ +BV6+zVAD (shown in white). TNF $\alpha$ +zVAD treatment significantly increased NIT-1 cell death over 48 hours (Figure 6A,B,C), and this caspase-independent cell death was reduced in RIPK1 $\Delta$  cells (Figure 6A,B). Cell death in response to TNF $\alpha$ +zVAD was strongly amplified by addition of BV6 (Figure 6A,B,C), and this effect was again abrogated in NIT-1 RIPK1 $\Delta$  cells (Figure 6A,B). The increased cell death observed with TNF $\alpha$ +zVAD or TNF $\alpha$ +BV6+zVAD treatment occurred when caspase 3/7 activity was significantly reduced compared to vehicle-treated control cells (Figure 6D), and in the absence of genomic DNA laddering (Figure 6E). As in NIT-1 cells, we found that INS-1 cells are susceptible to

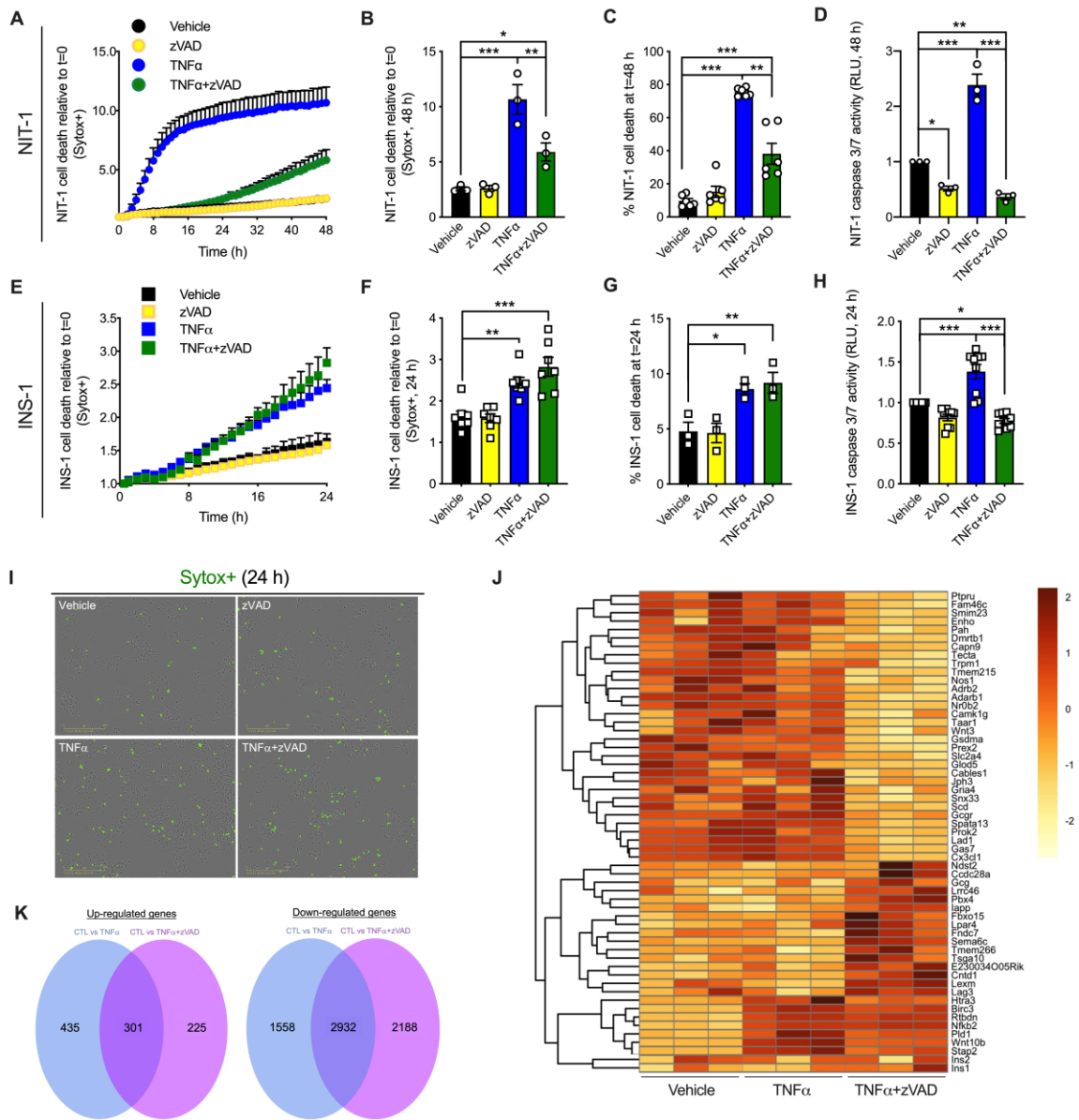


**Figure 5: NIT-1 and INS-1  $\beta$  cells are susceptible to TNF $\alpha$ -induced cell death when caspases are inhibited.**

A) NIT-1 CTL cell death was monitored over 48 h as described, and B) quantified at 48 h post treatment (n=3). Cell culture treatment conditions are indicated by color (black: vehicle, yellow: 50  $\mu$ M zVAD, blue: 40 ng/mL TNF $\alpha$ , green: TNF $\alpha$ +zVAD) and  $\beta$ -cell

lines are indicated by shapes (NIT-1 CTL: circles, INS-1: squares). C) Percent NIT-1 CTL cell death was quantified 48 h after treatment with zVAD, TNF $\alpha$  or a combination thereof using the Sartorius IncuCyte S3 advanced label-free classification analysis software module (n=6). D) NIT-1 CTL cell caspase 3/7 activity was quantified 48 h post treatment and expressed relative to vehicle treated cells (n=3). E) INS-1 cell death was monitored over 24 h, and F) quantified at 24 h post treatment (n=7). G) Percent INS-1 cell death was quantified 24 h after treatment using the Sartorius IncuCyte S3 advanced label-free classification analysis software module, as described (n=3). H) INS-1 cell caspase 3/7 activity was quantified 24 h post treatment and expressed relative to vehicle treated cells (n=9). I) Representative IncuCyte images illustrate Sytox green positive INS-1 cells 24 h post treatment. J) Heatmap displaying genes with significantly different expression among groups. High expression is shown in dark red and low expression in light yellow (n=3). K) Venn diagrams displaying (left) the number of genes up-regulated commonly by TNF $\alpha$  and TNF $\alpha$ +zVAD (301), up-regulated specifically by TNF $\alpha$  (435), or up-regulated specifically by TNF $\alpha$ +zVAD (225), and (right) the number of genes down-regulated commonly by TNF $\alpha$  and TNF $\alpha$ +zVAD (2932), down-regulated specifically by TNF $\alpha$  (1558), or down-regulated specifically by TNF $\alpha$ +zVAD (2188). A-H) Data are presented as mean  $\pm$  SEM and were analyzed by one-way ANOVA followed by Sidák post-test and multiple comparisons correction. \* $p < 0.05$ ; \*\* $p < 0.01$ ; \*\*\* $p < 0.001$  as indicated. J,K) Differentially expressed genes were identified at  $p < 0.05$ ,  $p$ -values were corrected for false discovery rate using the Benjamini-Hochberg method, and corrected  $p < 0.05$  was used to identify significantly different gene expression.

TNF $\alpha$ +zVAD-induced cell death that is amplified by BV6 co-treatment (Figure 6F,G,H). Representative cell death images are shown in Figure 6I. These data indicate that caspase-independent TNF $\alpha$ -induced NIT-1 and INS-1 cell death is regulated by RIPK1 and cIAPs.

D. RIPK3 promotes TNF $\alpha$ -induced INS-1 cell death when caspases are inhibited.

RIPK3 has been shown to promote TNF $\alpha$ -induced cell death when caspase activity is inhibited in several cell types<sup>255,264,275</sup>. To determine whether RIPK3 plays a role in caspase-independent TNF $\alpha$ -induced  $\beta$ -cell death, we generated NIT-1 RIPK3 deficient cells (NIT-1 RIPK3 $\Delta$ , shown in diamonds) containing an 80 base pair insertion in exon 6 of the Rpk3 gene. As before, we found that TNF $\alpha$  treatment significantly increased NIT-1 CTL cell death and caspase 3/7 activity (Figure 7A,B). NIT-1 RIPK3 $\Delta$  cells were also susceptible to TNF $\alpha$ -induced cell death after 48 hours, although this cell death and caspase 3/7 activity were reduced compared to NIT-1 CTL cells (Figure 7A,B). NIT-1 RIPK3 $\Delta$  cells were completely protected from TNF $\alpha$ -induced cell death when caspases were inhibited with zVAD (Figure 7A,B), conditions under which NIT-1 CTL cell death was significantly increased. Next, INS-1 cells were treated with TNF $\alpha$ , zVAD or GSK'872 (a small molecule RIPK3 . kinase inhibitor) individually or in combination and evaluated over 24 hours. Treatment with GSK'872 at 5 mM did not alter INS-1 cell death (Figure 7C) or caspase 3/7 activity (Figure 7D) compared to vehicle treated control cells after 24 hours. As before, TNF $\alpha$  increased cell death and caspase 3/7 activity (Figure 7C,D), and co-treatment with TNF $\alpha$ +GSK'872 resulted in similar degrees of cell death and caspase 3/7 activity as TNF $\alpha$  alone (Figure 7C,D).

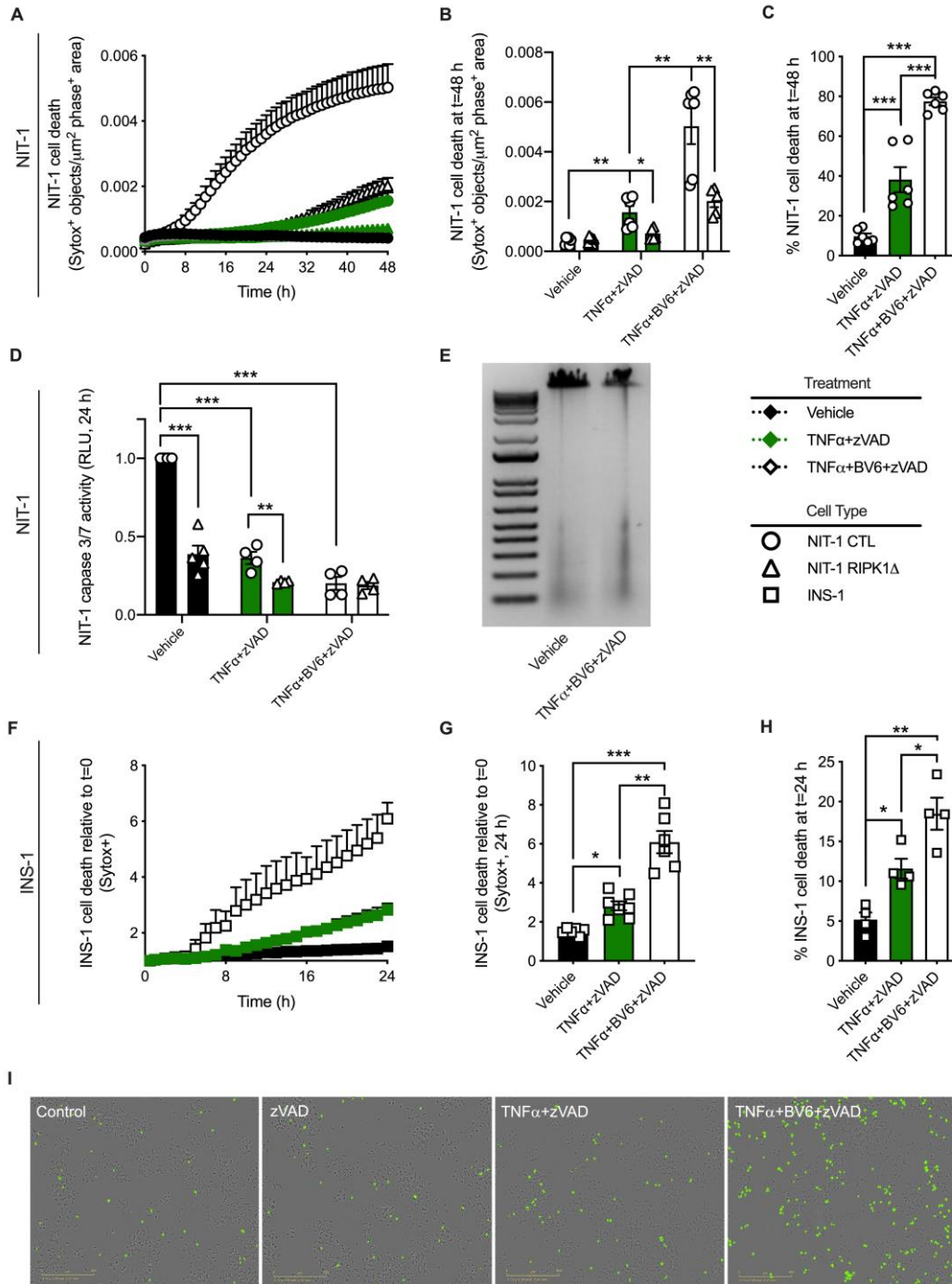


**Figure 6: RIPK1 and cIAPs regulate TNF $\alpha$ -induced NIT-1 and INS-1  $\beta$ -cell death when caspases are inhibited.**

A) NIT-1 CTL and NIT-1 RIPK1 $\Delta$  cell death was monitored over 48 h, and B) quantified at 48 h post treatment (n=5-6). Cell culture treatment conditions are indicated by color

(black: vehicle, green: 40 ng/ml TNF $\alpha$  + 50  $\mu$ M zVAD, white: TNF $\alpha$ +zVAD + 5  $\mu$ M BV6) and  $\beta$ -cell lines are indicated by shapes (NIT-1 CTL: circles, NIT-1 RIPK1 $\Delta$ : triangles, INS-1: squares). C) Percent NIT-1 CTL cell death was quantified 48 h after treatment with vehicle, TNF $\alpha$  +zVAD or TNF $\alpha$ +BV6+zVAD using the Sartorius IncuCyte S3 advanced label-free classification analysis software module, as described (n=6). D) NIT-1 CTL and RIPK1 $\Delta$  cell caspase 3/7 activity was quantified 24 h post treatment and expressed relative to vehicle treated NIT-1 CTL cells (n=4-5). E) Genomic DNA was isolated from NIT-1 CTL cells following treatment with vehicle or TNF $\alpha$ +BV6+zVAD for 8 h, then visualized on an agarose gel. F) INS-1 cell death was monitored over 24 h, and G) quantified at 24 h post treatment (n=5-6). H) Percent INS-1 cell death was quantified 24 h after treatment using the Sartorius IncuCyte S3 advanced label-free classification analysis software module (n=4). I) Representative IncuCyte images illustrate Sytox green positive INS-1 cells 24 h post treatment. Data are presented as mean  $\pm$  SEM and were analyzed by one-way ANOVA followed by Sidák post-test and multiple comparisons correction. \* $p$  < 0.05; \*\* $p$  < 0.01; \*\*\* $p$  < 0.001 as indicated.

In contrast, TNF $\alpha$ +zVAD treatment elicited INS-1 cell death when caspases were inhibited (Figure 7C,D), and addition of GSK'872 (5 mM) under these conditions (TNF $\alpha$ +zVAD+GSK'872) resulted in significantly less cell death than TNF $\alpha$ +zVAD treatment with no difference in caspase 3/7 activity (Figure 7C,D).

We next evaluated INS-1 cells overexpressing RIPK3. Overexpression of RIPK3 in pcDNA3-mRipk3 INS-1 cells was verified at the RNA and protein levels by qRT-PCR and immunoblot analysis (Figure 7E,F). Neither basal nor TNF $\alpha$ -induced (Figure 7G) cell death was altered in pcDNA-3-Empty versus pcDNA3-mRipk3 INS-1 cells. However, TNF $\alpha$ +zVAD treatment caused significantly more cell death in RIPK3 overexpressing pcDNA3-mRipk3 cells compared to control pcDNA-3-Empty cells (Figure 7G). Following treatment with TNF $\alpha$ +zVAD, RIPK3 co-immunoprecipitated with MLKL and caspase 8 from RIPK3 overexpressing INS-1 cell lysates (Figure 7H). Likewise, MLKL co-immunoprecipitated with RIPK3 and caspase 8 under these conditions (Figure 7I). These data indicate that TNF $\alpha$  treatment induces  $\beta$ -cell apoptosis that occurs with caspase 3/7 activation. In contrast, TNF $\alpha$ +zVAD treatment induces a form of  $\beta$ -cell death that occurs when caspase activity is inhibited, is mediated by RIPK3 and is associated with formation of RIPK3-MLKL protein complexes.

E. Mouse islets cells are susceptible to TNF $\alpha$ -induced cell death when cIAPs or caspases are inhibited.

Previous studies have found that TNF $\alpha$  promotes cell death in immortalized  $\beta$ -cell lines<sup>246,247</sup>, but that primary islet cells are resistant to TNF $\alpha$ -induced death<sup>276</sup>. We first confirmed that molecular components of TNF receptor signaling including TNFR1, RIPK1, CASP8, RIPK3 and MLKL are expressed in mouse islets at the mRNA and

protein levels (Figure 8A,B). Using our real time cell imaging and analysis platform, we confirmed that treatment with TNF $\alpha$  alone (shown in blue) did not significantly increase dispersed mouse islet cell death after 24 hours (Figure 8C). However, in line with our NIT-1 and INS-1 cell findings, inhibition of cIAPs with BV6 significantly increased TNF $\alpha$ -induced mouse islet cell death (Figure 8C, shown in purple). Interestingly, TNF $\alpha$  also increased mouse islet cell death when caspase 3/7 activity was inhibited with zVAD (Figure 8C,D, shown in green). Representative mouse islet cell death images are shown in Figure 8E. These data suggest that primary mouse islet cells are susceptible to TNF $\alpha$ -induced cell death under certain conditions such as when cIAPs or caspases are inhibited.

F. Ripk3 promotes TNF $\alpha$ -induced mouse islet cell death when caspases are inhibited.

We next tested whether RIPK3 contributes to TNF $\alpha$ -induced mouse islet cell death when caspases are inhibited. Like previous experiments in mouse islet cells, TNF $\alpha$  failed to increase cell death after 24 hours, while TNF $\alpha$ +zVAD treatment significantly increased islet cell death (Figure 8F, left panel). Addition of the RIPK3 inhibitor GSK'872 significantly reduced mouse islet cell death in response to TNF $\alpha$ +zVAD, but not TNF $\alpha$  alone (Figure 8F, right panel), and caspase 3/7 activity was not significantly altered by GSK'872 treatment (Figure 8G). We next evaluated Ripk3<sup>-/-</sup> islets, in which we confirmed loss of RIPK3 expression (Figure 8H). Rates of basal cell death were not different between untreated Ripk3<sup>+/+</sup> and Ripk3<sup>-/-</sup> islets cells (Figure 8I). In contrast to our findings with Ripk3<sup>+/+</sup> islet cells, TNF $\alpha$ +zVAD treatment failed to increase cell death in Ripk3<sup>-/-</sup> islets compared to vehicle-treated cells (Figure 8J,K). These data indicate that

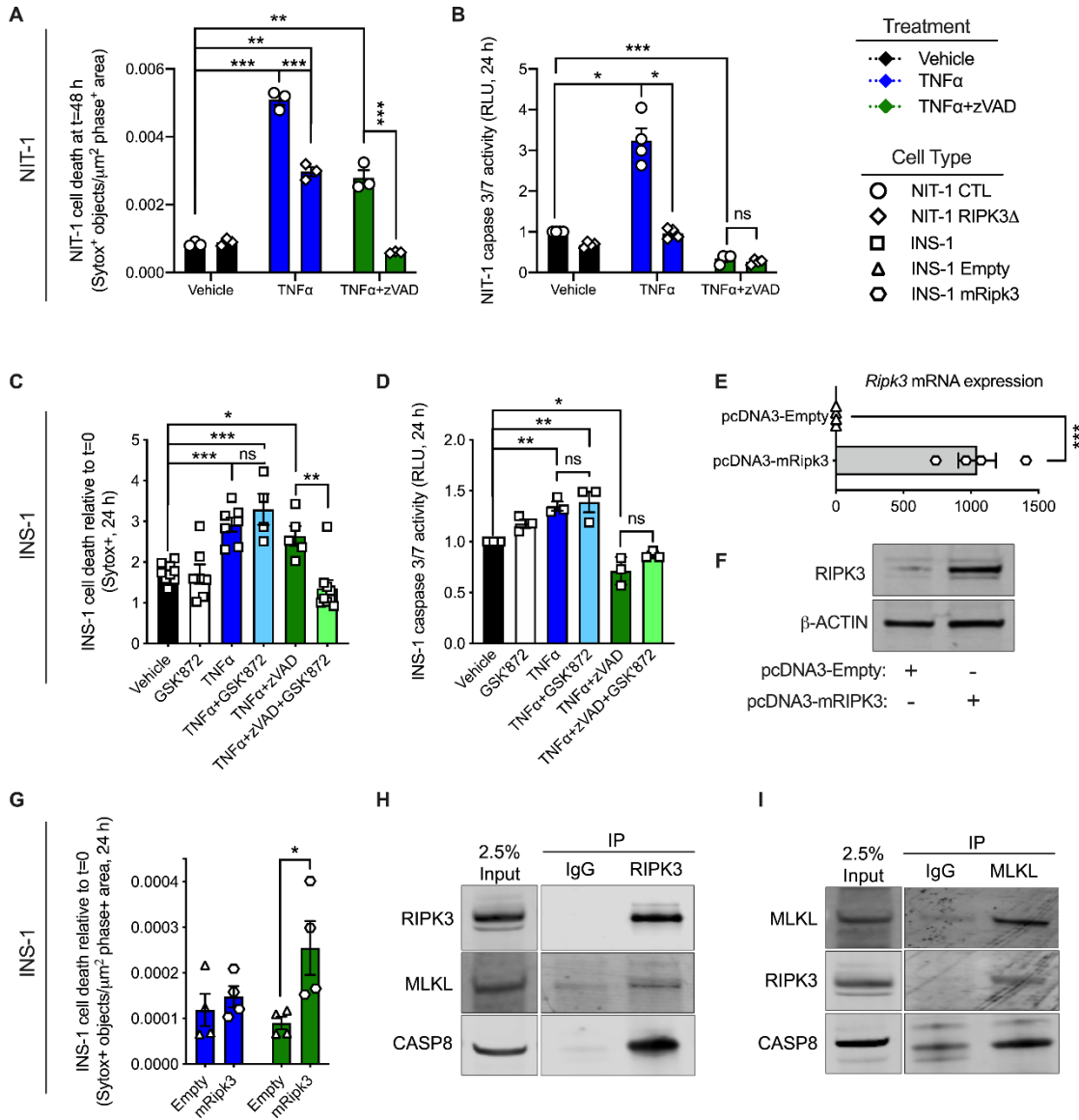


**Figure 7: RIPK3 promotes TNF $\alpha$ -induced INS-1 cell death when caspases are inhibited.**

A) NIT-1 CTL and NIT-1 RIPK3 $\Delta$  cell death was quantified 48 h post treatment (n=3). Cell culture treatment conditions are indicated by color (black: vehicle, blue: 40 ng/ml TNF $\alpha$ , green: 40 ng/ml TNF $\alpha$  + 50  $\mu\text{M}$  zVAD) and  $\beta$ -cell lines are indicated by shapes (NIT-1 CTL: circles, NIT-1 RIPK3 $\Delta$ : diamonds, INS-1: squares, INS-1 Empty: triangles, INS-1 mRIPK3: hexagons). B) NIT-1 CTL and RIPK3 $\Delta$  cell caspase 3/7 activity was

quantified 24 h post treatment and expressed relative to vehicle treated NIT-1 CTL cells (n=4). C) INS-1 cell death was quantified 24 h post treatment relative to t=0 (n=4-9). Cell culture treatment conditions are indicated by color (black: vehicle, white: 5  $\mu$ M GSK'872, blue: 40 ng/ml TNF $\alpha$ , light blue: TNF $\alpha$ +GSK'872, green: TNF $\alpha$  + 50  $\mu$ M zVAD, light green: TNF $\alpha$ +zVAD+GSK'872). D) INS-1 cell caspase 3/7 activity was quantified 24 h post treatment and expressed relative to vehicle treated cells (n=3). E) *Ripk3* RNA expression (n=4) and F) RIPK3 protein expression were quantified in control (pcDNA3-Empty: triangles) and Ripk3 overexpressing (pcDNA3-mRipk3: hexagons) INS-1 cells. G) INS-1 pcDNA3-Empty and pcDNA3-mRipk3 cell death was quantified 24 h post TNF $\alpha$  or TNF $\alpha$ +zVAD treatment (n=4). H) Immunoblot analysis of proteins immunoprecipitated with anti-RIPK3 following 24 h TNF $\alpha$ +zVAD treatment (n=3). I) Immunoblot analysis of proteins immunoprecipitated with anti-MLKL following 24 h TNF $\alpha$ +zVAD treatment (n=3). Data are presented as mean  $\pm$  SEM and were analyzed by one-way ANOVA followed by Sidák post-test and multiple comparisons correction. \* $p$  < 0.05; \*\* $p$  < 0.01; \*\*\* $p$  < 0.001; ns,  $p$  > 0.05 as indicated.

TNF $\alpha$  treatment elicits primary mouse islet cell death when caspases are inhibited, and that this form of cell death is mediated by RIPK3.

G. Ripk3<sup>-/-</sup> mice are protected from STZ-induced hyperglycemia *in vivo*.

We next characterized glucose homeostasis in Ripk3<sup>+/+</sup> and Ripk3<sup>-/-</sup> mice before and after administration of the  $\beta$ -cell toxin streptozotocin (STZ) to evaluate their susceptibility to hyperglycemia *in vivo* (Figure 9A). Prior to multiple low dose STZ treatment, Ripk3<sup>+/+</sup> and Ripk3<sup>-/-</sup> mice exhibited similar glucose tolerance, with no difference in blood glucose before or 10, 20, 30, 60, 90 or 120 minutes after intraperitoneal glucose administration (Figure 8B). In contrast, following 5 days of low dose STZ and a 5-day recovery, Ripk3<sup>-/-</sup> mice displayed significantly lower blood glucose than Ripk3<sup>+/+</sup> mice 60, 90 and 120 minutes after glucose injection (Figure 9C). Non-fasting blood glucose concentrations were also significantly reduced in Ripk3<sup>-/-</sup> compared to Ripk3<sup>+/+</sup> mice 7, 9 and 14 days after initiating STZ treatment (data displayed in Figures 9D,E). These data indicate that Ripk3<sup>-/-</sup> mice are protected from STZ-induced hyperglycemia and glucose intolerance *in vivo*.

## **Discussion**

Acquiring a better understanding of the mechanisms that underly  $\beta$ -cell death may lead to new treatments for diabetes, a disease in which  $\beta$ -cell loss results in insufficient insulin release and hyperglycemia<sup>30,242</sup>. TNF $\alpha$  has been recognized as a mediator of  $\beta$ -cell dysfunction and death in T1D for more than two decades<sup>243,244,246,247,250</sup>, and recent clinical studies found that treatment with TNF $\alpha$  neutralizing antibodies improves  $\beta$ -cell function in individuals with recently diagnosed T1D<sup>245,252</sup>. Although TNF $\alpha$  has been recognized as a cytotoxin for nearly 50 years<sup>277</sup>, the mechanisms by which TNF receptor

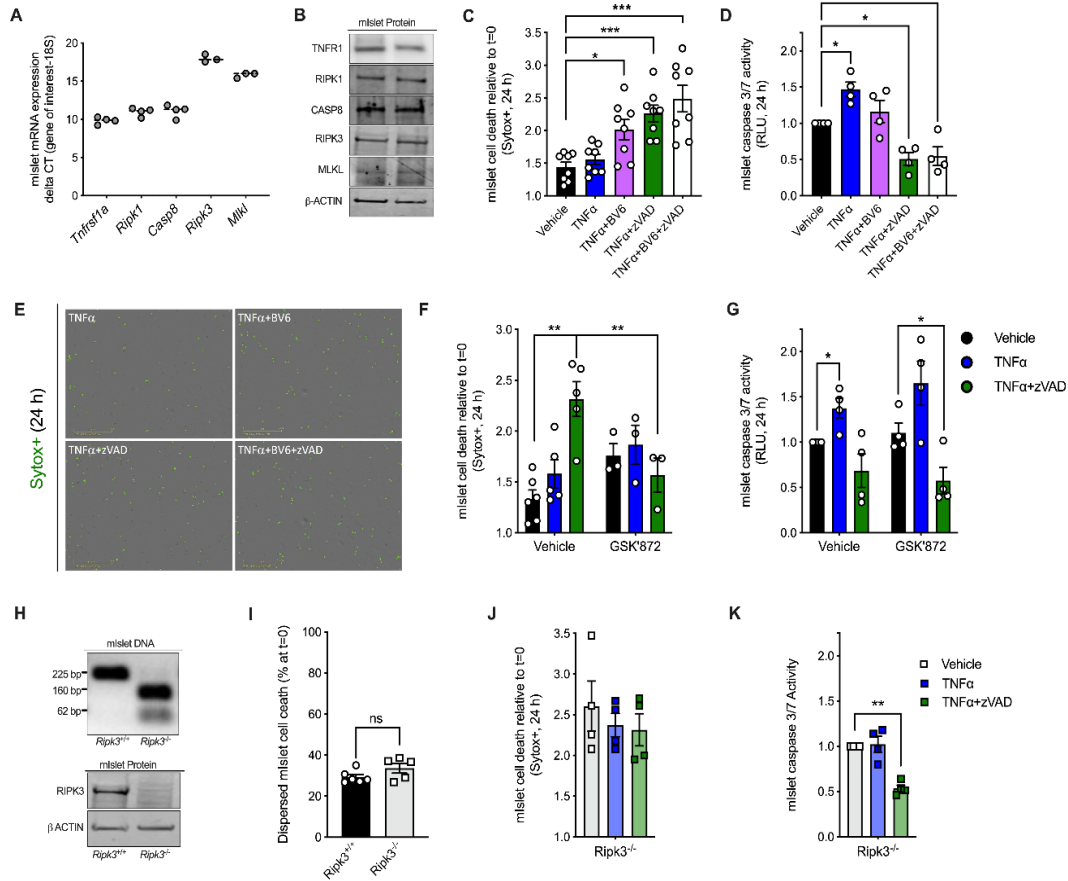


**Figure 8: Mouse islets cells are susceptible to TNF $\alpha$ -induced cell death when cIAPs or caspases are inhibited.**

A) Mouse islet cells express components of the TNF $\alpha$  signaling pathway at the RNA and B) protein levels. C) Mouse islet cell death was quantified 24 h post treatment relative to t=0 (n=8). Cell culture treatment conditions are indicated by color (black: vehicle, blue: 40 ng/ml TNF $\alpha$ , purple: TNF $\alpha$  + 5  $\mu$ M BV6, green: TNF $\alpha$  + 50  $\mu$ M zVAD, white: TNF $\alpha$ +BV6+zVAD. D) Mouse islet cell caspase 3/7 activity was quantified 24 h post treatment and expressed relative to vehicle treated cells (n=4). E) Representative IncuCyte images illustrate Sytox green positive mouse islet cells 24 h post treatment. F) Mouse islet cell death was quantified 24 h after treatment with vehicle, TNF $\alpha$  or

TNF $\alpha$ +zVAD in the absence (left) or in the presence (right) of the RIPK3 inhibitor GSK'872 (5 mM, n=3-5). G) Mouse islet cell caspase 3/7 activity was quantified 24 h after treatment with vehicle, TNF $\alpha$  or TNF $\alpha$ +zVAD in the absence (left) or in the presence (right) of the RIPK3 inhibitor GSK'872 (n=4). H) Mouse genotyping and islet immunoblot analysis confirmed loss of RIPK3 expression in Ripk3<sup>-/-</sup> compared to Ripk3<sup>+/+</sup> mice. I) Basal cell death rate was quantified in Ripk3<sup>+/+</sup> and Ripk3<sup>-/-</sup> mouse islet cells (n=5-6). J) Ripk3<sup>-/-</sup> mouse islet cell death was monitored for 24 h and quantified 24 h post treatment relative to t=0 (n=4). K) Mouse islet cell caspase 3/7 activity was quantified 24 h post treatment and expressed relative to vehicle treated cells (n=4). Data are presented as mean  $\pm$  SEM and were analyzed by Student's t-test or one-way ANOVA followed by Sidák post-test and multiple comparisons correction, as described. \* $p < 0.05$ ; \*\* $p < 0.01$ ; ns,  $p > 0.05$  as indicated.

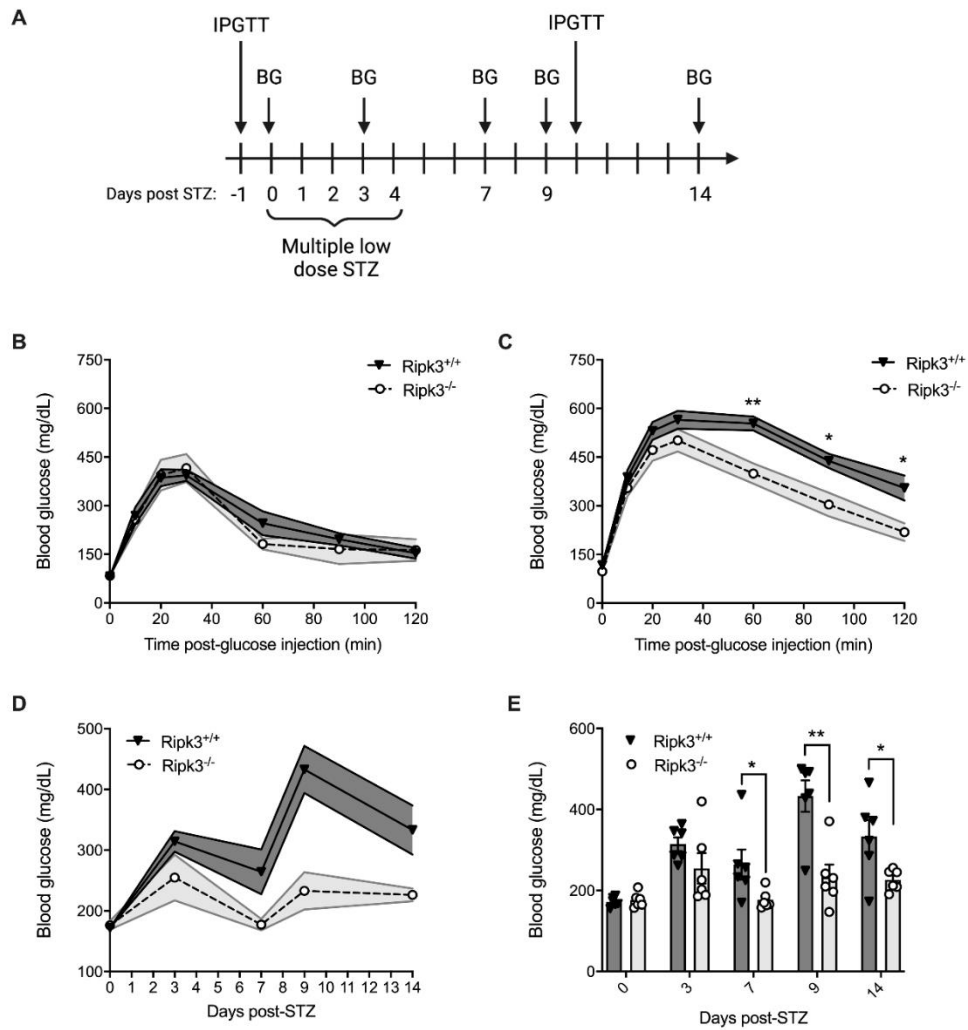


**Figure 9: Ripk3<sup>-/-</sup> mice are protected from STZ-induced hyperglycemia *in vivo*.**

A) Schematic of multiple low dose-streptozotocin (STZ) treatment and blood glucose monitoring. B) Prior to STZ treatment, glucose tolerance was evaluated by intraperitoneal glucose tolerance test (IPGTT) in Ripk3<sup>+/+</sup> and Ripk3<sup>-/-</sup> mice (n=6/group). C) 10 days after starting STZ treatment, glucose tolerance was evaluated by IPGTT in Ripk3<sup>+/+</sup> and Ripk3<sup>-/-</sup> mice (n=6/group). D,E) Non-fasting blood glucose was quantified in Ripk3<sup>+/+</sup> and Ripk3<sup>-/-</sup> mice 0, 3, 7, 9 and 14 days after STZ treatment (n=6/group), and data are displayed over time (D) and at individual time points (E). Data are presented as mean ±

SEM and were analyzed by Student's t-test. \* $p < 0.05$ ; \*\* $p < 0.01$ ; \*\*\* $p < 0.001$ ; ns,  $p > 0.05$ ; as indicated.

signaling elicit  $\beta$ -cell death have not been well characterized. In the present study, we applied knowledge from other cell types and utilized state-of-the-art, high-content live cell imaging and analysis techniques to test the hypothesis that RIPK1 and RIPK3 regulate TNF $\alpha$ -induced  $\beta$ -cell death in concert with caspase activity *in vitro*. Using NIT-1, INS-1 and isolated mouse islet cells and applying small molecule inhibitors of cIAPs, caspases and RIPK3, Ripk1 and Ripk3 gene editing, and RIPK3 overexpression and knockout models, we identified roles for RIPK1 and RIPK3 in regulation of TNF $\alpha$ -induced  $\beta$ -cell death and characterized factors that modify  $\beta$ -cell susceptibility to TNF $\alpha$ -induced cytotoxicity such as cIAPs, SMAC and caspase activation.

Previous studies have investigated TNF $\alpha$ -induced NF $\kappa$ B activation and FADD signaling in  $\beta$  cells<sup>246,247</sup>, but few have evaluated RIPK1, RIPK3 or MLKL<sup>191,278</sup>, components of TNF receptor signaling known to promote cell death in other cell types<sup>194,258,264</sup>. Notably, a recent study found that inhibition of RIPK1 promotes porcine islet viability and  $\beta$ -cell abundance<sup>191</sup>. In the present study, we found that NIT-1 RIPK1 $\Delta$  cells are strongly protected from TNF $\alpha$ -induced cell death (Figure 4A,B,C), that this is associated with reduced caspase 3/7 activation (Figure 4D), and that cIAPs repress TNF $\alpha$ -induced cell death in a RIPK1-dependent manner (Figure 4E,F), a mechanism that has been described in other cell types<sup>279,280</sup>.

Since protection of NIT-1 RIPK1 $\Delta$  cells from TNF $\alpha$ - and BV6-induced cell death was associated with decreased caspase 3/7 activity (Figure 4E-I), we interrogated the role of caspase activation in TNF $\alpha$ -induced  $\beta$ -cell death using zVAD, a small molecule pan-caspase inhibitor. Interestingly, TNF $\alpha$ +zVAD cotreatment significantly increased cell death in NIT-1 (Figure 5B,C) and INS-1 cells (Figure 5F,G), and this cell death occurred

in association with reduced caspase 3/7 activity (Figure 5D,H), suggesting a non-apoptotic form of caspase-independent cell death under these conditions. RNA sequencing revealed that a distinct transcriptional profile is present in TNF $\alpha$ +zVAD- compared to TNF $\alpha$ -treated INS-1 cells (Figure 5J,K), consistent with the idea that discrete mechanisms of TNF $\alpha$ -induced  $\beta$ -cell death occur when caspases are active versus inhibited. Interestingly, our RNA sequencing results identified lymphocyte expansion molecule (*Lexm*) and lymphocyte activation gene 3 (*Lag3*) as genes upregulated specifically by TNF $\alpha$ +zVAD treatment, suggesting that the form of cell death that occurs under these conditions is immune-relevant (Figure 5J). We further characterized this mechanism of caspase-independent  $\beta$ -cell death, observing that it is regulated downstream of TNF receptor signaling by cIAPs and RIPK1. We also observed that *Birc3*, the transcript for cIAP2, is significantly upregulated in response to either TNF $\alpha$  or TNF $\alpha$ +zVAD treatment (Figure 5J), indicating a role for cIAP2 in counter regulation of TNF $\alpha$ -induced  $\beta$ -cell death independent of caspase activity. Indeed, inhibition of cIAPs with BV6 also increased TNF $\alpha$ +zVAD induced cell death in a RIPK1-dependent manner (Figure 6A,B,C), revealing that NIT-1 and INS-1  $\beta$  cells are susceptible to a caspase-independent mechanism of TNF $\alpha$ -induced cell death that is regulated by cIAPs and RIPK1. Although either TNF $\alpha$  or TNF $\alpha$ +zVAD treatment significantly increased cell death in both NIT-1 and INS-1 cells, we found that the timing and magnitude of this cell death response varied between NIT-1 and INS-1 cells (Figure 4,5). These differences in susceptibility to TNF $\alpha$ - and TNF $\alpha$ +zVAD-induced cell death may be related to variations in expression of TNF receptor signaling components such as

caspase 8 and MLKL, which we found to be higher in NIT-1 versus INS-1 cells (Figure 3B).

Previous studies in non-islet cell types have shown that TNFR1 stimulation signals RIPK1 to activate RIPK3 under conditions of caspase inhibition, with RIPK3 then going on to promote necroptosis via MLKL<sup>264,281</sup>. Although apoptosis is widely viewed as the principal mechanism of  $\beta$ -cell death in diabetes<sup>282,283</sup>, necroptosis has recently been recognized as a form of programmed cell death that contributes to disease pathogenesis in disorders such as Alzheimer's disease and osteoarthritis<sup>267-269</sup>. Despite potential relevance to the islet inflammation and  $\beta$ -cell autoimmunity observed in T1D, however, non-apoptotic mechanisms of  $\beta$ -cell death have not been well studied<sup>284-286</sup>. Given our finding that  $\beta$  cells are susceptible to caspase-independent cell death, we evaluated the role of RIPK3 in this process. Consistent with the literature, we found that RIPK3 gene editing (Figure 7A,B) or small molecule inhibition of RIPK3 kinase activity (Figure 7C,D) abrogated TNF $\alpha$ -induced  $\beta$ -cell death when caspases were inhibited with zVAD. Moreover, we observed that RIPK3 co-immunoprecipitated with MLKL in RIPK3 overexpressing INS-1 cells following TNF $\alpha$ +zVAD treatment (Figure 7H,I). Notably, we also found that NIT-1 RIPK3 $\Delta$  cells exhibited reduced caspase 3/7 activation in response to TNF $\alpha$  treatment (Figure 7B), an outcome that did not arise with RIPK3 kinase inhibition in INS-1 cells (Figure 7D). These findings are in line with previous observations linking RIPK3 function with caspase 8 activation and apoptosis<sup>255,287</sup> and suggest that RIPK3 plays an important role in balancing  $\beta$ -cell fate decisions. Together, these data show that RIPK3 promotes TNF $\alpha$ -induced  $\beta$ -cell death when caspases are inhibited, indicative of  $\beta$  cell necroptosis.

In contrast to immortalized  $\beta$  cells<sup>246,247,288</sup>, mouse islet cells are known to be resistant to TNF $\alpha$ -induced cell death<sup>246,289</sup>, and our studies in mouse islet cells are consistent with these previous findings (Figure 8C,F). However, our studies revealed that small molecule inhibition of either cIAPs (with BV6) or caspases (with zVAD) sensitizes mouse islet cells to TNF $\alpha$ -induced cell death (Figure 6C). Notably, mouse islet cell death induced by TNF $\alpha$ +zVAD treatment was blocked by RIPK3 inhibition with GSK'872 (Figure 8F), and TNF $\alpha$ +zVAD treatment failed to increase cell death and in Ripk3<sup>-/-</sup> islet cells (Figure 8J). These data show that primary mouse islet cells are also susceptible to TNF $\alpha$ -induced, RIPK3-mediated cell death when caspases are inactivated. Together, our *in vitro* data indicate that therapeutic strategies targeting TNF receptor signaling molecules such as RIPK1 and RIPK3 could promote  $\beta$ -cell survival and improve glucose homeostasis in individuals with T1D.

In these studies, we examined dispersed islet cells to enable use of our high-content live cell imaging and analysis system. We found that these dispersed islet cells exhibited higher rates of basal cell death (Figure 8I) than did NIT-1 or INS-1 cells, and this may have limited the magnitude of primary islet cell death observed in our studies. Still, we identified clear changes in TNF $\alpha$ -induced mouse islet cell death under the conditions tested, and methodological advances may reveal even greater responses in future studies.

Some other drawbacks to our islet studies exist. The primary islet cell death measurements reported reflect all islet cell types and are not specific to  $\beta$  cells. Likewise, inhibition of RIPK3 with GSK'872 is expected to impact all islet cell types, and islets from Ripk3<sup>-/-</sup> mice exhibit knockout in all cell types. Thus, additional studies are needed to characterize the signaling pathways of interest specifically in primary  $\beta$  cells.

To evaluate the role of this signaling pathway in  $\beta$ -cell death *in vivo*, we subjected Ripk3<sup>+/+</sup> and Ripk3<sup>-/-</sup> mice to multiple low dose STZ, a  $\beta$ -cell toxin used to model the  $\beta$ -cell loss that occurs in T1D. Although glucose tolerance was not different between Ripk3<sup>+/+</sup> and Ripk3<sup>-/-</sup> mice prior to STZ treatment (Figure 9B), Ripk3<sup>-/-</sup> mice displayed significantly lower blood glucose than Ripk3<sup>+/+</sup> mice during IPGTTs 10 days after starting STZ (Figure 9C). In addition, Ripk3<sup>-/-</sup> mice exhibited reduced non-fasting blood glucose 7-, 9-, and 14-days after initiating STZ treatment (Figure 9D,E). Given that STZ selectively kills  $\beta$  cells, we ascribe the reduced hyperglycemia observed in Ripk3<sup>-/-</sup> mice to a protection from STZ-induced  $\beta$ -cell death. However, it is possible that loss of RIPK3 in tissues outside the islet contributed to the observed phenotype, and additional studies are required to determine whether loss of RIPK3 specifically in  $\beta$  cells improves glucose homeostasis in this model. Likewise, additional studies are needed to understand the roles of  $\beta$ -cell RIPK1 and RIPK3 in diabetogenic  $\beta$ -cell loss *in vivo*. For example, Zhao and colleagues found that loss of RIPK3 failed to protect transplanted islets from T cell-mediated destruction<sup>201</sup>, and ER stress was shown to promote RIPK3-dependent IL1 $\beta$  production and NF $\kappa$ B-mediated inflammation in mouse and human islets<sup>278</sup>. Thus, RIPK3 may have additional functions in the islet outside of those studied here. Evaluation of  $\beta$ -cell specific Ripk3 knockout mice would help to clarify the role of RIPK3 in these processes, and use of other models such as NOD mice and kinase dead Ripk1 D138N mice<sup>290</sup> are also needed to establish the relevance of TNF $\alpha$ -mediated  $\beta$ -cell loss in the pathogenesis of diabetes *in vivo*.

It has been hypothesized that  $\beta$ -cell necroptosis could promote islet autoimmunity, inflammation and  $\beta$ -cell loss in T1D<sup>167</sup>, but at this time it is not known how caspase

inactivation, which promotes RIPK3-mediated cell death *in vitro*, might occur *in vivo*. However, certain viruses inhibit caspase activity<sup>291,292</sup> and there is significant evidence linking viral infection with T1D onset<sup>293,294</sup>. Other factors associated with viral infection such as double stranded viral RNA<sup>295</sup> and IFN $\gamma$ <sup>296</sup> have also been shown to promote cell death via RIPK1 and RIPK3. Thus, studies to evaluate the relationship between caspase activity, viral responses and mechanisms of  $\beta$ -cell death are warranted. In the current study, we used a synthetic caspase inhibitor (zVAD) to prevent caspase activation. We attribute the ability of zVAD to promote RIPK3-mediated cell death to its inhibition of caspase 8, a molecule of central importance in regulating cell fate. Since zVAD is a pan-caspase inhibitor, however, it is possible that inhibition of caspases other than caspase 8 contributed to our findings. Although we confirmed that zVAD inhibits caspase 8 and caspase 3/7 activation, it is also possible that zVAD has unknown off-target effects. Studies using  $\beta$ -cell specific caspase 8 knockout mice are of interest to further characterize caspase-independent  $\beta$ -cell death.

#### Acknowledgment

All text and figures from studies in this section has been published as a part of a manuscript submitted to *Molecular Metabolism*<sup>168</sup>.

Contreras CJ, Mukherjee N, Branco RCS, Lin L, Hogan MF, Cai EP, Oberst AA, Kahn SE, Templin AT. RIPK1 and RIPK3 regulate TNF $\alpha$ -induced  $\beta$ -cell death in concert with caspase activity. *Mol Metab.* 2022 Aug 24;65:101582. doi:

10.1016/j.molmet.2022.101582. PMID: 36030035; PMCID: PMC9464965.

## **Chapter 4 – Investigating the role of RIPK1 in TNF $\alpha$ and IFN $\gamma$ -induced $\beta$ -cell cytotoxicity**

### **Introduction**

In this chapter, I aim to investigate the role of RIPK1 in  $\beta$ -cell cytotoxicity induced by proinflammatory cytokines, TNF $\alpha$  and IFN $\gamma$ . The focus is on understanding  $\beta$ -cell kinase signaling, gene expression profile and death triggered by these cytokines, and whether targeting RIPK1 alters these processes. Additionally, I examine the role of RIPK1 in mediating  $\beta$ -cell autoimmunity in T1D. In vivo transplantation experiments were conducted by Dr. Erica P. Cai's lab at Indiana Biosciences Research Institute and kinome profiling was performed in collaboration with Dr. Steve Angus at Indiana University School of Medicine.

In addition to genetic susceptibility, environmental factors like viral infections have been implicated in T1D pathogenesis. Interferons (IFNs) are cytokines that possess powerful immunomodulatory and antiviral properties that play a central role in pathological immune responses in autoimmune diseases. In the context of T1D, IFNs mediate inflammatory  $\beta$ -cell stress responses in part by increasing inflammatory gene expression, kinase signaling, and autoantigen presentation (<sup>188,297,298</sup>). IFNs mediate their effect via the JAK-STAT signaling pathway, resulting in upregulation of interferon-stimulated genes (ISG). We and others have observed that IFN $\gamma$ , in combination with TNF $\alpha$  induces  $\beta$ -cell death *in vitro* <sup>299</sup>. Interestingly, previously published literature shows that TNF $\alpha$  + IFN $\gamma$  treatment induces mouse islet cell death in a caspase 3-independent fashion <sup>156</sup>. Multiple studies have explored the role of IFN $\gamma$  treatment on islets that can lead to non-apoptotic forms of cell death. Two studies of IL-1 $\beta$  + IFN $\gamma$ -

mediated cell death in rat insulinoma cells and rat islets revealed that the loss of  $\beta$ -cell viability induced by these cytokines was not associated with increased caspase 3 activity or annexin V positivity<sup>154,155</sup>. Similarly, another study found that IFN $\gamma$  and synthetic double-stranded RNA induced NO-dependent necrosis of rat islet cells<sup>157</sup>.

Both TNF $\alpha$  and IFN $\gamma$  are proinflammatory cytokines known to be key mediators of  $\beta$ -cell cytotoxicity in T1D. Clinical studies aiming to reduce TNF $\alpha$  and IFN $\gamma$  signaling in individuals with early T1D have shown beneficial effects in increasing endogenous insulin production. Etanercept and golimumab, both targeted to inhibit TNF $\alpha$  signaling, have significantly improved C-peptide levels in new-onset T1D<sup>245,252</sup>. Additionally, a study has shown beneficial effect of JAK inhibitor, baricitinib, on recent onset T1D. Individuals who received baricitinib showed improved  $\beta$ -cell function, compared to placebo<sup>300</sup>. Inhibitors of JAK1 and JAK2 affect both IFN $\gamma$  production from T cells and JAK-STAT signaling in  $\beta$  cells<sup>301</sup>. These studies emphasize the importance of TNF $\alpha$  and IFN $\gamma$  signaling in early T1D pathogenesis.

IFNs also mediate expression of major histocompatibility (MHC) class I proteins on the surface of  $\beta$  cells<sup>302</sup>, another histopathological hallmark of T1D. This is associated with increased STAT1 phosphorylation and leads to production of chemoattractants that can increase the ability of cytotoxic CD8<sup>+</sup> T cells to target  $\beta$  cells<sup>303</sup>. Studies from Helen E. Thomas's group has shown that not only does IFN $\gamma$  lead to upregulation of MHC I expression of  $\beta$  cells, it is important for homing and proliferation of autoreactive T cells<sup>301</sup>.

RIPK1 is a known mediator of both TNF $\alpha$  and IFN $\gamma$  signaling in non-islet cell types. A study found that IFN $\gamma$ -induced necrosis proceeds via RIPK1-RIPK3 necrosome

formation, suggesting necroptotic cell death in mouse embryonic fibroblasts (MEFs) <sup>185</sup>.

In the previous chapter, we have shown that RIPK1 and RIPK3 can regulate TNF $\alpha$ -induced  $\beta$ -cell loss, in concert with caspase activation. In these studies, I aimed to explore whether RIPK1 regulates inflammatory gene expression, kinase signaling and cell death in  $\beta$  cells.

## **Results**

### **A. RIPK1 is a T1D-relevant mediator of TNF $\alpha$ + IFN $\gamma$ signaling in $\beta$ cells**

The cytotoxic functions of RIPK1 are regulated in part via its kinase activity <sup>187,304</sup>. We show that TNF $\alpha$ +IFN $\gamma$  treatment increases RIPK1 phosphorylation at Ser 166 in mouse islets and  $\beta$ iPSCs (Fig. 10A,B), suggesting initiation of necroptosis signaling in these cells. We explored to publicly available HPAP data and found that *Ripk1* expression is increased in T1D donors compared to non-diabetic control (Fig. 10C).

Immunofluorescence staining of human pancreas sections also revealed that RIPK1 is highly expressed in human  $\beta$  cells (Fig. 10D). These data indicate that RIPK1 is a crucial molecular component of TNF $\alpha$ + IFN $\gamma$ -mediated signaling in  $\beta$  cells.

### **B. RIPK1 mediates TNF $\alpha$ - and IFN $\gamma$ -relevant kinase signaling in a mouse $\beta$ cells**

To characterize the role of RIPK1 in  $\beta$ -cell kinase signaling, we performed kinome profiling to evaluate kinase signaling in control and *Ripk1* gene edited NIT-1  $\beta$ -cell line (Fig. 11A,B). First, kinome profiling revealed that RIPK1 kinase activity is reduced in RIPK1 gene edited (*Ripk1 $\Delta$ ) mouse NIT-1  $\beta$  cells. We found activity of TNF $\alpha$ - (IKKB, ASK1/3, JNK1/2/3, MLKL) and IFN $\gamma$ -(PKR, MTOR) related kinases to be differentially regulated in RIPK1 deficient cells. Several of these kinases have been linked to  $\beta$ -cell loss. For example, JNK was found to mediate TNF $\alpha$ + IFN $\gamma$ -induced MIN6N8 cell death,*

associated with production of ROS and loss of mitochondrial membrane potential<sup>305</sup>. Cytokine exposure increases PKR activity in INS1  $\beta$ -cells and rat islets<sup>306</sup>. These data indicate that RIPK1 contributes to T1D-relevant signaling in  $\beta$  cells.

### C. RIPK1 mediates TNF $\alpha$ - and IFN $\gamma$ -relevant gene expression in a mouse $\beta$ cells

Recent studies have uncovered roles for RIPK1 in regulating inflammatory gene expression<sup>187,307</sup>. The effects of RIPK1 on transcription has been attributed to I $\kappa$ B kinase (IKK) and NF $\kappa$ b, with this transcriptional regulation thought to modulate the pro-death actions of RIPK1<sup>308–310</sup>. To understand the role of RIPK1 in transcriptional regulation in  $\beta$  cells, we performed RNA sequencing (RNA seq) of control and RIPK1 gene edited (Ripk1 $\Delta$ ) mouse NIT-1  $\beta$  cells (Fig. 12A). These studies found striking effects of RIPK1 on  $\beta$ -cell gene expression that are relevant to  $\beta$ -cell cytotoxicity in T1D. Expression of TNF $\alpha$ - (*Nfkb1/2*, *Ask1/3*, *Jnk1/2*, *Casp3/7*, *Ripk3* and *Mkl1*) and IFN $\gamma$ - (*Jak1*, *Sting1*, *cGas*, *H2-K1*, *H2-Q2*, *H2-Q6*, *H2-Dma*) related transcripts were highly differentially regulated in RIPK1 deficient cells. We also found that loss of RIPK1 kinase activity in Ripk1<sup>D138N/D138N</sup> islets abrogated upregulation of several genes and caspase 3/7 activity increased by TNF $\alpha$ +IFN $\gamma$  treatment in wild type (WT) islets (Fig. 12B,C). These studies show that RIPK1 promotes TNF $\alpha$ - and IFN $\gamma$ - mediated  $\beta$ -cell cytotoxicity in part via roles on inflammatory gene expression.

### D. RIPK1 promotes TNF $\alpha$ +IFN $\gamma$ -induced cell death in mouse $\beta$ -cell lines

As mentioned previously, RIPK1 promotes both caspase-dependent apoptosis and caspase-independent necroptosis in non-islet cell types<sup>311,312</sup>. We have previously shown that RIPK1 mediates TNF $\alpha$ -induced  $\beta$  cells (see Chapter 3), and TNF $\alpha$ +IFN $\gamma$  induces activation of RIPK1 via phosphorylation in mouse  $\beta$  cells and human  $\beta$ iPSCs (Figure

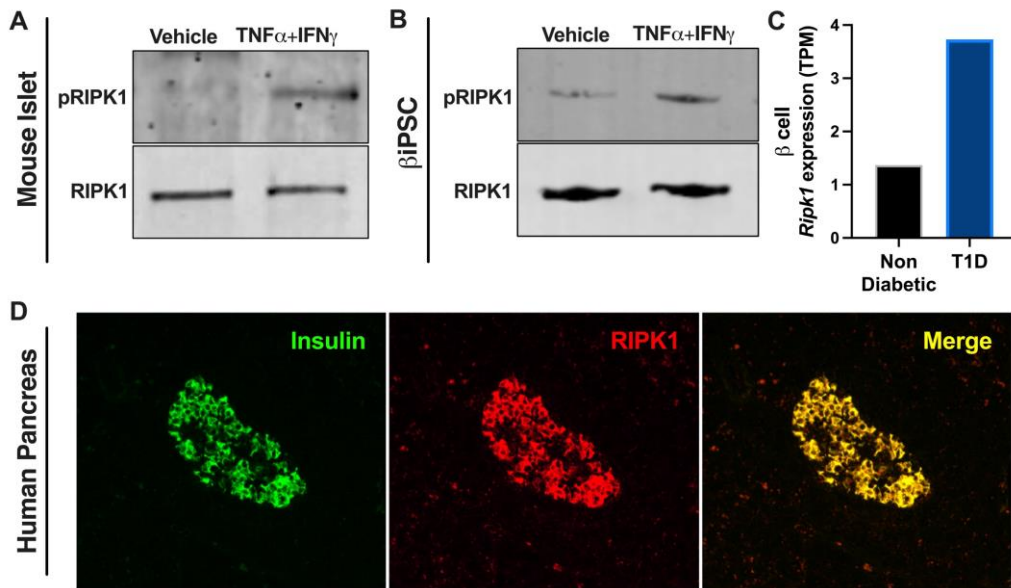


**Figure 10: RIPK1 is a T1D-relevant mediator of TNF $\alpha$ + IFN $\gamma$  signaling in  $\beta$  cells.** Phosphorylated RIPK1 and total RIPK1 expression observed in A) isolated mouse islet and B) human  $\beta$ -like iPSCs treated overnight with TNF $\alpha$ + IFN $\gamma$  (40ng/ml and 100ng/ml respectively). C) HPAP data showing *Ripk1* expression in  $\beta$  cells of non-diabetic (black bar) and T1D (blue bar) individuals. D) RIPK1 protein is abundant in human  $\beta$ -cells *in situ*.

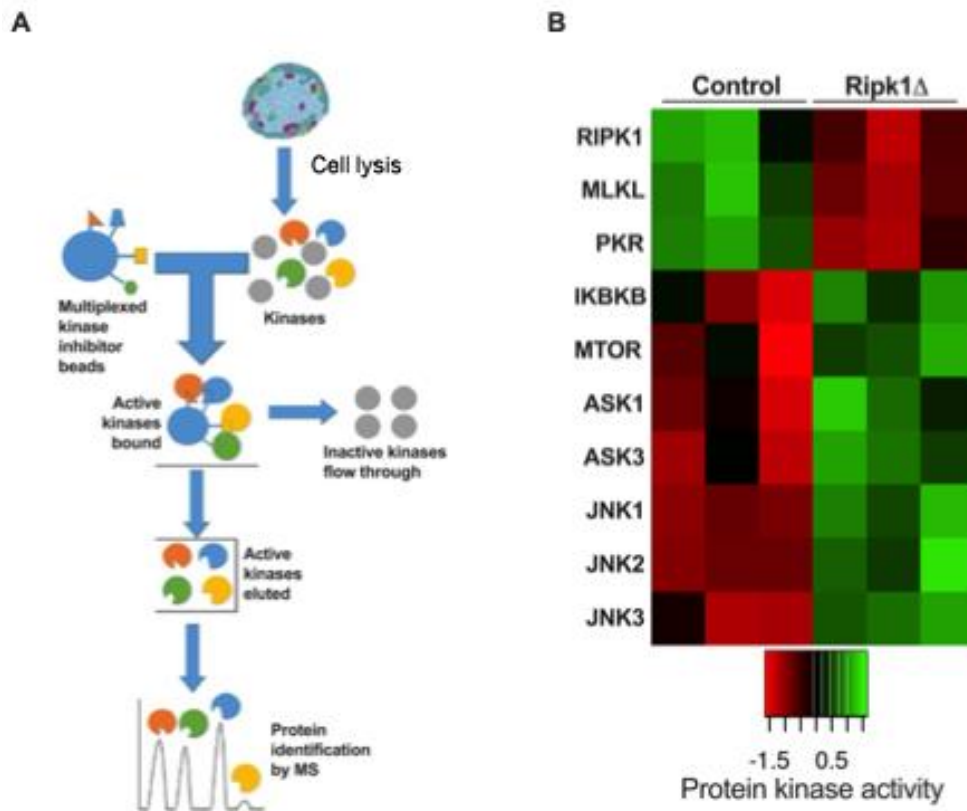


**Figure 11: RIPK1 mediates TNF $\alpha$ - and IFN $\gamma$ -relevant kinase signaling in a mouse  $\beta$  cells.**

A) Kinome profiling schematic adapted from Yu, Int J. Mol. Sci, 2021. B) Effects of RIPK1 on NIT-1  $\beta$ -cell kinase activity.

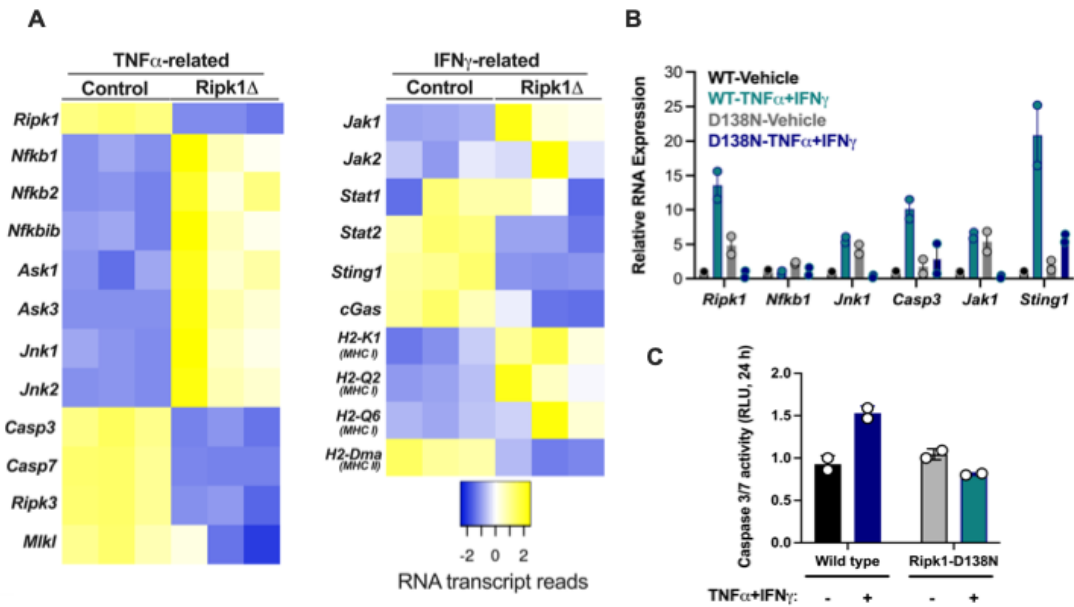


**Figure 12: RIPK1 mediates TNF $\alpha$ - and IFN $\gamma$ -relevant gene expression in a mouse  $\beta$  cells.**

A) RNA sequencing heatmap showing effects of RIPK1 on NIT-1  $\beta$ -cell TNF $\alpha$ - and IFN $\gamma$ -relevant RNA expression. B) RNA expression and C) Caspase 3/7 activity in WT and Ripk1<sup>D138N/D138N</sup> islets treated with TNF $\alpha$ + IFN $\gamma$  (40ng/ml and 100ng/ml respectively).

10A,B). To investigate whether RIPK1 kinase activation mediates TNF $\alpha$ +IFN $\gamma$ - induced  $\beta$ -cell death, we analyzed RIPK1 kinase inhibitor (SZM'679) treated native NIT-1 2055, NIT-1 CTL and MIN6-K8  $\beta$  cells (Fig. 13) *in vitro*. We observed that TNF $\alpha$ +IFN $\gamma$  induced significant cell death in all the cell types relative to vehicle (Fig. 13 A,B;D-G). Interestingly, the addition of SZM'679 reduced TNF $\alpha$ +IFN $\gamma$ - induced NIT-1 2055 and NIT-CTL cell death and caspase 3/7 activity (Fig. 13A-E), but not in MIN6-K8 (Fig. 13F,G)  $\beta$ -cell death. This data suggests that TNF $\alpha$ +IFN $\gamma$ - induced RIPK1 kinase activation is an important feature in NIT-1  $\beta$  cells, derived from a T1D mouse model. These findings indicate that RIPK1 kinase activity mediates TNF $\alpha$ +IFN $\gamma$ - induced NIT-1  $\beta$ -cell death *in vitro*.

#### E. RIPK1 kinase inhibition alters NIT 1 $\beta$ -cell MHC I expression *in vitro*

We have shown that RIPK1 mediated TNF $\alpha$ - and IFN $\gamma$ - relevant inflammatory gene expression and TNF $\alpha$ +IFN $\gamma$ - induced  $\beta$ -cell death. IFN $\gamma$  increases the expression of Class I major histocompatibility complex (MHC I), which is induced on  $\beta$  cells during destructive insulinitis.  $\beta$ -cell MHC I upregulation has been observed in human<sup>313-315</sup> and NOD mice<sup>316,317</sup>, and is temporally associated with initiation of insulinitis<sup>318</sup>. RIPK1 promotes inflammation via transcriptional regulation, kinase signaling and immunogenic cell death, but the role of RIPK1 in  $\beta$  cell-to-immune cell crosstalk has not been well characterized. We aimed to investigate the role of RIPK1 kinase activity in modulating IFN $\gamma$ -induced  $\beta$ -cell MHC I expression in native NIT-1 2055  $\beta$  cells *in vitro*. Overnight IFN $\gamma$  treatment induced increase in NIT-1 2055 MHC I expression (Fig. 14) and addition of small molecule RIPK1 kinase inhibitor, SZM' 679, significantly reduced this increase (Fig. 14 A,B). SZM'679 treatment alone does not alter NIT-1 2055 MHC I expression

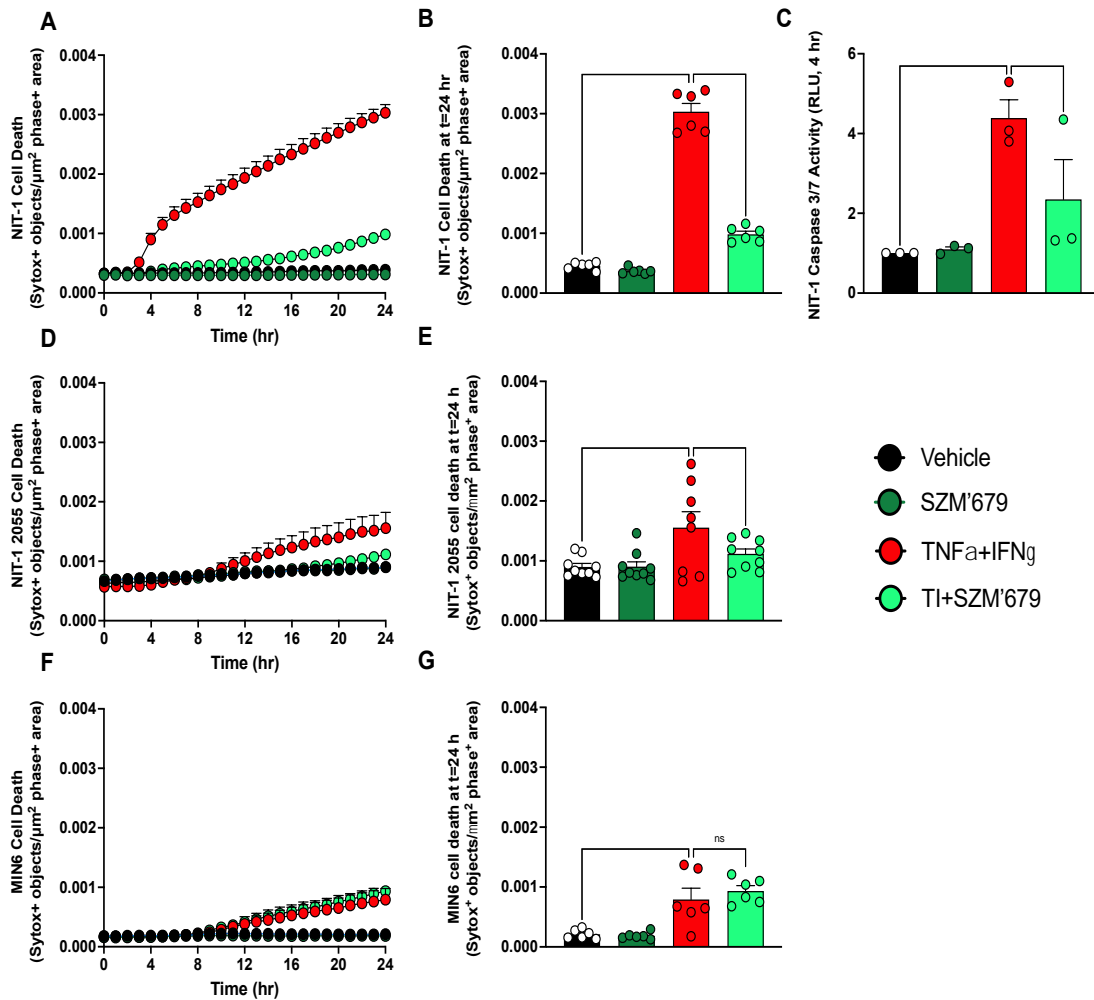


**Figure 13: RIPK1 promotes TNF $\alpha$ +IFN $\gamma$ -induced cell death in mouse  $\beta$ -cell lines.**

A) NIT-1 CTL B) NIT-1 2055 and F) MIN6K8 cell death was monitored over 24 h as described, and B,E and G) quantified at 24 h post treatment (n=6-7). C) NIT-1 CTL caspase 3/7 activity was measured at 4 h post treatment. Cell culture treatment conditions are indicated by color (black: vehicle, dark green: 1  $\mu\text{M}$  SZM'679, red: 40 ng/mL TNF $\alpha$ + 100ng/ml IFN $\gamma$ , light green: TNF $\alpha$ +IFN+SZM'679).

(data not shown). This data suggests that  $\beta$ -cell MHC I expression in NIT-1 2055 cells is dependent on RIPK1 kinase activity.

#### F. Loss of RIPK1 tend to protect transplanted $\beta$ cells from autoimmune-associated $\beta$ -cell loss

We next determined whether loss of RIPK1 in gene edited NIT-1 *Ripk1 $\Delta$*   $\beta$  cells protect from autoimmune-mediated  $\beta$ -cell killing after transplantation *in vivo*. NIT-1 CTL or *Ripk1 $\Delta$*  cells expressing firefly luciferase (*Luc2*) was transplanted on opposite flanks of 8-week-old female non-diabetic NSG mice lacking T-, B- and NK immune cells.

Following  $\beta$ -cell transplantation, we quantified *in vivo* graft luminescence by IVIS imaging after administration of splenocytes isolated from diabetic NOD mice. NIT-1 *Ripk1 $\Delta$*   $\beta$  cells were found to be protected from autoimmune-mediated killing compared to NIT-1 CTL cells (Fig. 15B-D). This indicates that functions of  $\beta$ -cell RIPK1 related to inflammatory gene expression, kinase signaling and/or cell death signaling participate in diabetic splenocyte-mediated  $\beta$ -cell death *in vivo*.

#### **Discussion**

$\beta$ -cell demise in T1D occur via 1) cytokine signaling that elicits immunogenic  $\beta$ -cell stress and 2) loss of immune tolerance leading to autoimmune  $\beta$ -cell destruction.  $\text{TNF}\alpha$  and  $\text{IFN}\gamma$  are major pro-inflammatory cytokines implicated to synergistically lead to  $\beta$ -cell death in T1D. While studies of cytokine induced  $\beta$ -cell death have primarily focused on caspase-dependent apoptosis, we and others have shown that cytokine signaling can induce caspase-independent forms of  $\beta$ -cell loss. Our previous studies have found that RIPKs play a crucial role in mediating caspase-independent necroptotic cell death in  $\beta$  cells. We found that *Ripk1* expression is upregulated in  $\beta$  cells from T1D versus non-

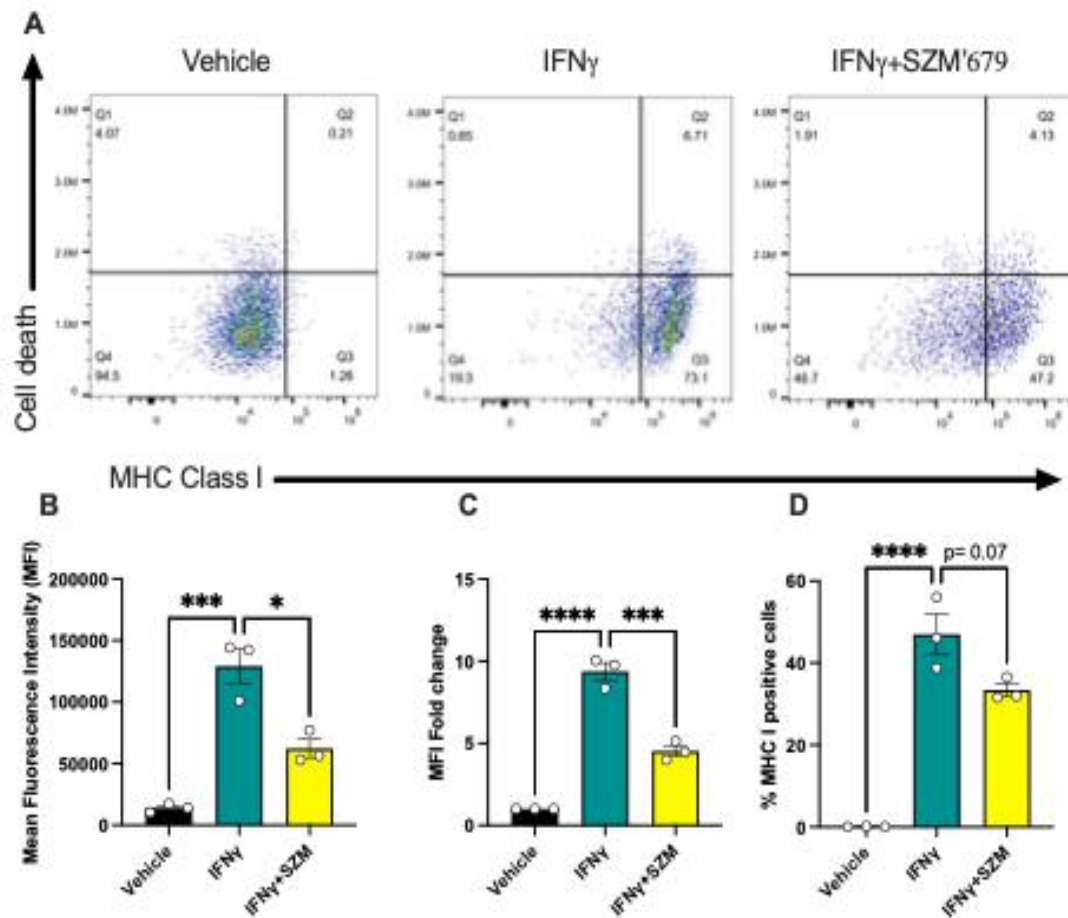


**Figure 14: RIPK1 kinase inhibition alters NIT 1  $\beta$ -cell MHC I expression *in vitro*.**

NIT-1 2055 cells were treated overnight and changes in MHC I expression was observed by flow cytometry. A) Representative plots are shown. B) Mean fluorescence intensity (MFI), C) MFI fold change and D) percent MHC I positive cells with vehicle (black), IFN $\gamma$  alone (2000IU/ml, teal) and IFN $\gamma$ +SZM'679 (1 $\mu$ M SZM'679) is shown.

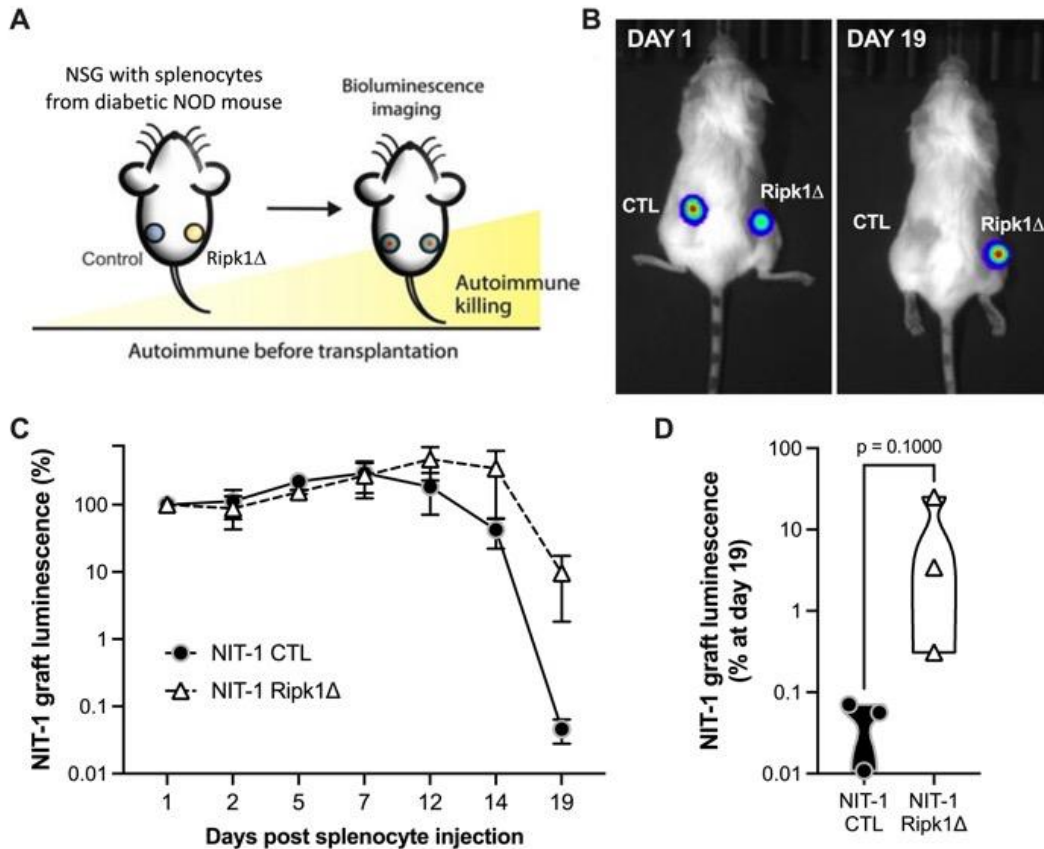


**Figure 15: NOD splenocyte-mediated killing of NIT-1 CTL and Ripk1Δ cells *in vivo*.**

A) Schematic of NIT-1 cell transplantation procedure. Briefly, NIT-1 CTL or Ripk1Δ cells expressing firefly luciferase (Luc2) was transplanted on opposite flanks of 8-week-old female non-diabetic NSG mice lacking T-, B- and NK immune cells. Following  $\beta$ -cell transplantation, *in vivo* graft luminescence was quantified by IVIS imaging (PerkinElmer) after administration of splenocytes isolated from anti-PD-L1 treated female NOD mice. B) Representative images of *in vivo* graft luminescence. C) Graft luminescence was monitored over 19 days and D) quantified at day 19 post diabetic splenocyte administration. (n=3)

diabetic organ donors<sup>188</sup> and human  $\beta$ -cells exhibit abundant RIPK1 protein expression *in situ* (Fig. 10C). RIPK1 has both kinase and scaffolding functions, and these mediate its action on inflammatory gene expression, caspase-dependent apoptosis and caspase-independent necroptosis. Although recent studies indicate RIPK1 has cytotoxic effects in  $\beta$  cells, the role of RIPK1 in autoimmune-associated  $\beta$ -cell loss in T1D is not well understood.

RIPK1 is a key shared mediator of TNF $\alpha$  and IFN $\gamma$  signaling in non-islet cell types<sup>259,319–322</sup>. In this chapter, we applied knowledge from other cell types to investigate how loss of  $\beta$ -cell RIPK1 expression or RIPK1 kinase function alters TNF $\alpha$ - and IFN $\gamma$ -induced gene expression, islet cell and  $\beta$ -cell death. We found that overnight treatment of TNF $\alpha$ +IFN $\gamma$  induces increased RIPK1 phosphorylation in mouse islets and  $\beta$ -like hiPSCs (Fig. 10 A,B), suggesting that TNF $\alpha$ +IFN $\gamma$ -induced  $\beta$ -cell cytotoxicity is mediated by RIPK1 kinase activity. We investigated whether RIPK1 deficiency alters activation of  $\beta$ -cell kinases. We found that RIPK1 deficiency alters several kinases known to have roles in TNF $\alpha$  and IFN $\gamma$  signaling, again emphasizing the role of RIPK1 in TNF $\alpha$  + IFN $\gamma$  signaling in  $\beta$  cells. Furthermore, we identified roles for RIPK1 in TNF $\alpha$ - and IFN $\gamma$ -related gene expression in NIT-1  $\beta$  cells and successfully observed similar gene expression patterns in islets obtained from kinase dead Ripk1<sup>D138N/D138N</sup> mice.

TNF $\alpha$  + IFN $\gamma$  can induce  $\beta$  cell death *in vitro*. We next aimed to understand whether small molecule RIPK1 kinase inhibition alters TNF $\alpha$  + IFN $\gamma$ -induced  $\beta$ -cell death. We found that RIPK1 kinase inhibition using SZM'679 successfully blocked TNF $\alpha$  + IFN $\gamma$ -induced cell death in NIT-1  $\beta$  cell lines (NIT-1 CTL and NIT-1 2055 cells), but not in MIN6K8 cells. This observation suggests that RIPK1 kinase activation may play a more

crucial role in T1D  $\beta$  cells compared to non-diabetic control  $\beta$  cells and could be a potential target to inhibit  $\beta$ -cell demise in early T1D. Future studies utilizing RIPK1 small molecule inhibitors to observe TNF $\alpha$  + IFN $\gamma$ -induced cell death of human  $\beta$ -like iPSCs derived from non-diabetic and T1D individuals would provide additional information on the relative importance of RIPK1 in diabetic versus non-diabetic  $\beta$  cell.

IFNs can induce  $\beta$ -cell MHC I expression, thereby promoting  $\beta$ -cell-to-immune cell crosstalk and  $\beta$ -cell autoimmune attack. We treated NIT-1 2055 cells with IFN $\gamma$  to observe increased MHC I expression. We next treated these cells with RIPK1 kinase inhibitor, SZM'679, and observed that SZM'679 treatment tends to reduce  $\beta$ -cell MHC I expression. To our knowledge, this is one of the first studies to show that RIPK1 kinase modulation is capable of altering  $\beta$ -cell MHC I surface expression, thereby influencing  $\beta$ -cell-to-immune cell interaction. Furthermore, RIPK1 deficient NIT-1 cells were found to be protected against autoimmune killing by splenocytes obtained diabetic NOD mice. This preliminary study characterized the role of RIPK1 in  $\beta$ -cell replacement therapy.

These studies have uncovered a novel role of RIPK1 in cytokine-induced  $\beta$ -cell cytotoxicity in T1D. Future studies will investigate whether  $\beta$ -cell specific RIPK1 deficiency protects NOD mice from spontaneous diabetes development. Further treatment of NOD mice with SZM'679 will allow us to investigate whether RIPK1 kinase inhibition can be a potential target to prevent or treat T1D.

## **Chapter 5 – Investigating the role of caspase 3/7 activation and RIPK1 kinase activity in endoplasmic reticulum stress-induced $\beta$ -cell death**

### **Introduction**

Endoplasmic reticulum (ER) stress is a major contributor of  $\beta$ -cell dysfunction and death, and studies in non-islet cell types have linked RIPKs to ER stress-induced caspase-independent cell death. In these studies, I first explore whether ER stress can induce caspase-independent  $\beta$ -cell death using  $\beta$ -cell lines and isolated mouse islets.

Additionally, I investigate if targeting RIPK1 alters ER stress-induced  $\beta$ -cell loss in vitro and hyperglycemia in vivo. Kinome profiling experiments was performed by Dr. Steve Angus at Indiana University School of Medicine.

One of the major contributors of  $\beta$ -cell dysfunction and death in both T1D and T2D has been attributed to ER stress. Monitoring protein flux through the ER is crucial to maintain ER homeostasis and avoid stress. Increased demand for insulin can often exceed the ER capacity, leading to accumulation of unfolded protein and ER stress. Moreover, established  $\beta$ -cell stressors such as free fatty acids and proinflammatory cytokines have been demonstrated to cause ER stress (see chapter 1). Under unresolved ER stress, the unfolded protein response (UPR) is activated which plays a significant role in determining cell survival and death. During periods of ER stress, the folding chaperone BiP is recruited away from PERK, ATF6 and IRE1, resulting in activation of these signaling intermediates. ATF4, CHOP, ATF6 and XBP1 proteins are generated, driving transcriptional responses intended to inhibit global translation and expansion of ER protein folding capacity to remediate ER stress. When the UPR fails to restore ER homeostasis, cell death efforts are activated. The primary mechanism of ER stress-

mediated cell death upon unresolved stress is apoptosis<sup>323</sup>. Apoptosis is majorly triggered by permeabilization of the outer mitochondrial membrane, governed by B-cell lymphoma 2 (BCL-2) associated protein family, leading to release of cytochrome c into the cytoplasm. This allows for formation of apoptosome and subsequent activation of procaspase-9<sup>324</sup>. Other mechanisms of mitochondrial membrane permeabilization, downstream of UPR activation, have also been recognized<sup>323</sup>.

While studies of ER-stress induced  $\beta$ -cell death has been majorly focused on caspase-driven apoptosis, Hagenlocher et al. has recently observed that inhibition of caspases using a pan-caspase inhibitor (QVD) failed to protect INS-1 and MIN6  $\beta$  cells from thapsigargin-induced cell death<sup>325</sup>. Studies in non-islet cell types have noted a role of RIPKs in mediating ER stress-induced cell death. Saveljeva et al. showed that several ER stress-inducing agents triggered TNFR1-mediated necroptosis in a mouse fibroblast cell line, independent of autocrine production of TNF $\alpha$ , and this cell death could be inhibited by RIPK1 inhibitor, necrostatin-1 (Nec-1)<sup>326</sup>. On the other hand, a novel CHOP activator was found to induce RIPK-driven necroptosis in A549 human lung cancer cells<sup>327</sup>. We have shown in the previous chapters that RIPK1 is an important mediator of TNF $\alpha$ - and IFN $\gamma$ -induced  $\beta$ -cell cytotoxicity. However, the role of RIPK1 in ER stress-induced  $\beta$ -cell death is not well understood.

In this chapter, I aim to investigate the role of caspase activation in ER stress-induced  $\beta$ -cell loss. Using a small molecule pan-caspase inhibitor (zVAD-FMK) and ER stress-inducing agents such as thapsigargin and tunicamycin, I investigate the role of caspase 3/7 activation in ER stress-induced islet cell and  $\beta$ -cell death. We found that while ER stress-induced  $\beta$ -cell loss occurs in concert with caspase 3/7 activation, inhibition of

caspases with zVAD-FMK fails to protect against thapsigargin- and tunicamycin-induced  $\beta$ -cell death. We hypothesized that this caspase-independent form of cell death is mediated by RIPK1. To investigate the role of RIPK1 in this caspase-independent form of  $\beta$ -cell death, utilizing small molecule RIPK1 kinase inhibitor (SzM'679), we investigate ER stress-induced  $\beta$ -cell death *in vitro*. To study the role of RIPK1 in ER-stress induced hyperglycemia *in vivo*, we opted to use control and RIPK1 kinase dead (*Ripk1*<sup>D138N/D138N</sup>) mice with spontaneous mutation in the insulin 2 gene (Akita mice), that leads to incorrect folding of the insulin protein producing ER stress and toxicity in pancreatic  $\beta$  cells.

## **Results**

### **A. Inhibition of caspase activity fails prevent ER stress-induced $\beta$ -cell death**

We initially aimed to confirm previous findings that caspase inhibition does not prevent thapsigargin-induced  $\beta$ -cell death<sup>325</sup>, utilizing our validated synthetic pan-caspase inhibitor (zVAD-FMK). Thapsigargin treatment strongly induced NIT-1 cell death after 48 h, and cell death was unaltered by addition of zVAD (Fig. 16). As expected, thapsigargin-induced cell death was associated with increased caspase 3/7 activity, while thapsigargin+zVAD treatment significantly reduced caspase 3/7 activity (Fig. 16A-C). In INS-1  $\beta$  cells, we again found that either thapsigargin alone or thapsigargin+zVAD treatment increased cell death significantly (Fig. 16D,E). We validated our findings in isolated mouse islets. We found that thapsigargin treatment increased islet cell death and addition of zVAD failed to prevent this increase in cell death (Fig. 16F,G). We next determined whether this phenomenon was specific to thapsigargin-induced  $\beta$ -cell death. We utilized another well-characterized ER stress-inducing agent, tunicamycin, to observe whether tunicamycin-induced  $\beta$ -cell death is dependent on caspase activation.

Interestingly, tunicamycin treatment had similar effects to thapsigargin treatment, and addition of zVAD again failed to protect from tunicamycin-induced cell death (Fig. 17A-E). These data indicate that although ER stress induces cell death in association with caspase activation, inhibition of caspase activation fails to protect against ER stress-induced  $\beta$ -cell death. This suggests that ER stress may elicit non-apoptotic forms of  $\beta$ -cell death in diabetes.

B. Ripk1 CRISPR-gene edited NIT-1  $\beta$  cells are resistant to ER stress-induced death independent of caspase activity

We next studied RIPK1 deficient NIT-1 Ripk1 $\Delta$   $\beta$  cells to determine whether RIPK1 plays a role in ER stress-induced NIT-1 cell death. We found that in comparison to control cells, NIT-1 Ripk1 $\Delta$  cells were strongly protected from thapsigargin- or tunicamycin-induced cell death both when caspases were active and when they were inhibited (Fig. 18A,B and D,E). Caspase 3/7 activation was significantly reduced in RIPK1-deficient NIT-1 Ripk1 $\Delta$   $\beta$  cells (Fig. 18C), which is consistent with the requirement of RIPK1 for caspase activation.

C. RIPK1 kinase inhibition fails to protect against thapsigargin-induced NIT-1  $\beta$ -cell death

RIPK1 kinase domain phosphorylates its downstream target, RIPK3, to induce necroptotic cell death. RIPK1 mediated necroptosis signaling downstream of TNF $\alpha$  is well studied, and we have previously shown that small molecule RIPK1 kinase inhibition, using SZM'679, significantly reduced TNF $\alpha$ +IFN $\gamma$ -induced NIT-1 cell death. To investigate the role of RIPK1 kinase activity in thapsigargin-induced  $\beta$ -cell death, we next treated NIT-1 CTL cells with thapsigargin, in the presence or absence of SZM'679.

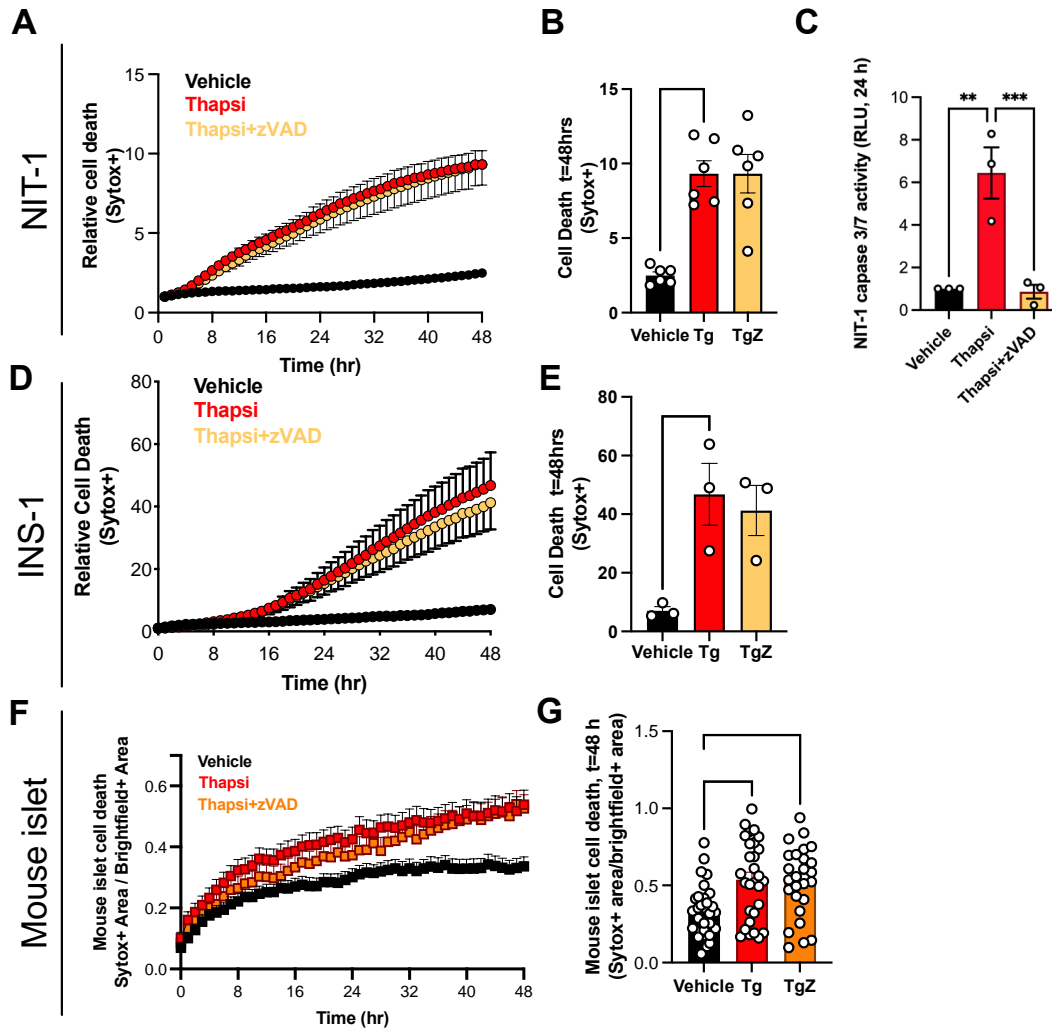


**Figure 16: Inhibition of caspase activity does not prevent thapsigargin-induced  $\beta$ -cell death.**

A Sartorius IncuCyte S3 live cell imaging and analysis instrument was used to monitor cell death via quantification of Sytox green positive cells. Cell culture treatment conditions are indicated by color (black: vehicle, red: 50 nM Thapsigargin, orange: Thapsigargin+zVAD, 50  $\mu$ M zVAD). A) NIT-1 CTL, D) INS-1 and F) mouse islet cell death was monitored for 48 h following treatment. B, E, G) cell death was quantified at 48 h. C) NIT-1 caspase 3/7 activity was measured at 24 h post-treatment. Data are presented

as mean  $\pm$  SEM and were analyzed by Ordinary one-way ANOVA. \* $p < 0.05$ ; \*\* $p < 0.01$ ;  
\*\*\* $p < 0.001$ ; ns,  $p > 0.05$ ; as indicated.

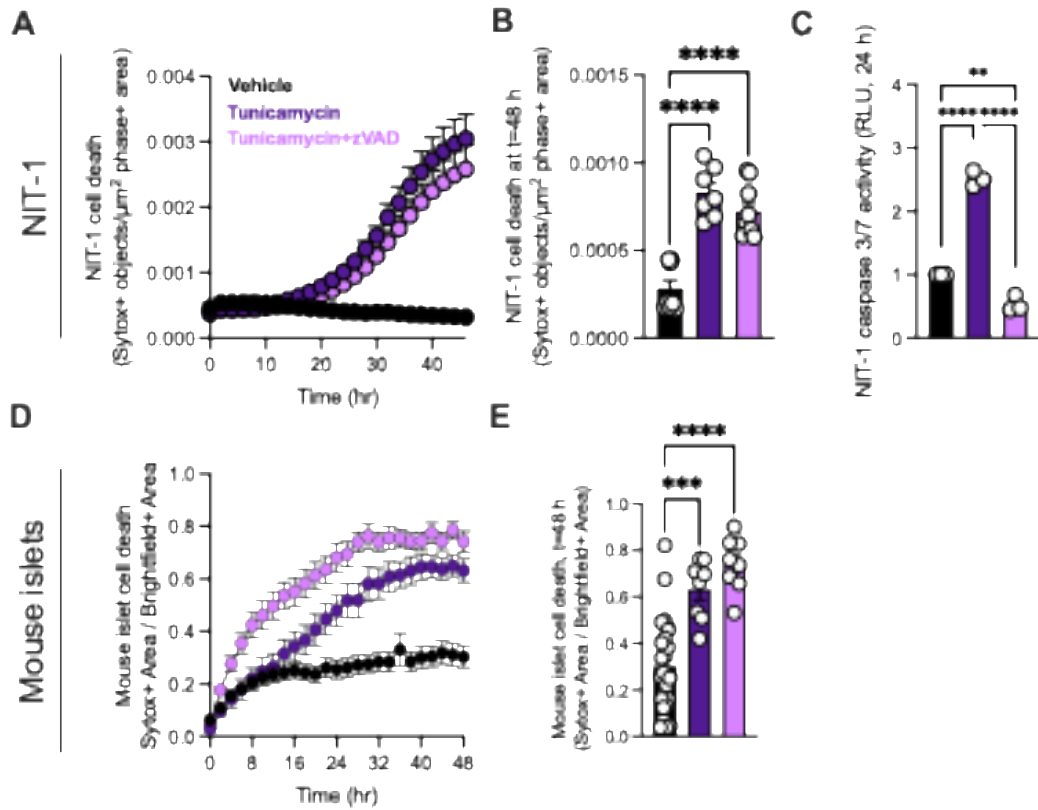


**Figure 17: Inhibition of caspase activity does not prevent tunicamycin-induced  $\beta$ -cell death.**

Cell culture treatment conditions are indicated by color (black: vehicle, purple: 1  $\mu$ M Tunicamycin, violet: Tunicamycin+zVAD, 50  $\mu$ M zVAD). A) NIT-1 CTL, D) mouse islet cell death was monitored for 48 h following treatment. B,E) cell death was quantified at 48 h. C) NIT-1 caspase 3/7 activity was measured at 24 h post-treatment. Data are presented as mean  $\pm$  SEM and were analyzed by Ordinary one-way ANOVA. \* $p$  < 0.05; \*\* $p$  < 0.01; \*\*\* $p$  < 0.001; \*\*\*\* $p$  < 0.0001; ns,  $p$  > 0.05; as indicated.

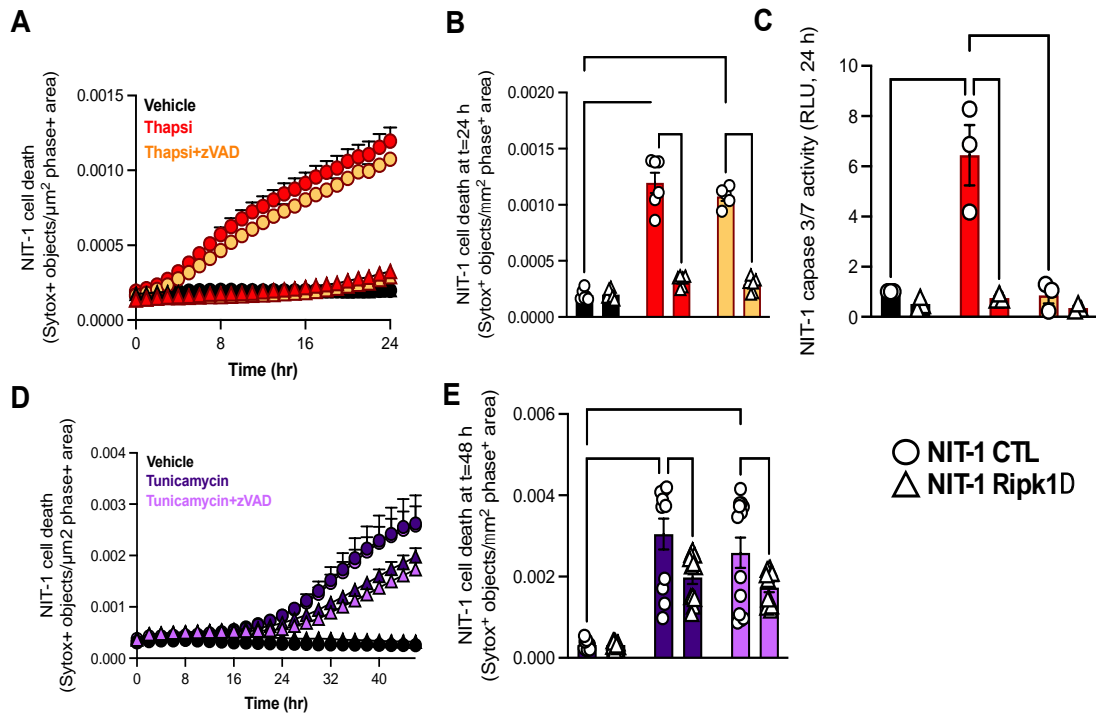


**Figure 18: Ripk1 CRISPR-gene edited NIT-1  $\beta$  cells are resistant to ER stress-induced death independent of caspase activity.**

Cell culture treatment conditions are indicated by color (black: vehicle, red: 50 nM Thapsigargin, orange: Thapsigargin+zVAD, purple: 1  $\mu$ M Tunicamycin, violet: Tunicamycin+zVAD).  $\beta$ -cell lines are indicated by shapes (NIT-1 CTL: circles, NIT-1 RIPK1 $\Delta$ : triangles). A) Cell death was monitored over 24 h and B) quantified at 24 h. C) NIT-1 caspase 3/7 activity was measured at 24 h. Data are presented as mean  $\pm$  SEM and were analyzed by 2-way ANOVA. \* $p < 0.05$ ; \*\* $p < 0.01$ ; \*\*\* $p < 0.001$ ; \*\*\*\* $p < 0.0001$ ; ns,  $p > 0.05$ ; as indicated.

Interestingly, SMZ'679 failed to protect against thapsigargin-induced NIT-1 cell death over 24 h (Fig. 19A-C). Furthermore, in contrast to the role of SZM'679 in reducing TNF $\alpha$ +IFN $\gamma$  caspase 3/7 activation in NIT-1  $\beta$  cells (refer to Fig. 13C of chapter 4), thapsigargin-induced caspase 3/7 activation was unaltered with addition of SZM'679 (Fig. 19C). These data indicate a unique kinase independent role of RIPK1 in mediating ER-stress induced  $\beta$ -cell loss.

D. RIPK1 kinase dead mice are not protected from ER stress-induced hyperglycemia *in vivo*

We generated RIPK1 kinase dead mice with Akita mutation to study the role of RIPK1 kinase activation in ER stress-induced hyperglycemia. The Akita strain is a well-characterized monogenic model with spontaneous mutation in the insulin 2 gene, leading to misfolding of insulin protein. This is known to result in  $\beta$ -cell toxicity, reduced  $\beta$ -cell mass and reduced insulin secretion. Akita mice used for this study were on a C57BL/6J background and develop hyperglycemia, hypoinsulinemia, polydipsia and polyuria by 3-4 weeks of age. Although diabetic phenotype is known to be more severe and progressive in male mice versus females, we chose to monitor both male and female mice to account for sexual difference in phenotype.

We monitored blood glucose levels in male and female wild type (Ripk1<sup>+/+</sup> and Akita.Ripk1<sup>+/+</sup>) and RIPK1 kinase dead (Ripk1<sup>D138N/D138N</sup> and Akita.Ripk1<sup>D138N/D138N</sup>) mice from 5 to 10 weeks of age. We observed that both male and female Ripk1<sup>+/+</sup> and Ripk1<sup>D138N/D138N</sup> mice had similar blood glucose levels over the 5 weeks (Fig. 20). In contrast, the Akita.Ripk1<sup>+/+</sup> and Akita.Ripk1<sup>D138N/D138N</sup> mice had significant hyperglycemia, starting at 5 weeks of age. However, the loss of RIPK1 kinase

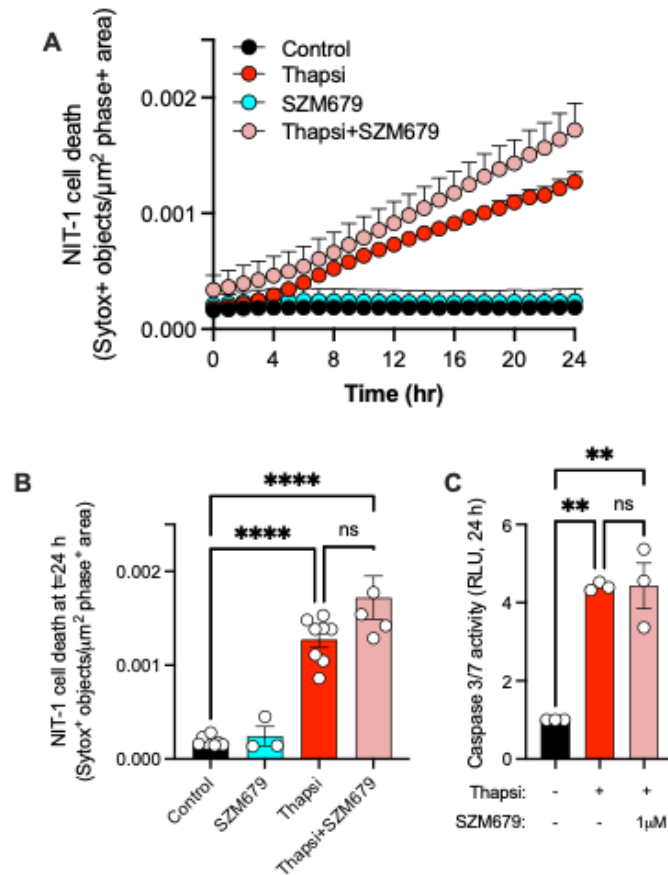


**Figure 19: RIPK1 kinase inhibition fails to protect against thapsigargin-induced NIT-1  $\beta$ -cell death.**

Cell culture treatment conditions are indicated by color (black: vehicle, red: 50 nM Thapsigargin, blue: 1  $\mu\text{M}$  SZM'679, peach: Thapsigargin+SZM'679). NIT-1 cell death was A) monitored over 24 h, and B) quantified at 24 h. NIT-1 caspase 3/7 activity was measured at 24 h post treatment. Data are presented as mean  $\pm$  SEM and were analyzed by one-way ANOVA. \* $p < 0.05$ ; \*\* $p < 0.01$ ; \*\*\* $p < 0.001$ ; \*\*\*\* $p < 0.0001$ ; ns,  $p > 0.05$ ; as indicated.

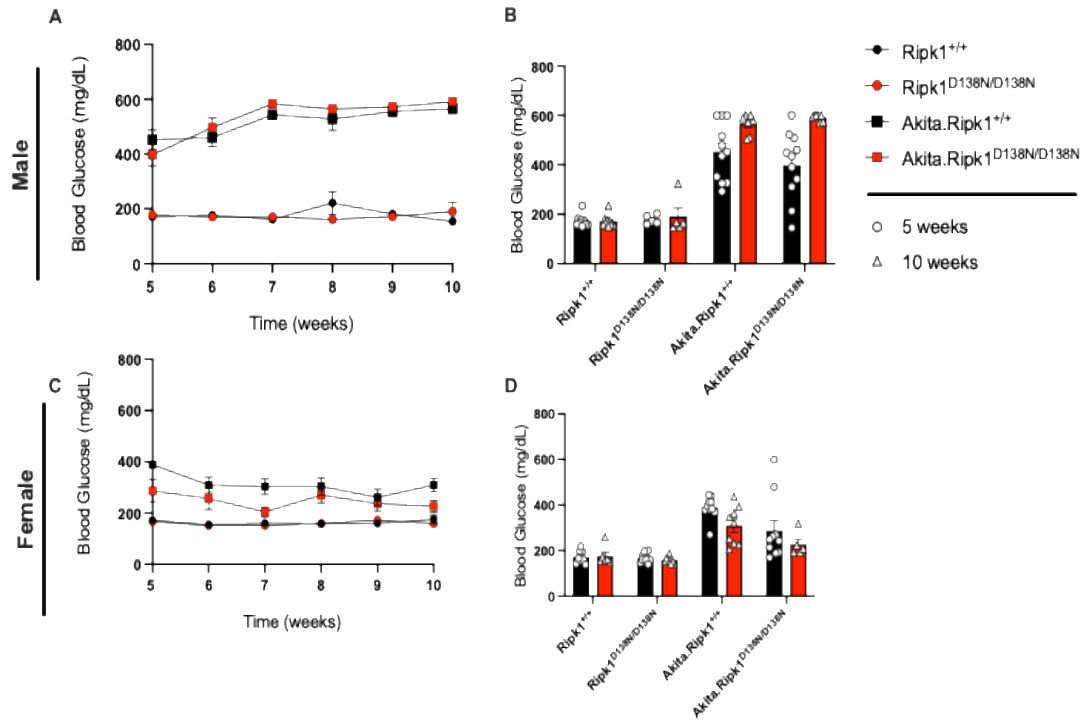


**Figure 20: RIPK1 kinase dead mice are not protected against ER stress-induced hyperglycemia *in vivo*.**

Blood glucose was monitored in A) male and C) female Ripk1<sup>+/+</sup> (black, circles), Ripk1<sup>D138N/D138N</sup> (red, circles), Akita.Ripk1<sup>+/+</sup> (black, squares) and Akita.Ripk1<sup>D138N/D138N</sup> (red, squares) from 5- to 10-weeks of age. B,D) Blood glucose quantified at 5 (circles) and 10 (square) weeks of age.

activation failed to protect against hyperglycemia in Ripk1<sup>D138N/D138N.Akita</sup> mice (Fig. 20).

These data indicate that RIPK1 kinase activation does not mediate development of diabetic phenotype in mice bearing *Ins2*<sup>Akita</sup> mutation.

## **Discussion**

In  $\beta$  cells, the ER plays a crucial role as the site for assembly and processing of insulin, which accounts for almost half of the total protein production in the cell. Unresolved ER stress can activate cell death signaling. Apoptosis is however not the only way for a cell to die. In the previous chapters, we have investigated the susceptibility of  $\beta$  cells to pro-inflammatory cytokine induced necroptosis, an inflammatory form of PCD. Since ER stress plays a crucial causative role in  $\beta$ -cell loss and onset of both T1D and T2D, there is a critical need for a better understanding of the molecular mechanisms that can regulate ER stress-mediated death, with the hope to identify new therapeutic targets to prevent or cure diabetes.

In this chapter, I aim to understand whether caspase activation is crucial for ER stress-induced  $\beta$ -cell death. In line with previously published data<sup>325</sup>, we observed that commonly used ER stress-inducing agents such as thapsigargin and tunicamycin led to  $\beta$ -cell caspase 3/7 activation and cell death, indicating apoptotic cell death as primary mode of ER stress-induced  $\beta$ -cell loss. However, inhibition of caspase activation using a pan-caspase inhibitor (zVAD-FMK) failed to prevent  $\beta$ -cell death. It is possible that although apoptosis is the primary route a  $\beta$  cell may choose to die, inhibiting this pathway may induce a switch to necrotic forms of cell death. Our RIPk1 small molecule kinase inhibition (SZM'679) data is also similar to Hagenlocher et al.'s data where use of a

different RIPK1 small molecule kinase inhibitor (Nec-1) had failed to protect INS-1 and MIN6  $\beta$  cells from thapsigargin-induced cell death.

It is important to understand the different modalities of  $\beta$ -cell death downstream of different  $\beta$ -cell stressors. Several recent studies in non-islet cell types have identified alternative cell death induction by ER stress including autophagic cell death, necroptosis, pyroptosis, as well as ferroptosis<sup>328</sup>. Extending on my study of RIPKs in  $\beta$  cell cytotoxicity, I questioned whether ER stress induced-cell death was dependent on RIPK1. While RIPK1 deficiency in NIT-1 *Ripk1 $\Delta$*  cells strongly protected against thapsigargin and tunicamycin-induced  $\beta$ -cell death, inhibition of RIPK1 kinase activation using either a small molecule inhibitor or a genetic model of kinase dead mutation failed to protect against ER stress-induced  $\beta$ -cell *in vitro* or hyperglycemia *in vivo*. These data suggest that although RIPK1 might play a role in ER stress-mediated  $\beta$ -cell death, it is unlikely that this requires RIPK1 kinase activation. Although RIPK1 kinase dead mice were not protected from hyperglycemia in Akita mice, it is possible that the *Ins2<sup>Akita</sup>* mutation is too robust to see differences in glucose homeostasis *in vivo*, that cannot be restored by *Ripk1<sup>D138N/D138N</sup>* mutation. Future studies may focus on investigating a dose dependent effect of thapsigargin- or tunicamycin- induced cell death in isolated islets obtained from WT (*Ripk1<sup>+/+</sup>*) and *Ripk1<sup>D138N/D138N</sup>* *in vitro*.

As discussed previously, RIPK1 is a multifunctional protein with distinct kinase and scaffolding functions. Although, ER stress-inducing necroptosis has been discovered, there is still significant discrepancy in literature that has led to lack of precise molecular mechanism. Our results indicate that in  $\beta$  cells, RIPK1 kinase function might not be crucial in eliciting ER stress-mediated cell cytotoxicity. Since *Ripk1<sup>-/-</sup>* mice are

embryonically lethal, future studies utilizing RIPK1 specific PROTAC (protein targeting chimera) that temporally and efficiently degrades the protein <sup>329</sup>, or a small molecule inhibitor targeted towards the scaffolding domain of RIPK1 can expand our knowledge on its role in ER stress-induced  $\beta$ -cell loss.

## **Chapter 6 – RIPK3 promotes islet amyloid-induced $\beta$ -cell loss and glucose intolerance in a humanized mouse model of T2D**

### **Introduction**

RIPK3 has been recently implicated in cell death and inflammation in amyloid-associated neurodegenerative diseases. However, the role of RIPK3 in islet amyloid-associated  $\beta$ -cell cytotoxicity is unknown. In this chapter, I investigate the role of RIPK3 in islet amyloid-induced  $\beta$ -cell cytotoxicity and islet inflammation. I develop techniques to visualize islet amyloid deposition, cell death and caspase 3/7 activation in amyloid-prone mouse islets in real-time. Furthermore, I generate and utilize an amyloid-prone whole-body RIPK3 knockout mice to investigate if loss of RIPK3 protects against amyloid-associated glucose intolerance and  $\beta$ -cell loss in vivo. In vitro islet function data were generated by Dr. Michael Kalwat at Indiana Biosciences Research Institute. In vivo GSIS data were generated in collaboration with the Islet Physiology Core and Translational Core at Indiana University School of Medicine. Macrophage depleted islets were generated by Dr. Steven Kahn's laboratory at University of Washington, Seattle.

Type 2 diabetes (T2D) is a global epidemic characterized by insulin resistance, loss of functional  $\beta$ -cell mass and hyperglycemia<sup>331,332</sup>. Islet amyloid deposits are present in the majority of individuals with T2D, where they are associated with islet inflammation, decreased  $\beta$ -cell mass and increased  $\beta$ -cell death<sup>20,87,88,94</sup>. Islet amyloidosis occurs via aggregation of human islet amyloid polypeptide (hIAPP), a  $\beta$ -cell secretory product that is co-secreted with insulin<sup>58,333</sup>. In contrast to hIAPP, rodent IAPP (rIAPP) does not aggregate to form amyloid<sup>333,89</sup>, so mouse models with  $\beta$ -cell expression of hIAPP have been developed to model islet amyloidosis in T2D<sup>334,335</sup>. Several studies have found that

oligomeric forms of hIAPP directly elicit  $\beta$ -cell cytotoxicity, either by disrupting cell membranes<sup>89,90,336,337</sup> or by inducing receptor-mediated cell death signaling<sup>91,338</sup>. In addition, islet amyloid formation is thought to mediate  $\beta$ -cell loss by eliciting cytokine (*Il1 $\beta$* , *Tnf*, *Il6*) and chemokine (*Ccl2*, *Cxcl1*) production from islet macrophages<sup>93,94,237,339</sup>. Although prior research has established that amyloid formation is an important mediator of islet inflammation and  $\beta$ -cell cytotoxicity in T2D, the molecular mechanisms that underlie this process remain incompletely understood.

Recent studies of amyloid-induced cytotoxicity in Alzheimer's disease (AD) identified receptor interacting protein kinase 3 (RIPK3) as a mediator of neuronal cell loss in this disease<sup>267,340,341</sup>. RIPK3 is a multifunctional protein that regulates inflammation and cell death signaling in diverse cell types including neurons<sup>267</sup>, hepatocytes<sup>342</sup>, immune cells<sup>343</sup> and  $\beta$  cells<sup>168,278</sup>. RIPK3 promotes inflammation in part by mediating IL-1 $\beta$ , IL-6, CXCL1 and CCL2 synthesis<sup>343–345</sup>, and it also participates in apoptotic and necroptotic cell death signaling via effects on caspase activation<sup>255,346</sup> and mixed lineage kinase domain like pseudokinase (MLKL) phosphorylation, respectively<sup>342,347</sup>. Yang and colleagues previously showed that RIPK3 promotes islet inflammation following ER stress<sup>278</sup>, and we recently reported that RIPK3 contributes to TNF $\alpha$ -induced  $\beta$ -cell death<sup>168</sup>. However, the role of RIPK3 in islet amyloid-induced  $\beta$ -cell cytotoxicity and hyperglycemia has not been evaluated previously.

We hypothesized that RIPK3 mediates amyloid-induced  $\beta$ -cell loss and hyperglycemia in T2D. To test this hypothesis, we used a well characterized humanized mouse model of T2D with  $\beta$ -cell specific expression of hIAPP that develops endogenous islet amyloid deposits both *in vitro* and *in vivo*<sup>334,238,348–350</sup>. We performed *in vitro*

studies to quantify islet amyloid deposition, islet cell death and caspase 3/7 activity in real-time using islets isolated from WT, Ripk3<sup>-/-</sup>, hIAPP and hIAPP;Ripk3<sup>-/-</sup> mice. We evaluated hIAPP-stimulated inflammatory gene expression in WT and Ripk3<sup>-/-</sup> bone marrow derived macrophages (BMDM) *in vitro*, and we characterized the role of RIPK3 in glucose stimulated insulin secretion (GSIS) *in vitro* and *in vivo*. Finally, we performed *in vivo* studies to examine body weight, glucose homeostasis, islet amyloid deposition and  $\beta$ -cell area in WT, Ripk3<sup>-/-</sup>, hIAPP and hIAPP;Ripk3<sup>-/-</sup> mice in response to HFD feeding. To our knowledge, this study is the first to evaluate the role of RIPK3 in HFD- and islet amyloid-induced b-cell cytotoxicity and hyperglycemia in a mouse model of T2D.

## **Results**

### **A. Real time quantification of islet amyloid deposition, islet cell death and caspase 3/7 activity *in vitro***

We first quantified endogenous islet amyloid formation, islet cell death and caspase 3/7 activity in wild type mouse islets that express non-amyloidogenic rIAPP (WT) and hIAPP islets that express amyloidogenic hIAPP (hIAPP) following culture in 16.7mM glucose media for 96 h. These experiments utilized a high-content live cell imaging and analysis platform that enables quantification of parameters of interest in real time in intact islets. Using Thioflavin S to visualize amyloid fibrils<sup>351</sup>, we found that amyloid deposits were present in hIAPP islets starting 24 h after culture in 16.7 mM glucose media (Figure 21A). Significant islet amyloid deposition was present in hIAPP islets after 48 h and 96 h of culture (Figure 21B-D), while as expected amyloid deposits were not observed in WT islets at any time during the 96 h culture period (Figure 21A-D). We

next quantified islet cell death in real time using Sytox green, a membrane impermeable DNA binding dye<sup>352</sup>. We found that 16.7 mM glucose treatment increased cell death in both WT and hIAPP islets over the first 24 h (Figure 21E). However, islet cell death was significantly higher in amyloid-prone hIAPP islets compared to amyloid-free WT islets 48 h (Figure 21F) and 96 h (Figure 21G) post 16.7 mM glucose treatment, times at which amyloid formation was occurring in hIAPP but not WT islets (Figure 21E-H). Treatment with 16.7 mM glucose significantly increased caspase 3/7 activity in both WT and hIAPP islets over time (Figure 21I,J), with glucose-induced caspase 3/7 activation being higher in amyloid-forming hIAPP islets compared to WT islets after 48 h and 96 h of culture (Figure 21J). Notably, we observed that RIPK3 protein expression and MLKL phosphorylation were upregulated in amyloid-laden hIAPP islets compared to amyloid-free WT islets *in vitro*, indicating a role for RIPK3 in amyloid-induced islet cell death (Figure 21K-M). These data suggest that amyloid deposition leads to increased islet cell death that occurs in association with elevated caspase 3/7 and RIPK3 activity.

**B. Loss of RIPK3 protects from amyloid-induced islet cell death *in vitro*.**

To investigate the role of RIPK3 in amyloid-induced islet cell death, we next evaluated islets isolated from WT, *Ripk3*<sup>-/-</sup>, hIAPP and hIAPP;*Ripk3*<sup>-/-</sup> mice. Following 48 h and 96 h of culture in 16.7 mM glucose, both hIAPP and hIAPP;*Ripk3*<sup>-/-</sup> islets exhibited significant amyloid deposition, the quantity of which was not different between genotypes (Figure 22A-C). In contrast, we found that hIAPP;*Ripk3*<sup>-/-</sup> islets were protected from amyloid-induced cell death compared to hIAPP islets with intact RIPK3 expression after both 48 h and 96 h of culture (Figure 22D-F).

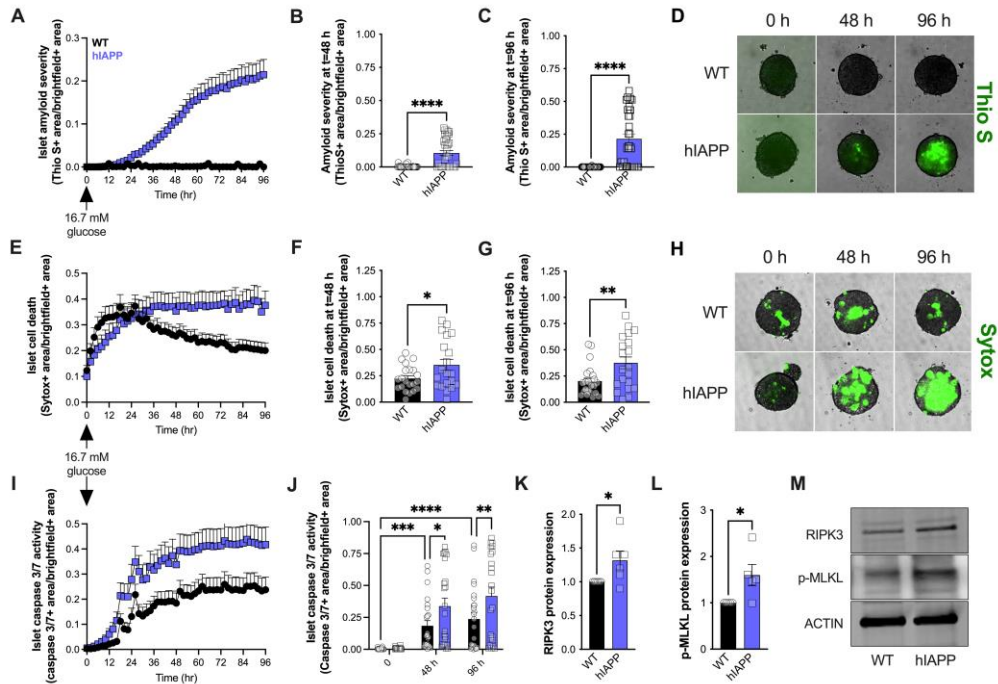


**Figure 21: Real-time quantification of endogenous islet amyloid formation and islet cell death *in vitro*.**

Islet amyloid deposition, islet cell death and caspase 3/7 activity were quantified in intact islets isolated from WT (black, circles) and hIAPP (purple, squares) mice. A) Islet amyloid severity (Thio S+ area/brightfield+ area) was monitored every 2 h for 96 h and quantified at B) 48 h and C) 96 h post culture in 16.7mM glucose (n=34-35 islets from 4 mice per genotype). D) Representative images of islet amyloid deposition are shown. E) Islet cell death (Sytox+ area/brightfield+ area) was monitored every 2 h for 96 h and quantified at F) 48 h and G) 96 h post culture in 16.7mM glucose (n=20-23 islets from 3 mice per genotype). H) Representative images of islet cell death are shown. I) Islet caspase 3/7 activity (caspase 3/7+ area/brightfield+ area) was monitored every 2 h for 96 h and quantified at J) 0, 48 and 96 h post culture in 16.7mM glucose (n=23-24 islets from 3 mice per genotype). K) RIPK3 and L) phospho-MLKL protein expression were quantified in WT and hIAPP islets following culture in 16.7mM glucose (n=5-6 per

genotype). M) Representative images of RIPK3, phospho-MLKL and ACTIN protein expression are shown. \* $p < 0.05$ ; \*\* $p < 0.01$ ; \*\*\* $p < 0.001$ ; \*\*\*\* $p < 0.0001$ .

Following culture in 16.7 mM glucose for 48 h, caspase 3/7 activity was increased both in amyloid-forming hIAPP islets and in hIAPP;Ripk3<sup>-/-</sup> islets compared to amyloid-free WT islets (Figure 22G). Similar to our previous experiments (Figure 21 K,M), amyloid formation in hIAPP islets was associated with increased *Ripk3* mRNA expression, and we found that the amyloid-induced increase in *Ripk3* expression was abrogated in hIAPP;Ripk3<sup>-/-</sup> islets (Figure 22H). Figure 22I illustrates loss of RIPK3 protein expression in Ripk3<sup>-/-</sup> islets. These results indicate that RIPK3 promotes amyloid-induced islet cell death downstream of amyloid deposition *per se*.

### C. RIPK3 promotes hIAPP-induced inflammatory gene expression in macrophages *in vitro*.

We next examined the role of RIPK3 in hIAPP-induced inflammatory gene expression *in vitro*. We first compared *Ripk3* expression in isolated islets, BMDMs and INS-1  $\beta$  cells, and consistent with previous reports we found that *Ripk3* is expressed in each of these cell types (Figure 23A). We also observed that isolated islets express the macrophage marker *Emr1* (Figure 23B), suggesting that a portion of islet *Ripk3* expression may come from macrophages. To characterize the contribution of islet *Ripk3* expression from  $\beta$  cells versus macrophages more directly, we treated isolated islets with clodronate liposomes to deplete macrophages (Figures 23C-E). We found that clodronate-liposome treatment reduced islet *Emr1* expression by ~75% compared to islets treated with PBS liposomes (Figure 23D), indicating efficient clodronate-mediated macrophage depletion in this model. Islet *Ripk3* expression was also significantly reduced following clodronate-liposome treatment (Figure 23C), and the degree of *Ripk3* expression was correlated with the degree of *Emr1* expression in both PBS-liposome and clodronate-liposome treated

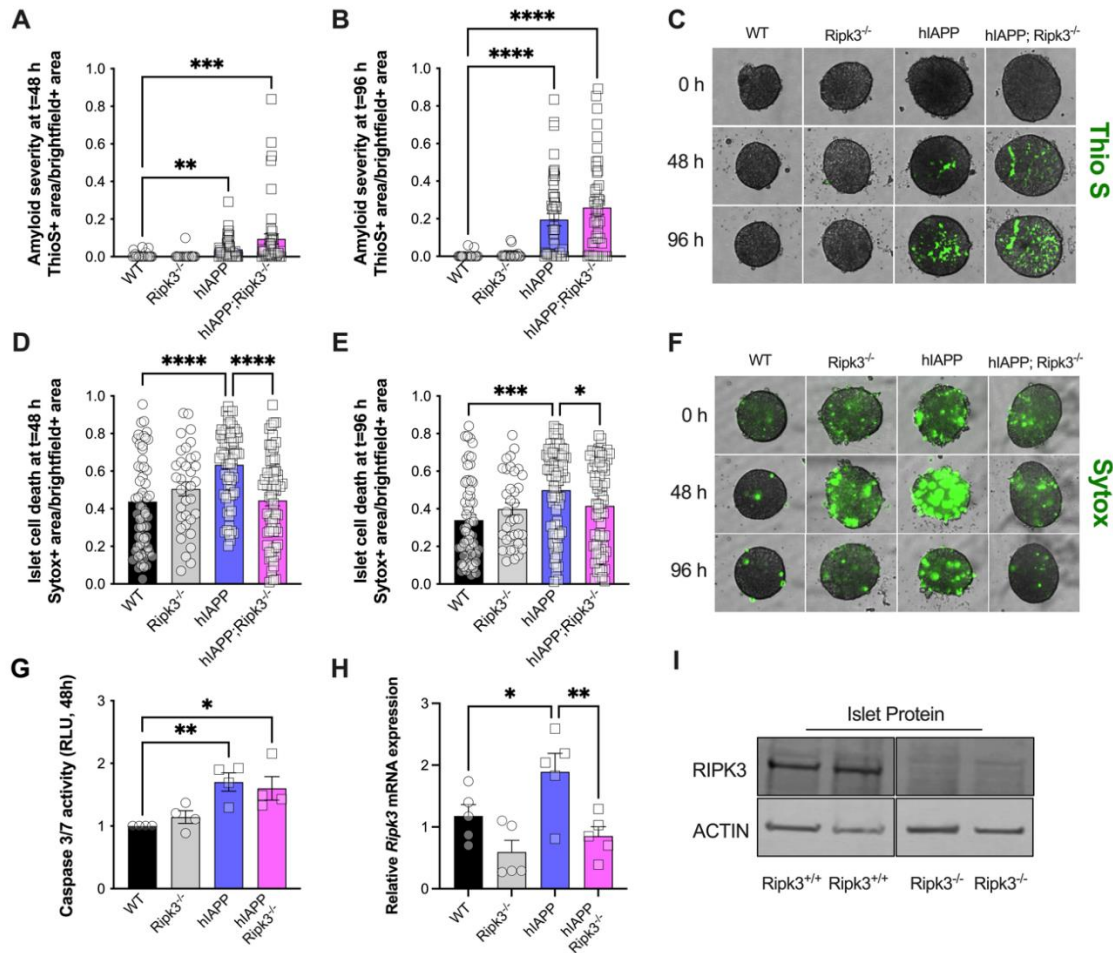


**Figure 22: Loss of RIPK3 protects from amyloid-induced islet cell death *in vitro*.**

Islet amyloid deposition, islet cell death and caspase 3/7 activity were quantified in intact islets isolated from WT (black, circles), Rlpk3<sup>-/-</sup> (grey, circles), hIAPP (purple, squares) and hIAPP;Rlpk3<sup>-/-</sup> (pink, squares) mice. Islet amyloid severity (Thio S+ area/brightfield+ area) was quantified at A) 48 h and B) 96 h post culture in 16.7mM glucose (n=24-48 islets from 3-6 mice per genotype). C) Representative images of islet amyloid deposition are shown. Islet cell death (Sytox+ area/brightfield+ area) was quantified at D) 48 h and E) 96 h post culture in 16.7mM glucose (n=36-72 islets from 4-8 mice per genotype). F) Representative images of islet cell death are shown. G) Caspase 3/7 activity was quantified in WT, Rlpk3<sup>-/-</sup>, hIAPP and hIAPP;Rlpk3<sup>-/-</sup> islets 48 h post

culture in 16.7mM glucose and expressed relative to WT islets (n=4 per genotype). H) *Ripk3* RNA expression was quantified in WT, *Ripk3*<sup>-/-</sup>, hIAPP and hIAPP;*Ripk3*<sup>-/-</sup> islets following culture in 16.7mM glucose for 48 h (n=5 per genotype). I) RIPK3 protein expression was quantified in WT and *Ripk3*<sup>-/-</sup> mouse islets. Representative images of RIPK3 and ACTIN protein expression from non-consecutive lanes on the same membrane are shown. \*p<0.05; \*\*p<0.01; \*\*\*p<0.001; \*\*\*\*p<0.0001.

islets (Figure 23E). These data indicate that in addition to  $\beta$  cells, macrophages are an important source of *Ripk3* expression in isolated islets. We next exposed WT and *Ripk3*<sup>-/-</sup> BMDMs to non-amyloidogenic synthetic rIAPP or amyloidogenic synthetic hIAPP for 16 h. Synthetic hIAPP, but not rIAPP, significantly increased *Ripk3* expression in WT BMDMs, and this effect was blocked in *Ripk3*<sup>-/-</sup> BMDMs (Figure 23F). In addition, we found that synthetic hIAPP increased *Tnf* (Figure 23G), *Il1b* (Figure 23H) and *Nos2* (Figure 23I) expression in WT BMDMs, and these effects were ameliorated in *Ripk3*<sup>-/-</sup> BMDMs (Figure 3J). Together, these data indicate that loss of RIPK3 in macrophages mitigates islet amyloid-induced inflammation.

D. Characterization of metabolic phenotypes in chow-fed WT, *Ripk3*<sup>-/-</sup>, hIAPP and hIAPP;*Ripk3*<sup>-/-</sup> mice.

To evaluate the role of RIPK3 in metabolic phenotypes *in vivo*, we first examined chow-fed 8-12 week old WT, *Ripk3*<sup>-/-</sup>, hIAPP and hIAPP;*Ripk3*<sup>-/-</sup> mice. Mice from all groups exhibited similar glucose tolerance (Figure 24A,B), fasting blood glucose (Figure 24C), insulin tolerance (Figure 24D,E) and fasting serum insulin (Figure 24F) at this time. Following *in vivo* intraperitoneal glucose challenge, WT, *Ripk3*<sup>-/-</sup>, hIAPP and hIAPP;*Ripk3*<sup>-/-</sup> mice exhibited similar insulin release 2 min and 10 min post glucose injection (Figure 24G). Moreover, *in vitro* GSIS (Figure 24H) and insulin content (Figure 24I) were similar between islets isolated from WT and *Ripk3*<sup>-/-</sup> mice. These data indicate that glucose homeostasis and  $\beta$ -cell secretory function are similar between young chow-fed WT, *Ripk3*<sup>-/-</sup>, hIAPP and hIAPP;*Ripk3*<sup>-/-</sup> mice.

E. Loss of RIPK3 protects against and islet amyloid-induced glucose intolerance following HFD *in vivo*.

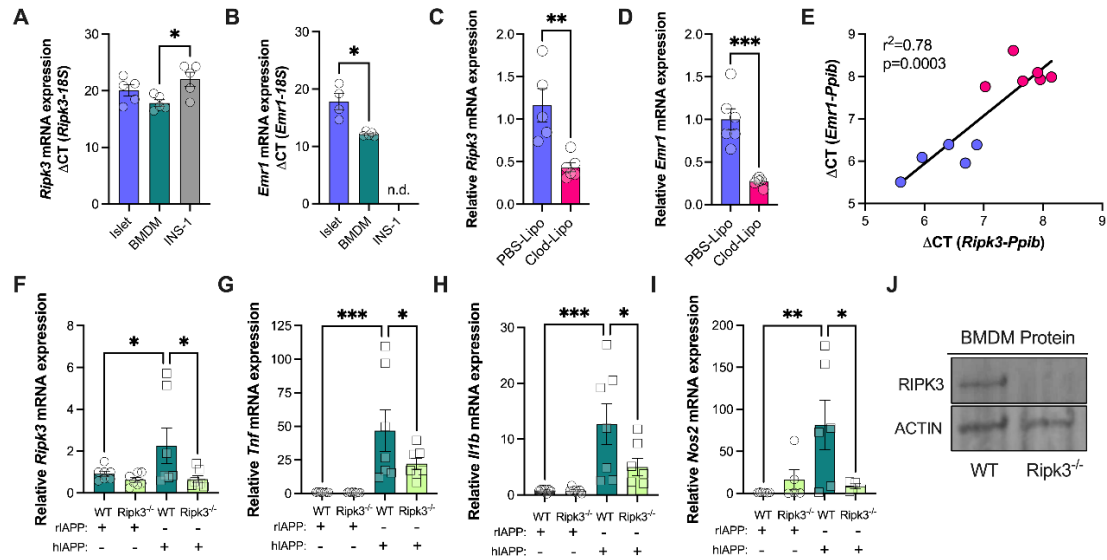


**Figure 23: RIPK3 promotes synthetic hIAPP-induced inflammatory gene expression in macrophages *in vitro*.**

A) *Ripk3* and B) *Emr1* RNA expression was quantified in mouse islets (purple), bone marrow derived macrophage (BMDMs) (dark green) and INS-1  $\beta$  cells (grey) and expressed as  $\Delta$ CT to *18S* rRNA (n=4-5 per cell type). Isolated mouse islets were cultured with PBS- (purple) or clodronate-containing liposomes (red) for 48 h. Expression of C) *Ripk3* and D) *Emr1* RNA was quantified and expressed relative to *Ppib* RNA levels using the  $2^{-\Delta\Delta C_t}$  method (n=5-6 per condition). E) Simple regression analysis of  $\Delta$ CT values of *Emr1* (*Emr1* - *Ppib* RNA) and *Ripk3* (*Ripk3* - *Ppib* RNA) within PBS-liposome (purple) and clodronate-liposome (red) treated islets was performed. BMDMs isolated from WT mice (dark green) or *Ripk3*<sup>-/-</sup> mice (light green) were treated with synthetic rodent IAPP (circles) or synthetic human IAPP (squares) for 16 h. Expression of F) *Ripk3*, G) *Tnf*, H) *Il1b* and I) *Nos2* RNA was quantified and normalized to *18S* rRNA levels using the  $2^{-\Delta\Delta C_t}$  method (n=7 per condition). J) RIPK3 protein expression was evaluated in WT and

Ripk3<sup>-/-</sup> BMDMs and representative immunoblots are shown. \*p<0.05; \*\*p<0.01;  
\*\*\*p<0.001.

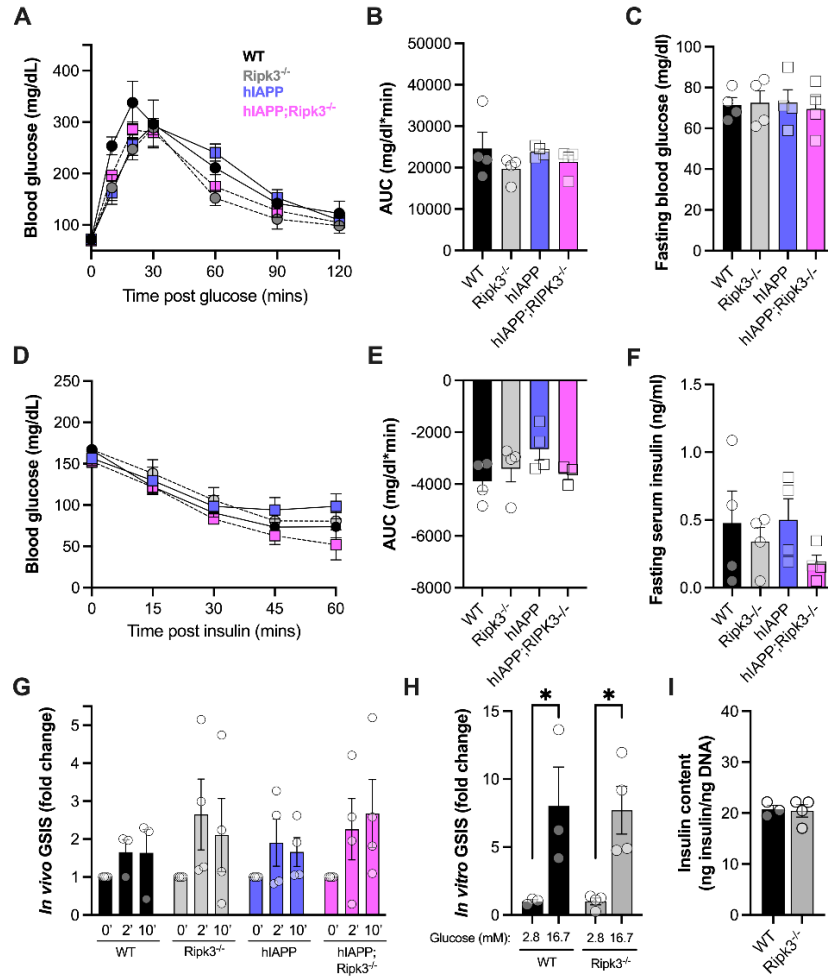


**Figure 24: Characterization of metabolic phenotypes in chow-fed WT, Ripk3<sup>-/-</sup>, hIAPP and hIAPP;Ripk3<sup>-/-</sup> mice.**

8–12-week-old WT (black, circles), Ripk3<sup>-/-</sup> (grey, circles), hIAPP (purple, squares) and hIAPP;Ripk3<sup>-/-</sup> (pink, squares) mice fed a normal chow diet were examined. A) Glucose tolerance was evaluated by intraperitoneal glucose tolerance test (IPGTT) and B) quantified as incremental area under the curve (iAUC, mg/dl\*min) after overnight fast (n=4 mice per genotype). C) Fasting blood glucose was measured by handheld glucometer after overnight fast (n=4 mice per genotype). D) Insulin tolerance was evaluated by intraperitoneal insulin tolerance test (IPITT) and E) quantified as

decremental area under the curve (dAUC, mg/dl\*min) after 2 hr fast (n=3-4 mice per genotype). F) Fasting serum insulin was measured after overnight fast (n=4 mice per genotype). G) *In vivo* glucose stimulated insulin secretion (GSIS) was performed and serum insulin levels quantified at 0-, 2- and 10-mins following glucose challenge (n=3-4 mice per genotype). *In vitro* GSIS was performed on islets isolated from 8-12-week-old WT and Ripk3<sup>-/-</sup> mice, then H) insulin secretion (fold change) and I) insulin content was measured (n=3-4 mice per genotype). \*p<0.05.

We next evaluated the role of RIPK3 in HFD- and islet amyloid-induced glucose homeostasis *in vivo*. We quantified body weight, non-fasting blood glucose, glucose tolerance and insulin tolerance in WT, Ripk3<sup>-/-</sup>, hIAPP and hIAPP;Ripk3<sup>-/-</sup> mice during and after 52 weeks of HFD feeding. All groups of mice gained body weight over the HFD feeding period (Figure 25A), and after 52 weeks of HFD hIAPP;Ripk3<sup>-/-</sup> mice exhibited higher body weight than WT, Ripk3<sup>-/-</sup> or hIAPP mice (Figure 25B). Non-fasting blood glucose concentrations were not different between groups over the course of the 52-week HFD feeding period (Figure 25C), and at study end non-fasting blood glucose (Figure 25D) and non-fasting serum insulin (Figure 25E) were not different between groups. In contrast, we found that islet amyloid-prone hIAPP mice exhibited significant glucose intolerance compared to WT mice after 52 weeks of HFD feeding, whereas hIAPP;Ripk3<sup>-/-</sup> mice were protected from amyloid-associated glucose intolerance (Figure 25F,G). Despite the higher body weight in hIAPP;Ripk3<sup>-/-</sup> mice at study end, insulin tolerance was not different among groups after HFD (Figure 25H,I). These data indicate that RIPK3 contributes to islet amyloid-induced glucose intolerance *in vivo*.

**F. RIPK3 deficient mice are protected from islet amyloid-induced  $\beta$ -cell loss *in vivo*.**

To determine whether RIPK3 contributes to islet amyloid-induced  $\beta$ -cell loss *in vivo*, we next performed immunohistochemistry and quantitative microscopy on pancreas sections isolated from WT, Ripk3<sup>-/-</sup>, hIAPP and hIAPP;Ripk3<sup>-/-</sup> mice following 52 weeks of HFD feeding. We found that average islet area was not different between WT, Ripk3<sup>-/-</sup>, hIAPP and hIAPP;Ripk3<sup>-/-</sup> mice (Figure 26A). As expected, islet amyloid deposition was absent in pancreases from WT and Ripk3<sup>-/-</sup> mice that express rIAPP (Figure 26B). In contrast,

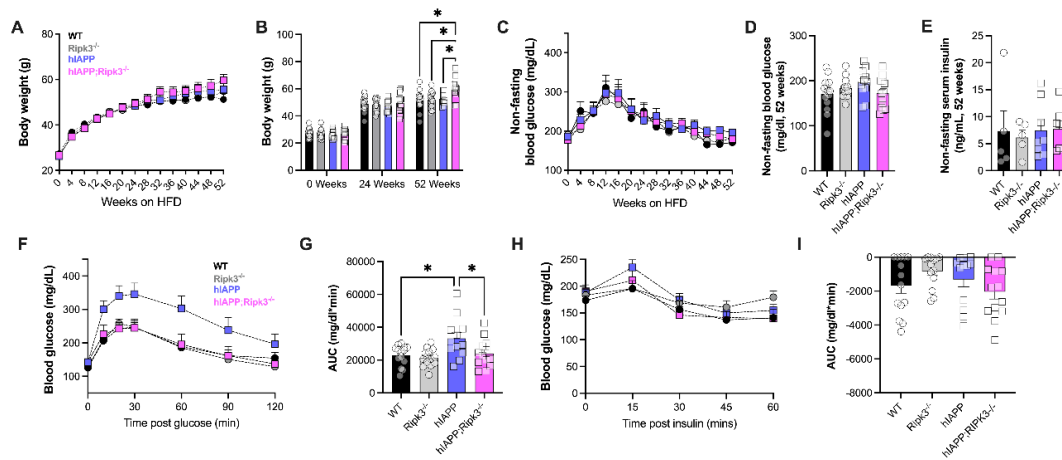


**Figure 25: Loss of RIPK3 protects against amyloid-induced glucose intolerance *in vivo*.**

8-10-week-old WT (black, circles), *Ripk3*<sup>-/-</sup> (grey, circles), hIAPP (purple, squares) and hIAPP;*Ripk3*<sup>-/-</sup> (pink, squares) mice were subjected to high-fat diet (HFD) feeding for 52 weeks. A) Body weight was monitored every 4 weeks for 52 weeks and B) quantified after 0, 24 and 52 weeks of HFD (n=12-14 mice per genotype). C) Non-fasting blood glucose was monitored every 4 weeks for 52 weeks and D) quantified after 52 weeks of HFD (n=12-14 mice per genotype). E) Non-fasting serum insulin was measured after 52 weeks of HFD feeding. F) Glucose tolerance was evaluated by intraperitoneal glucose tolerance test (IPGTT) and G) quantified as incremental area under the curve (iAUC, mg/dl\*min) after overnight fast (n=12-14 mice per genotype). H) Insulin tolerance was evaluated by intraperitoneal insulin tolerance test (IPITT) and I) quantified as decremental area under the curve (dAUC, mg/dl\*min) after 2 h fast (n=12-14 mice per genotype). \*p<0.05.

significant islet amyloid deposition was observed in both hIAPP and hIAPP;Ripk3<sup>-/-</sup> pancreas sections, and the degree of islet amyloid deposition was not different between these genotypes (Figure 26B). Additionally, we found that  $\beta$ -cell area was significantly reduced in amyloid-laden hIAPP versus amyloid-free WT pancreas sections ( $63.8 \pm 3.1\%$  versus  $73.7 \pm 0.7\%$  b-cell area), and that hIAPP;Ripk3<sup>-/-</sup> pancreases were partially protected from this amyloid-induced  $\beta$ -cell loss ( $69.5\% \pm 1.8\%$  b-cell area) (Figure 26C). Representative images of islets are shown in Figure 26D. These data suggest that loss of RIPK3 protects from amyloid-induced  $\beta$ -cell loss *in vivo* via mechanisms downstream of amyloid deposition *per se*.

## **Discussion**

Islet amyloid deposition was first identified as a pathological feature of diabetes in 1901<sup>10</sup>, and numerous studies since then have established islet amyloid as a hallmark of the islet lesion in T2D<sup>5,20,88,334,335</sup>. Although islet amyloid is known to contribute to reduced  $\beta$ -cell mass, insufficient insulin secretion and hyperglycemia in T2D<sup>87,88,238,334,350</sup>, the mechanisms that underlie this process remain incompletely understood. Here, we generated and evaluated islet amyloid-prone hIAPP mice with whole body loss of RIPK3, a recently recognized regulator of  $\beta$ -cell fate<sup>168,278</sup>. Our *in vitro* studies quantified amyloid deposition and cell death in intact isolated islets in real time, examined amyloid-induced caspase activation, and evaluated hIAPP-stimulated inflammatory gene expression. In addition, we performed *in vivo* studies on mice fed a HFD for 52 weeks to characterize the role of RIPK3 in islet amyloid deposition, amyloid-induced  $\beta$ -cell loss and hyperglycemia *in vivo*. Using this approach, we found that RIPK3 contributes to islet

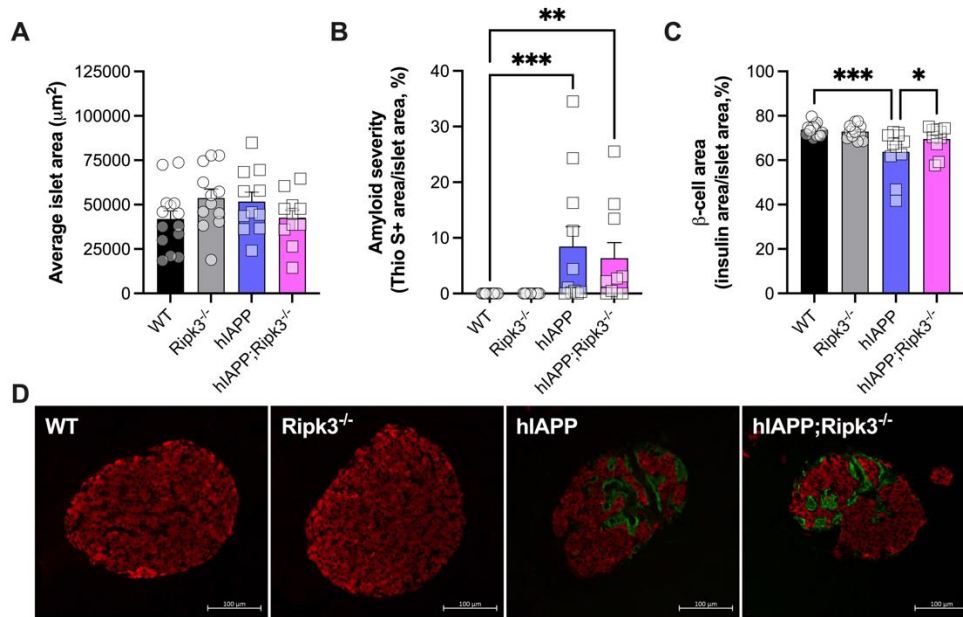


**Figure 26: Loss of RIPK3 ameliorates amyloid-induced  $\beta$ -cell loss *in vivo*.** After 52 weeks of HFD feeding, immunohistochemistry was performed on WT (black, circles), Ripk3<sup>-/-</sup> (grey, circles), hIAPP (purple, squares) and hIAPP;Ripk3<sup>-/-</sup> (pink, squares) mouse pancreas sections. **A**) Average islet area ( $\text{mm}^2$ ), **B**) amyloid severity (Thio S+ area/islet area, %) and **C**)  $\beta$ -cell area (insulin+ area/islet area, %) were quantified (n=11-14 genotype). **D**) Representative images of pancreatic islets from WT, Ripk3<sup>-/-</sup>, hIAPP and hIAPP;Ripk3<sup>-/-</sup> mouse pancreas sections are shown. Scale bar=100  $\mu\text{m}$ . \*p<0.05; \*\*p<0.01; \*\*\*p<0.001.

amyloid-induced inflammation,  $\beta$ -cell loss and glucose intolerance in a humanized mouse model of T2D.

In the present study, we evaluated potential roles of RIPK3 in amyloid-induced  $\beta$ -cell cytotoxicity. As described, our findings suggest that loss of RIPK3 protects from amyloid-induced islet cell death downstream of amyloid formation *per se*, likely via reduced amyloid-associated islet inflammation and  $\beta$ -cell death signaling. Given that RIPK3 can promote both caspase-mediated apoptosis<sup>255,346</sup> and caspase-independent necroptosis<sup>342,347</sup>, we examined the roles of caspase 3/7 activity and RIPK3 expression in amyloid-induced  $\beta$ -cell loss *in vitro*. Similar to previous reports<sup>134,353</sup>, we found that caspase activity was increased over time in association with islet amyloid deposition and islet cell death. However, our studies also found that protection from amyloid-induced cell death in hIAPP;Ripk3<sup>-/-</sup> islets was not coincident with reduced caspase 3/7 activity, and although hIAPP;Ripk3<sup>-/-</sup> islets were protected from amyloid-induced cell death, it was not blocked completely. Considering that we also observed increased RIPK3 expression and MLKL phosphorylation in amyloid-laden islets, our data indicate that both caspase-dependent mechanisms such as apoptosis and caspase-independent mechanisms such as necroptosis may contribute to amyloid-induced islet cell death *in vitro*. In this context, our findings are in agreement with a previous study showing that loss of caspase 8 in  $\beta$  cells reduces, but does not completely prevent, amyloid-induced  $\beta$ -cell death<sup>353</sup>. We propose a model wherein amyloid formation activates RIPK3 in coordination with caspase 8, and that RIPK3 promotes amyloid-induced islet cell death via caspase 3/7 independent actions. This model is in line with studies in other cell types that show caspase 8 and RIPK3 coordinately regulate caspase-dependent apoptosis and

caspase-independent necroptosis signaling<sup>341,343,354</sup>. Our findings are also in agreement with recent observations of RIPK3 in AD pathogenesis<sup>267,355</sup> and suggest potential overlapping mechanisms of amyloid-associated cytotoxicity in AD and T2D.

In addition to its role in apoptotic and necroptotic cell death signaling, RIPK3 also regulates cytokine and chemokine production in immune cells<sup>345,356,357</sup>. Since islet amyloid deposition elicits cytokine production from islet resident macrophages<sup>93,94</sup> and synthetic hIAPP treatment increases inflammatory gene expression in macrophages and dendritic cells<sup>93,358</sup>, we reasoned that the protection from amyloid-induced cell death observed in hIAPP;*Ripk3*<sup>-/-</sup> islets could be related to effects on RIPK3-mediated inflammation<sup>356,357,359</sup>. Indeed, we found that clodronate liposome-mediated depletion of islet macrophages reduced *Ripk3* expression *in vitro*, confirming that macrophages are an important source of islet *Ripk3* expression. In line with previous findings<sup>93,358</sup>, we observed that synthetic hIAPP treatment increased *Tnf*, *Il1b* and *Nos2* gene expression in WT BMDMs, and this was associated with increased *Ripk3* expression. In contrast, we found that *Ripk3*<sup>-/-</sup> BMDMs were protected from synthetic hIAPP-induced inflammatory gene expression. Although RIPK3 has previously been shown to promote TNF $\alpha$ , IL1 $\beta$  and iNOS synthesis<sup>343,344,356,360</sup>, our findings reveal this is also the case with hIAPP-stimulated inflammatory gene expression. Given these findings, we propose that macrophage RIPK3 promotes amyloid-induced islet inflammation separately from the known roles of RIPK3 in  $\beta$  cells<sup>168,278</sup>. As such, additional studies are needed to determine the relative importance of RIPK3 signaling in  $\beta$  cells versus macrophages in islet amyloid-induced  $\beta$ -cell cytotoxicity.

To explore the role of RIPK3 in T2D pathogenesis, we evaluated amyloid-free WT and Ripk3<sup>-/-</sup> mice as well as islet amyloid-prone hIAPP and hIAPP;Ripk3<sup>-/-</sup> mice *in vivo*. Prior to islet amyloid formation, we found that young, chow-fed WT, Ripk3<sup>-/-</sup>, hIAPP and hIAPP;Ripk3<sup>-/-</sup> mice had similar glucose tolerance, fasting blood glucose, insulin tolerance and fasting serum insulin. These findings contrast with those of Roychowdhury et al.<sup>361</sup>, and may be related to the different Ripk3 mutant mouse models used<sup>362</sup> and/or varying insulin secretory function between the different genetic backgrounds utilized in our studies<sup>363</sup>. Using our established HFD-feeding paradigm, we found that HFD led to islet amyloid deposition in both hIAPP and hIAPP;Ripk3<sup>-/-</sup> mice. While hIAPP mice exhibited glucose intolerance and reduced  $\beta$ -cell area following HFD, hIAPP;Ripk3<sup>-/-</sup> mice were protected from these impairments. The protection from glucose intolerance and  $\beta$ -cell loss observed in hIAPP;Ripk3<sup>-/-</sup> mice was not associated with improved insulin sensitivity or reduced islet amyloid deposition compared to hIAPP mice with intact RIPK3 expression, suggesting that loss of RIPK3 led to improved  $\beta$ -cell function and/or survival in the face of islet amyloid deposition. Moreover, since hIAPP and hIAPP;Ripk3<sup>-/-</sup> mice exhibited similar glucose tolerance and insulin sensitivity prior to HFD feeding, the glucose tolerance phenotypes observed were likely related to the HFD-induced islet amyloid deposition that occurred over the study period. Although  $\beta$ -cell function was not the focus of the present study, we observed that WT and Ripk3<sup>-/-</sup> islets had similar GSIS and insulin content *in vitro*, that young chow-fed WT, Ripk3<sup>-/-</sup>, hIAPP and hIAPP;Ripk3<sup>-/-</sup> mice had similar GSIS *in vivo* and that WT, Ripk3<sup>-/-</sup>, hIAPP and hIAPP;Ripk3<sup>-/-</sup> mice had similar non-fasting serum insulin following HFD feeding. However, we cannot rule out the possibility that higher insulin secretion in hIAPP;Ripk3<sup>-/-</sup>

<sup>-/-</sup> compared to hIAPP mice contributed to their improved glucose tolerance after HFD, as we did not quantify serum insulin in those particular studies. Given that RIPK3 is known to interact with molecules involved in amplification of insulin secretion such as glutamate dehydrogenase and isocitrate dehydrogenase 1<sup>364</sup>, studies of RIPK3 in the amplifying pathway of insulin secretion would be informative. However, like our *in vitro* studies, our *in vivo* data indicate that the protection observed in hIAPP;Ripk3<sup>-/-</sup> mice was not due to reduced amyloid deposition *per se*, but rather decreased amyloid-associated  $\beta$ -cell cytotoxicity.

Limitations to our studies exist. First, although we used a humanized mouse model of hIAPP expression that approximates amyloid deposition phenotypes in human islets, additional studies in *bona fide* human islets are needed to confirm the role of RIPK3 in amyloid-induced islet cytotoxicity in T2D. Given that we examined a mouse model of whole body RIPK3 deficiency, the phenotypes observed in hIAPP;Ripk3<sup>-/-</sup> islets and mice could be due to effects of RIPK3 in  $\beta$  cells, macrophages or other cell types. Our previous work revealed that RIPK3 regulates TNF $\alpha$ -induced cytotoxicity in  $\beta$  cells<sup>168</sup>, and our current study identified a role for RIPK3 in hIAPP-stimulated inflammation in macrophages. Considering these findings, we believe RIPK3 could mediate amyloid-induced islet inflammation and  $\beta$ -cell death via actions in both cell types. However, additional studies using  $\beta$ -cell- or macrophage-specific models of RIPK3 deficiency are needed to determine whether loss of RIPK3 is beneficial due to reduced cell death signaling in  $\beta$  cells, decreased amyloid-induced cytokine production in macrophages, or both. Another caveat of our studies is that our quantification of cell death was performed using Sytox green, a membrane impermeable DNA-binding dye that labels both apoptotic

and necroptotic cells<sup>352</sup>. Thus, our technique was not able to identify whether dead cells arising with amyloid deposition underwent apoptosis or necroptosis. Additionally, amyloid-induced cell death was not quantified specifically in  $\beta$  cells but rather in all islet cell types. Although  $\beta$  cells comprise approximately 75% of mouse islets<sup>365</sup>, it is possible that other islet cell types such as  $\alpha$  cells,  $\delta$  cells or macrophages were also captured in our *in vitro* cell death quantification. Future studies will characterize the protective phenotypes observed with RIPK3 deficiency in greater detail. Despite these limitations, the studies presented here identify RIPK3 as a novel mediator of islet amyloid-associated inflammation,  $\beta$ -cell loss and glucose intolerance.

In conclusion, our studies uncovered a novel role for RIPK3 in amyloid-associated  $\beta$ -cell loss and glucose intolerance in T2D pathogenesis. We found that loss of RIPK3 protects from amyloid-induced  $\beta$ -cell cytotoxicity and hIAPP-induced inflammation *in vitro* as well as amyloid-associated  $\beta$ -cell loss and glucose intolerance *in vivo*. This protection was not related to decreased amyloid deposition *per se*, indicating that RIPK3 mediates  $\beta$ -cell cytotoxicity downstream of amyloid formation via effects on amyloid-induced cytokine production and/or  $\beta$ -cell death signaling. Although RIPK3 has been identified as a potential therapeutic target in several diseases including cancer<sup>366,367</sup>, acute kidney injury<sup>368,369</sup> and neurodegenerative diseases<sup>267,341,355,370</sup>, this work shows that therapeutics targeting RIPK3 may also reduce  $\beta$ -cell cytotoxicity and promote glucose homeostasis during T2D pathogenesis.

#### Acknowledgement

All text and figures from studies in this section has been published as a part of a manuscript submitted to *Molecular Metabolism*<sup>330</sup>.

Mukherjee N, Contreras CJ, Lin L, Colglazier KA, Mather EG, Kalwat MA, Esser N, Kahn SE, Templin AT. RIPK3 promotes islet amyloid-induced  $\beta$ -cell loss and glucose intolerance in a humanized mouse model of type 2 diabetes. *Mol Metab.* 2024 Jan. doi: 10.1016/j.molmet.2024.101877.

## **Chapter 7 – Conclusion**

This work investigates unknown mechanisms of  $\beta$ -cell survival and death. The findings outlined in this thesis are among the first to explore the role of receptor-interacting protein kinases in pancreatic  $\beta$  cells. Being professional secretory cells,  $\beta$  cells are responsible for insulin secretion to maintain glucose homeostasis.  $\beta$ -cell failure by loss of insulin action and/or production is a major contributor to the development of hyperglycemia. The studies performed in this dissertation aim to advance our understanding of  $\beta$ -cell demise through insights from cell death signaling in non-islet cell types, with the hope of uncovering new strategies to improve the health of individuals with diabetes.

Apoptosis has long been recognized as the primary mode of  $\beta$ -cell death. Prior studies have documented that  $\beta$ -cell death occurs in association with caspase 3 activation, chromatin condensation, nucleolar disintegration, DNA fragmentation, and annexin V positivity, displaying hallmarks of apoptosis<sup>132</sup>. Studies utilizing caspase-3 or caspase-8 deficient mouse models indeed show protection against STZ-induced hyperglycemia<sup>133,137</sup>. However, it was also observed that, with aging, loss of caspase 8 in  $\beta$  cells resulted in elevated  $\beta$ -cell death and glucose intolerance in chow-fed mice<sup>137</sup>. This observation indicates that  $\beta$  cells are capable of undergoing a form of cell death that does not rely on caspase activation. In this work, we utilize a small-molecule caspase inhibitor (zVAD-FMK) to ask whether  $\beta$ -cell death is dependent on caspase activation. Several  $\beta$ -cell stressors such as pro-inflammatory cytokines and ER stress-inducing agents trigger  $\beta$ -cell death, which is accompanied by increased caspase 3/7 activation. Interestingly, while zVAD-FMK reduces cytokine- or ER stress-induced caspase 3/7 activation, it fails

to protect against cell death in  $\beta$ -cell lines and mouse islets. This data supports the notion that  $\beta$  cells can undergo caspase-independent forms of cell death and we propose that non-apoptotic  $\beta$ -cell death may occur in the context of diabetes.

Recent advances in the field of cell death research have shifted the understanding of the mechanism of cell death from a binary “programmed and non-inflammatory” (apoptosis) versus a “non-programmed and inflammatory” (necrosis) framework. Forms of programmed cell death that can lead to cell lysis and inflammation have been identified. In this context, receptor-interacting protein kinases (RIPKs) have emerged as key regulators of cell death and inflammation. Although RIPKs have multiple functions, they are well-studied for mediating necroptosis, a caspase-independent form of programmed cell death. We sought to understand the role of RIPKs in  $\beta$ -cell cytotoxicity in diabetes.

While initially studied in the context of TNFR-mediated cell death signaling, RIPK1 has now been identified to mediate cell death downstream of other receptors including TLRs, TRAIL, and interferon receptors. Moreover, research in other cell types has revealed the roles of RIPK1 in gene expression and kinase signaling. The findings from this thesis reveal that beyond its involvement in  $\beta$ -cell death downstream of pro-inflammatory cytokines and ER stress, RIPK1 appears to play essential roles in  $\beta$ -cell survival, gene expression, and communication with immune cells. This work also exposes the distinct roles of  $\beta$ -cell RIPK1 in the context of the diabetogenic stimulus utilized for the studies. Although cytokine-mediated effects of RIPK1 seem to depend on its kinase activity, inhibiting RIPK1 kinase activation does not prevent  $\beta$ -cell death in the context of ER stress, suggesting a more complex role of RIPK1 in  $\beta$  cells. This

underscores the idea that cellular context defines the roles of specific proteins. Even though our understanding of RIPK1 in  $\beta$  cells is still evolving, RIPK1 may regulate not only cell survival but also  $\beta$ -cell maturity, secretory capacity, and interaction with the immune system. Future studies using  $\beta$ -cell-specific knockout models will be critical for elucidating the precise roles of RIPK1 in  $\beta$ -cell function and survival. Additionally, since RIPK1 is expressed in immune cells, comparing results from our global RIPK1 kinase dead model to an immune-cell-specific and  $\beta$ -cell-specific RIPK1 kinase dead model will be critical to understanding the relative contribution of RIPK1 kinase activation to  $\beta$ -cell cytotoxicity in diabetes. Understanding these mechanisms could lead to novel therapeutic approaches to preserve  $\beta$ -cell function and prevent diabetes progression by targeting RIPK1 kinase signaling pathways in  $\beta$  cells and/or immune cells. Furthermore, data from this thesis show that the small molecule RIPK1 inhibitor, SZM' 679, significantly reduces cytokine-mediated  $\beta$ -cell death and MHC I expression. Future efforts will be targeted toward investigating whether SZM' 679 is capable of preventing or delaying diabetes progression in mouse models of T1D *in vivo*.

RIPKs are also relevant in the context of T2D, as evidenced by the results obtained from studies on islet amyloid in this thesis (Chapter 6). Pancreatic islet amyloid deposition is observed in the majority of individuals with T2D and is associated with  $\beta$ -cell dysfunction, death, and islet inflammation. Efforts toward enhancing the disaggregation or disintegration of amyloid deposits to reduce amyloid-associated  $\beta$ -cell cytotoxicity have not been significantly fruitful. Recent studies have also aimed to develop antibodies targeting pathological IAPP oligomeric species that have shown some  $\beta$ -cell protection and improved glucose homeostasis<sup>371</sup>. However, a different approach to

combat amyloid-associated  $\beta$ -cell toxicity has been anti-inflammatory strategies targeted toward reducing amyloid-associated inflammation downstream of amyloid deposition. Prior research and findings from this thesis show that reduced amyloid-induced pro-inflammatory response from macrophages is a possible therapeutic strategy and this work identified RIPK3 to be a potential target in this regard. Future studies aimed toward studying glucose homeostasis in an amyloid-prone immune-cell-specific RIPK3 deficient model would be critical to better understand the role of immune cell RIPK3 in islet amyloid-associated pathology. Moreover, the development and use of a RIPK3 small molecule kinase inhibitor would greatly improve our tool kit to study the effects of RIPK3 kinase inhibition *in vitro* and *in vivo*.

Our findings highlight the complexity of cell death signaling pathways and raise intriguing questions about the intrinsic properties of  $\beta$  cells that influence their susceptibility to different forms of cell death. Understanding these differences will be crucial to determine whether distinct populations of  $\beta$  cells within islets or from different individuals exhibit varying susceptibility to stress and/or maybe more prone to one form of cell death over another. This knowledge could pave the way for personalized medicine approaches aimed at protecting  $\beta$  cells from death and preventing the development of diabetes.

In conclusion, this thesis represents one of the pioneering efforts to investigate the role of receptor-interacting protein kinases (RIPKs) in  $\beta$ -cell cytotoxicity and the development of diabetes. Our research reveals new insights into how RIPKs contribute to  $\beta$ -cell death, kinase activation, and gene expression, highlighting their significant impact on  $\beta$ -cell health and function. While many questions remain unanswered, this work

establishes a foundation for a more comprehensive understanding of RIPKs in  $\beta$ -cell dynamics, encompassing both health and disease.

## References

1. Facts & figures. *International Diabetes Federation* <https://idf.org/about-diabetes/diabetes-facts-figures/>.
2. Williams, R. *et al.* Global and regional estimates and projections of diabetes-related health expenditure: Results from the International Diabetes Federation Diabetes Atlas, 9th edition. *Diabetes Res Clin Pract* **162**, 108072 (2020).
3. Mukherjee, N., Lin, L., Contreras, C. J. & Templin, A. T.  $\beta$ -Cell Death in Diabetes: Past Discoveries, Present Understanding, and Potential Future Advances. *Metabolites* **11**, 796 (2021).
4. Colglazier, K. A., Mukherjee, N., Contreras, C. J. & Templin, A. T. RISING STARS: Evidence for established and emerging forms of  $\beta$ -cell death. *J Endocrinol* **262**, e230378 (2024).
5. Maclean, N. & Ogilvie, R. F. Quantitative estimation of the pancreatic islet tissue in diabetic subjects. *Diabetes* **4**, 367–376 (1955).
6. Maclean, N. & Ogilvie, R. F. Observations on the Pancreatic Islet Tissue of Young Diabetic Subjects. *Diabetes* **8**, 83–91 (1959).
7. Doniach, I. & Morgan, A. G. Islets of Langerhans in Juvenile Diabetes Mellitus. *Clinical Endocrinology* **2**, 233–248 (1973).
8. Stefan, Y. *et al.* Quantitation of Endocrine Cell Content in the Pancreas of Nondiabetic and Diabetic Humans. *Diabetes* **31**, 694–700 (1982).
9. Klöppel, G., Drenck, C. R., Oberholzer, M. & Heitz, P. U. Morphometric evidence for a striking B-cell reduction at the clinical onset of type 1 diabetes. *Virchows Arch A Pathol Anat Histopathol* **403**, 441–452 (1984).

10. Opie, E. L. The relation of diabetes mellitus to lesions of the pancreas. Hyaline degeneration of the islands of Langerhans. *J Exp Med* **5**, 527–540 (1901).
11. Johnson, K. H. & Stevens, J. B. Light and Electron Microscopic Studies of Islet Amyloid in Diabetic Cats. *Diabetes* **22**, 81–90 (1973).
12. Rahier, J., Guiot, Y., Goebbels, R. M., Sempoux, C. & Henquin, J. C. Pancreatic beta-cell mass in European subjects with type 2 diabetes. *Diabetes Obes Metab* **10 Suppl 4**, 32–42 (2008).
13. MacCallum W. T. Hypertrophy of the islands of Langerhans in diabetes mellitus. *Am J Med Sci* **133**, 432 (1907).
14. Ogilvie RF. The islands of langerhans in 19 cases of obesity. *J Pathol Bacteriol.* **37**, 473–481 (1933).
15. Klöppel, G., Löhr, M., Habich, K., Oberholzer, M. & Heitz, P. U. Islet pathology and the pathogenesis of type 1 and type 2 diabetes mellitus revisited. *Surv Synth Pathol Res* **4**, 110–125 (1985).
16. Guiot, Y., Sempoux, C., Moulin, P. & Rahier, J. No decrease of the beta-cell mass in type 2 diabetic patients. *Diabetes* **50**, S188 (2001).
17. Cohrs, C. M. *et al.* Dysfunction of Persisting  $\beta$  Cells Is a Key Feature of Early Type 2 Diabetes Pathogenesis. *Cell Reports* **31**, 107469 (2020).
18. Saito, K., Yaginuma, N. & Takahashi, T. Differential volumetry of A,B and D cells in the pancreatic islets of diabetic and nondiabetic subjects. *Tohoku J. Exp. Med.* **129**, 273–283 (1979).

19. Sakuraba, H. *et al.* Reduced beta-cell mass and expression of oxidative stress-related DNA damage in the islet of Japanese Type II diabetic patients. *Diabetologia* **45**, 85–96 (2002).
20. Butler, A. E. *et al.* Beta-cell deficit and increased beta-cell apoptosis in humans with type 2 diabetes. *Diabetes* **52**, 102–110 (2003).
21. Jurgens, C. A. *et al.*  $\beta$ -cell loss and  $\beta$ -cell apoptosis in human type 2 diabetes are related to islet amyloid deposition. *Am. J. Pathol.* **178**, 2632–2640 (2011).
22. Wigger, L. *et al.* Multi-omics profiling of living human pancreatic islet donors reveals heterogeneous beta cell trajectories towards type 2 diabetes. *Nat Metab* **3**, 1017–1031 (2021).
23. Redondo, M. J. *et al.* The clinical consequences of heterogeneity within and between different diabetes types. *Diabetologia* **63**, 2040–2048 (2020).
24. Olehnik, S. K., Fowler, J. L., Avramovich, G. & Hara, M. Quantitative analysis of intra- and inter-individual variability of human beta-cell mass. *Sci Rep* **7**, 16398 (2017).
25. Ahlqvist, E., Prasad, R. B. & Groop, L. Subtypes of Type 2 Diabetes Determined From Clinical Parameters. *Diabetes* **69**, 2086–2093 (2020).
26. Kahn, S. E. The relative contributions of insulin resistance and beta-cell dysfunction to the pathophysiology of Type 2 diabetes. *Diabetologia* **46**, 3–19 (2003).
27. Vendrame, F., Zappaterreno, A. & Dotta, F. Markers of beta cell function in type 1 diabetes mellitus. *Minerva Med* **95**, 79–84 (2004).

28. Wrenshall, G. A., Bogoch, A. & Ritchie, R. C. Extractable Insulin of Pancreas: Correlation with Pathological and Clinical Findings in Diabetic and Nondiabetic Cases. *Diabetes* **1**, 87–107 (1952).
29. Cerasi, E. & Luft, R. The plasma insulin response to glucose infusion in healthy subjects and in diabetes mellitus. *European Journal of Endocrinology* **55**, 278–304 (1967).
30. Barker, A. *et al.* Age-dependent decline of  $\beta$ -cell function in type 1 diabetes after diagnosis: a multi-centre longitudinal study. *Diabetes Obes Metab* **16**, 262–267 (2014).
31. Yu, M. G. *et al.* Residual  $\beta$ -cell function and monogenic variants in long-duration type 1 diabetes patients. *J Clin Invest* **129**, 3252–3263 (2019).
32. Talchai, C., Xuan, S., Lin, H. V., Sussel, L. & Accili, D. Pancreatic  $\beta$  cell dedifferentiation as a mechanism of diabetic  $\beta$  cell failure. *Cell* **150**, 1223–1234 (2012).
33. Rui, J. *et al.*  $\beta$  Cells that Resist Immunological Attack Develop during Progression of Autoimmune Diabetes in NOD Mice. *Cell Metabolism* **25**, 727–738 (2017).
34. Karam, J. H., Grodsky, G. M. & Forsham, P. H. Excessive insulin response to glucose in obese subjects as measured by immunochemical assay. *Diabetes* **12**, 197–204 (1963).
35. Perley, M. J. & Kipnis, D. M. Plasma Insulin Responses to Oral and Intravenous Glucose: Studies in Normal and Diabetic Subjects. *J Clin Invest* **46**, 1954–1962 (1967).

36. Bonadonna, R. C. *et al.* Obesity and insulin resistance in humans: A dose-response study. *Metabolism* **39**, 452–459 (1990).
37. Mitrakou, A. *et al.* Role of reduced suppression of glucose production and diminished early insulin release in impaired glucose tolerance. *N Engl J Med* **326**, 22–29 (1992).
38. CHEN, M., BERGMAN, R. N., PACINI, G. & PORTE, D., JR. Pathogenesis of Age-Related Glucose Intolerance in Man: Insulin Resistance and Decreased  $\beta$ -Cell Function\*. *The Journal of Clinical Endocrinology & Metabolism* **60**, 13–20 (1985).
39. Utzschneider, K. M. *et al.* Oral disposition index predicts the development of future diabetes above and beyond fasting and 2-h glucose levels. *Diabetes Care* **32**, 335–341 (2009).
40. Quianzon, C. C. & Cheikh, I. History of insulin. *J Community Hosp Intern Med Perspect* **2**, 10.3402/jchimp.v2i2.18701 (2012).
41. Karamanou, M., Protogerou, A., Tsoucalas, G., Androutsos, G. & Poulakou-Rebelakou, E. Milestones in the history of diabetes mellitus: The main contributors. *World J Diabetes* **7**, 1–7 (2016).
42. Steiner, D. F. *et al.* The role of prohormone convertases in insulin biosynthesis: evidence for inherited defects in their action in man and experimental animals. *Diabetes Metab* **22**, 94–104 (1996).
43. Cnop, M. *et al.* Mechanisms of pancreatic beta-cell death in type 1 and type 2 diabetes: many differences, few similarities. *Diabetes* **54 Suppl 2**, S97-107 (2005).
44. Nishi, M. & Nanjo, K. Insulin gene mutations and diabetes. *J Diabetes Investig* **2**, 92–100 (2011).

45. Evans-Molina, C. *et al.* Glucose Regulation of Insulin Gene Transcription and Pre-mRNA Processing in Human Islets. *Diabetes* **56**, 827–835 (2007).
46. Alarcon, C., Verchere, C. B. & Rhodes, C. J. Translational Control of Glucose-Induced Islet Amyloid Polypeptide Production in Pancreatic Islets. *Endocrinology* **153**, 2082–2087 (2012).
47. Greenman, I. C., Gomez, E., Moore, C. E. J. & Herbert, T. P. The selective recruitment of mRNA to the ER and an increase in initiation are important for glucose-stimulated proinsulin synthesis in pancreatic  $\beta$ -cells. *Biochem J* **391**, 291–300 (2005).
48. Rhodes, C. J. & Halban, P. A. Newly synthesized proinsulin/insulin and stored insulin are released from pancreatic B cells predominantly via a regulated, rather than a constitutive, pathway. *Journal of Cell Biology* **105**, 145–153 (1987).
49. Rhodes, C. J., Lucas, C. A., Mutkoski, R. L., Orci, L. & Halban, P. A. Stimulation by ATP of proinsulin to insulin conversion in isolated rat pancreatic islet secretory granules. Association with the ATP-dependent proton pump. *J Biol Chem* **262**, 10712–10717 (1987).
50. Davidson, H. W., Wenzlau, J. M. & O'Brien, R. M. Zinc transporter 8 (ZnT8) and  $\beta$  cell function. *Trends in Endocrinology & Metabolism* **25**, 415–424 (2014).
51. Hou, J. C., Min, L. & Pessin, J. E. Insulin Granule Biogenesis, Trafficking and Exocytosis. *Vitam Horm* **80**, 473–506 (2009).
52. Riahi, Y. *et al.* Autophagy is a major regulator of  $\beta$ -cell insulin homeostasis. *Diabetologia* **59**, 1480–1491 (2016).

53. Pearson, G. L., Gingerich, M. A., Walker, E. M., Biden, T. J. & Soleimanpour, S. A. A Selective Look at Autophagy in Pancreatic  $\beta$ -Cells. *Diabetes* **70**, 1229–1241 (2021).
54. Hoboth, P. *et al.* Aged insulin granules display reduced microtubule-dependent mobility and are disposed within actin-positive multigranular bodies. *Proceedings of the National Academy of Sciences* **112**, E667–E676 (2015).
55. Cunningham, C. N. *et al.* Cells Deploy a Two-Pronged Strategy to Rectify Misfolded Proinsulin Aggregates. *Molecular Cell* **75**, 442–456.e4 (2019).
56. Muralidharan, C. *et al.* Pancreatic beta cell autophagy is impaired in type 1 diabetes. *Diabetologia* **64**, 865–877 (2021).
57. Masini, M. *et al.* Autophagy in human type 2 diabetes pancreatic beta cells. *Diabetologia* **52**, 1083–1086 (2009).
58. Kahn, S. E. *et al.* Evidence of Cosecretion of Islet Amyloid Polypeptide and Insulin by  $\beta$ -Cells. *Diabetes* **39**, 634–638 (1990).
59. Gorovits, N. & Charron, M. J. What we know about facilitative glucose transporters: Lessons from cultured cells, animal models, and human studies. *Biochemistry and Molecular Biology Education* **31**, 163–172 (2003).
60. Matschinsky, F. M. & Wilson, D. F. The Central Role of Glucokinase in Glucose Homeostasis: A Perspective 50 Years After Demonstrating the Presence of the Enzyme in Islets of Langerhans. *Front Physiol* **10**, 148 (2019).
61. Campbell, J. E. & Newgard, C. B. Mechanisms controlling pancreatic islet cell function in insulin secretion. *Nat Rev Mol Cell Biol* **22**, 142–158 (2021).

62. Evans-Molina, C. The Ailing  $\beta$ -Cell in Diabetes: Insights From a Trip to the ER: The 2023 Outstanding Scientific Achievement Award Lecture. *Diabetes* **73**, 545–553 (2024).
63. Wang, Z. & Thurmond, D. C. Mechanisms of biphasic insulin-granule exocytosis – roles of the cytoskeleton, small GTPases and SNARE proteins. *J Cell Sci* **122**, 893–903 (2009).
64. Trexler, A. J. & Taraska, J. W. Regulation of insulin exocytosis by calcium-dependent protein kinase C in beta cells. *Cell Calcium* **67**, 1–10 (2017).
65. Kalwat, M. A. & Cobb, M. H. Mechanisms of the Amplifying Pathway of Insulin Secretion in the  $\beta$  Cell. *Pharmacol Ther* **179**, 17–30 (2017).
66. Campbell-Thompson, M. *et al.* Insulinitis and  $\beta$ -Cell Mass in the Natural History of Type 1 Diabetes. *Diabetes* **65**, 719–731 (2015).
67. Coppieters, K. T. *et al.* Demonstration of islet-autoreactive CD8 T cells in insulitic lesions from recent onset and long-term type 1 diabetes patients. *Journal of Experimental Medicine* **209**, 51–60 (2012).
68. Keenan, H. A. *et al.* Residual Insulin Production and Pancreatic  $\beta$ -Cell Turnover After 50 Years of Diabetes: Joslin Medalist Study. *Diabetes* **59**, 2846–2853 (2010).
69. Hao, W. *et al.* Assessment of  $\beta$  Cell Mass and Function by AIRmax and Intravenous Glucose in High-Risk Subjects for Type 1 Diabetes. *J Clin Endocrinol Metab* **102**, 4428–4434 (2017).
70. Roep, B. O., Thomaidou, S., van Tienhoven, R. & Zaldumbide, A. Type 1 diabetes mellitus as a disease of the  $\beta$ -cell (do not blame the immune system?). *Nat Rev Endocrinol* **17**, 150–161 (2021).

71. Sims, E. K. *et al.* Teplizumab improves and stabilizes beta cell function in antibody-positive high-risk individuals. *Science Translational Medicine* **13**, eabc8980 (2021).
72. Evans-Molina, C. *et al.*  $\beta$  Cell dysfunction exists more than 5 years before type 1 diabetes diagnosis. *JCI Insight* **3**, e120877.
73. Erlich, H. *et al.* HLA DR-DQ Haplotypes and Genotypes and Type 1 Diabetes Risk: Analysis of the Type 1 Diabetes Genetics Consortium Families. *Diabetes* **57**, 1084–1092 (2008).
74. Barrett, J. C. *et al.* Genome-wide association study and meta-analysis finds over 40 loci affect risk of type 1 diabetes. *Nat Genet* **41**, 703–707 (2009).
75. Inshaw, J. R. J., Cutler, A. J., Crouch, D. J. M., Wicker, L. S. & Todd, J. A. Genetic Variants Predisposing Most Strongly to Type 1 Diabetes Diagnosed Under Age 7 Years Lie Near Candidate Genes That Function in the Immune System and in Pancreatic  $\beta$ -Cells. *Diabetes Care* **43**, 169–177 (2020).
76. Kaprio, J. *et al.* Concordance for Type 1 (insulin-dependent) and Type 2 (non-insulin-dependent) diabetes mellitus in a population-based cohort of twins in Finland. *Diabetologia* **35**, 1060–1067 (1992).
77. Knip, M. Pathogenesis of Type 1 Diabetes: Implications for Incidence Trends. *Hormone Research in Paediatrics* **76**, 57–64 (2011).
78. Graves, P. M. *et al.* Prospective study of enteroviral infections and development of beta-cell autoimmunity: Diabetes autoimmunity study in the young (DAISY). *Diabetes Research and Clinical Practice* **59**, 51–61 (2003).
79. Groot, P. F. de *et al.* Distinct fecal and oral microbiota composition in human type 1 diabetes, an observational study. *PLOS ONE* **12**, e0188475 (2017).

80. Knip, M. & Simell, O. Environmental Triggers of Type 1 Diabetes. *Cold Spring Harb Perspect Med* **2**, a007690 (2012).
81. The Concurrent Accumulation of Intra-Abdominal and Subcutaneous Fat Explains the Association Between Insulin Resistance and Plasma Leptin Concentrations | Diabetes | American Diabetes Association.  
<https://diabetesjournals.org/diabetes/article/51/4/1005/34624/The-Concurrent-Accumulation-of-Intra-Abdominal-and>.
82. DeFronzo, R. A. From the Triumvirate to the Ominous Octet: A New Paradigm for the Treatment of Type 2 Diabetes Mellitus. *Diabetes* **58**, 773–795 (2009).
83. Kahn, S. E., Hull, R. L. & Utzschneider, K. M. Mechanisms linking obesity to insulin resistance and type 2 diabetes. *Nature* **444**, 840–846 (2006).
84. Mahajan, A. *et al.* Refining the accuracy of validated target identification through coding variant fine-mapping in type 2 diabetes. *Nat Genet* **50**, 559–571 (2018).
85. Vasu, S. *et al.* MicroRNA Signatures as Future Biomarkers for Diagnosis of Diabetes States. *Cells* **8**, 1533 (2019).
86. Singer, R. A. & Sussel, L. Islet Long Noncoding RNAs: A Playbook for Discovery and Characterization. *Diabetes* **67**, 1461–1470 (2018).
87. Kahn, S. E., Andrikopoulos, S. & Verchere, C. B. Islet amyloid: a long-recognized but underappreciated pathological feature of type 2 diabetes. *Diabetes* **48**, 241–253 (1999).
88. Jurgens, C. A. *et al.*  $\beta$ -Cell Loss and  $\beta$ -Cell Apoptosis in Human Type 2 Diabetes Are Related to Islet Amyloid Deposition. *The American Journal of Pathology* **178**, 2632–2640 (2011).

89. Lorenzo, A., Razzaboni, B., Weir, G. C. & Yankner, B. A. Pancreatic islet cell toxicity of amylin associated with type-2 diabetes mellitus. *Nature* **368**, 756–760 (1994).
90. Lopes, D. H. J. *et al.* Amyloidogenicity and Cytotoxicity of Recombinant Mature Human Islet Amyloid Polypeptide (rhIAPP) \*. *Journal of Biological Chemistry* **279**, 42803–42810 (2004).
91. Abedini, A. *et al.* RAGE binds preamyloid IAPP intermediates and mediates pancreatic  $\beta$  cell proteotoxicity. *J Clin Invest* **128**, 682–698 (2018).
92. Chen, W. J. *et al.* Expression cloning and receptor pharmacology of human calcitonin receptors from MCF-7 cells and their relationship to amylin receptors. *Mol Pharmacol* **52**, 1164–1175 (1997).
93. Westwell-Roper, C. Y., Ehses, J. A. & Verchere, C. B. Resident macrophages mediate islet amyloid polypeptide-induced islet IL-1 $\beta$  production and  $\beta$ -cell dysfunction. *Diabetes* **63**, 1698–1711 (2014).
94. Meier, D. T. *et al.* Islet amyloid formation is an important determinant for inducing islet inflammation in high-fat-fed human IAPP transgenic mice. *Diabetologia* **57**, 1884–1888 (2014).
95. TATTERSALL, R. B. Mild Familial Diabetes with Dominant Inheritance. *QJM: An International Journal of Medicine* **43**, 339–357 (1974).
96. Hattersley, A. T. & Patel, K. A. Precision diabetes: learning from monogenic diabetes. *Diabetologia* **60**, 769–777 (2017).

97. Franco, E. D. *et al.* The effect of early, comprehensive genomic testing on clinical care in neonatal diabetes: an international cohort study. *The Lancet* **386**, 957–963 (2015).
98. Kayani, K., Mohammed, R. & Mohiaddin, H. Cystic Fibrosis-Related Diabetes. *Front Endocrinol (Lausanne)* **9**, 20 (2018).
99. Granados, A. *et al.* Cystic fibrosis related diabetes: Pathophysiology, screening and diagnosis. *Journal of Cystic Fibrosis* **18**, S3–S9 (2019).
100. Guo, J. H. *et al.* Glucose-induced electrical activities and insulin secretion in pancreatic islet  $\beta$ -cells are modulated by CFTR. *Nat Commun* **5**, 4420 (2014).
101. Hull, R. L. *et al.* Islet Interleukin-1 $\beta$  Immunoreactivity Is an Early Feature of Cystic Fibrosis That May Contribute to  $\beta$ -Cell Failure. *Diabetes Care* **41**, 823–830 (2018).
102. Moheet, A. *et al.* Lumacaftor/ivacaftor therapy fails to increase insulin secretion in F508del/F508del CF patients. *Journal of Cystic Fibrosis* **20**, 333–338 (2021).
103. Leturque, A., Burnol, A. F., Ferre, P. & Girard, J. Pregnancy-induced insulin resistance in the rat: assessment by glucose clamp technique. *American Journal of Physiology-Endocrinology and Metabolism* **246**, E25–E31 (1984).
104. American Diabetes Association. Gestational Diabetes Mellitus. *Diabetes Care* **27**, s88–s90 (2004).
105. You, H., Hu, J., Liu, Y., Luo, B. & Lei, A. Risk of type 2 diabetes mellitus after gestational diabetes mellitus: A systematic review & meta-analysis. *Indian J Med Res* **154**, 62–77 (2021).
106. Lapolla, A. & Metzger, B. E. *Gestational Diabetes: A Decade after the HAPO Study*. (Karger Medical and Scientific Publishers, 2019).

107. Lowe, W. L., Scholtens, D. M., Sandler, V. & Hayes, M. G. Genetics of Gestational Diabetes Mellitus and Maternal Metabolism. *Curr Diab Rep* **16**, 15 (2016).
108. Grankvist, K., Marklund, S. L. & Täljedal, I. B. CuZn-superoxide dismutase, Mn-superoxide dismutase, catalase and glutathione peroxidase in pancreatic islets and other tissues in the mouse. *Biochem J* **199**, 393–398 (1981).
109. Corbett, J. A. *et al.* Nitric Oxide Mediates IL-1 $\beta$ -Induced Islet Dysfunction and Destruction: Prevention by Dexamethasone. *Autoimmunity* **15**, 145–153 (1993).
110. Steer, S. A., Scarim, A. L., Chambers, K. T. & Corbett, J. A. Interleukin-1 stimulates beta-cell necrosis and release of the immunological adjuvant HMGB1. *PLoS Med* **3**, e17 (2006).
111. Gerber, P. A. & Rutter, G. A. The Role of Oxidative Stress and Hypoxia in Pancreatic Beta-Cell Dysfunction in Diabetes Mellitus. *Antioxid Redox Signal* **26**, 501–518 (2017).
112. Kaneto, H. *et al.* Apoptotic cell death triggered by nitric oxide in pancreatic beta-cells. *Diabetes* **44**, 733–738 (1995).
113. Tersey, S. A. *et al.* 12-Lipoxygenase Promotes Obesity-Induced Oxidative Stress in Pancreatic Islets. *Mol Cell Biol* **34**, 3735–3745 (2014).
114. Hernandez-Perez, M. *et al.* Inhibition of 12/15-Lipoxygenase Protects Against  $\beta$ -Cell Oxidative Stress and Glycemic Deterioration in Mouse Models of Type 1 Diabetes. *Diabetes* **66**, 2875–2887 (2017).
115. Prentki, M. & Corkey, B. E. Are the  $\beta$ -Cell Signaling Molecules Malonyl-CoA and Cystolic Long-Chain Acyl-CoA Implicated in Multiple Tissue Defects of Obesity and NIDDM? *Diabetes* **45**, 273–283 (1996).

116. Weir, G. C. Glucolipotoxicity,  $\beta$ -Cells, and Diabetes: The Emperor Has No Clothes. *Diabetes* **69**, 273–278 (2020).
117. Robertson, R. P., Zhang, H. J., Pyzdrowski, K. L. & Walseth, T. F. Preservation of insulin mRNA levels and insulin secretion in HIT cells by avoidance of chronic exposure to high glucose concentrations. *J Clin Invest* **90**, 320–325 (1992).
118. Lytrivi, M., Castell, A.-L., Poitout, V. & Cnop, M. Recent insights into mechanisms of  $\beta$ -cell lipo- and glucolipotoxicity in type 2 diabetes. *J Mol Biol* **432**, 1514–1534 (2020).
119. Lupi, R. *et al.* Prolonged Exposure to Free Fatty Acids Has Cytostatic and Pro-Apoptotic Effects on Human Pancreatic Islets: Evidence that  $\beta$ -Cell Death Is Caspase Mediated, Partially Dependent on Ceramide Pathway, and Bcl-2 Regulated. *Diabetes* **51**, 1437–1442 (2002).
120. El-Assaad, W. *et al.* Saturated Fatty Acids Synergize with Elevated Glucose to Cause Pancreatic  $\beta$ -Cell Death. *Endocrinology* **144**, 4154–4163 (2003).
121. Kharroubi, I. *et al.* Free Fatty Acids and Cytokines Induce Pancreatic  $\beta$ -Cell Apoptosis by Different Mechanisms: Role of Nuclear Factor- $\kappa$ B and Endoplasmic Reticulum Stress. *Endocrinology* **145**, 5087–5096 (2004).
122. Elmore, S. Apoptosis: A Review of Programmed Cell Death. *Toxicol Pathol* **35**, 495–516 (2007).
123. Kerr, J. F. R., Wyllie, A. H. & Currie, A. R. Apoptosis: A Basic Biological Phenomenon with Wide-ranging Implications in Tissue Kinetics. *Br J Cancer* **26**, 239–257 (1972).

124. Norbury, C. J. & Hickson, I. D. Cellular responses to DNA damage. *Annu Rev Pharmacol Toxicol* **41**, 367–401 (2001).
125. Vaux, D. L. & Korsmeyer, S. J. Cell death in development. *Cell* **96**, 245–254 (1999).
126. Chen, M. & Wang, J. Initiator caspases in apoptosis signaling pathways. *Apoptosis* **7**, 313–319 (2002).
127. Parrish, A. B., Freel, C. D. & Kornbluth, S. Cellular Mechanisms Controlling Caspase Activation and Function. *Cold Spring Harb Perspect Biol* **5**, a008672 (2013).
128. Boada-Romero, E., Martinez, J., Heckmann, B. L. & Green, D. R. The clearance of dead cells by efferocytosis. *Nat Rev Mol Cell Biol* **21**, 398–414 (2020).
129. Mandrup-Poulsen, T. beta-cell apoptosis: stimuli and signaling. *Diabetes* **50**, S58 (2001).
130. Hui, H., Dotta, F., Di Mario, U. & Perfetti, R. Role of caspases in the regulation of apoptotic pancreatic islet beta-cells death. *J Cell Physiol* **200**, 177–200 (2004).
131. Thomas, H. E., McKenzie, M. D., Angstetra, E., Campbell, P. D. & Kay, T. W. Beta cell apoptosis in diabetes. *Apoptosis* **14**, 1389–1404 (2009).
132. Yamada, K., Ichikawa, F., Ishiyama-Shigemoto, S., Yuan, X. & Nonaka, K. Essential role of caspase-3 in apoptosis of mouse beta-cells transfected with human Fas. *Diabetes* **48**, 478–483 (1999).
133. Liadis, N. *et al.* Caspase-3-Dependent  $\beta$ -Cell Apoptosis in the Initiation of Autoimmune Diabetes Mellitus. *Mol Cell Biol* **25**, 3620–3629 (2005).

134. Li, H. *et al.* Suppression of Caspase-3 Activation Protects Primary Islet  $\beta$ -Cells from the Cytotoxic Effects of Human Islet Amyloid Polypeptide. *Canadian Journal of Diabetes* **32**, 302 (2008).
135. Grunnet, L. G. *et al.* Proinflammatory cytokines activate the intrinsic apoptotic pathway in beta-cells. *Diabetes* **58**, 1807–1815 (2009).
136. Zaitseva, I. I. *et al.* Suppressor of cytokine signaling-1 inhibits caspase activation and protects from cytokine-induced beta cell death. *Cell. Mol. Life Sci.* **66**, 3787–3795 (2009).
137. Liadis, N. *et al.* Distinct In Vivo Roles of Caspase-8 in  $\beta$ -Cells in Physiological and Diabetes Models. *Diabetes* **56**, 2302–2311 (2007).
138. Emamaullee, J. A., Stanton, L., Schur, C. & Shapiro, A. M. J. Caspase inhibitor therapy enhances marginal mass islet graft survival and preserves long-term function in islet transplantation. *Diabetes* **56**, 1289–1298 (2007).
139. McCall, M. & James Shapiro, A. M. Update on Islet Transplantation. *Cold Spring Harb Perspect Med* **2**, a007823 (2012).
140. Pepper, A. R. *et al.* Engraftment Site and Effectiveness of the Pan-Caspase Inhibitor F573 to Improve Engraftment in Mouse and Human Islet Transplantation in Mice. *Transplantation* **101**, 2321–2329 (2017).
141. Emamaullee, J. A. *et al.* The caspase selective inhibitor EP1013 augments human islet graft function and longevity in marginal mass islet transplantation in mice. *Diabetes* **57**, 1556–1566 (2008).
142. McCall, M. *et al.* The caspase inhibitor IDN-6556 (PF3491390) improves marginal mass engraftment after islet transplantation in mice. *Surgery* **150**, 48–55 (2011).

143. Bellin, M. D. *et al.* Prolonged insulin independence after islet allotransplants in recipients with type 1 diabetes. *Am J Transplant* **8**, 2463–2470 (2008).
144. Matsumoto, S. *et al.* Improving efficacy of clinical islet transplantation with iodixanol-based islet purification, thymoglobulin induction, and blockage of IL-1 $\beta$  and TNF- $\alpha$ . *Cell Transplant* **20**, 1641–1647 (2011).
145. Onaca, N., Takita, M., Levy, M. F. & Naziruddin, B. Anti-inflammatory Approach With Early Double Cytokine Blockade (IL-1 $\beta$  and TNF- $\alpha$ ) Is Safe and Facilitates Engraftment in Islet Allotransplantation. *Transplant Direct* **6**, e530 (2020).
146. Fehsel, K., Kolb-Bachofen, V. & Kröncke, K.-D. Necrosis is the predominant type of islet cell death during development of insulin-dependent diabetes mellitus in BB rats. *Lab Invest* **83**, 549–559 (2003).
147. Hoorens, A., Stangé, G., Pavlovic, D. & Pipeleers, D. Distinction Between Interleukin-1–Induced Necrosis and Apoptosis of Islet Cells. *Diabetes* **50**, 551–557 (2001).
148. Majno, G. & Joris, I. Apoptosis, oncosis, and necrosis. An overview of cell death. *Am J Pathol* **146**, 3–15 (1995).
149. Buja, L. M., Eigenbrodt, M. L. & Eigenbrodt, E. H. Apoptosis and necrosis. Basic types and mechanisms of cell death. *Arch. Pathol. Lab. Med.* **117**, 1208–1214 (1993).
150. Davidovich, P., Kearney, C. J. & Martin, S. J. Inflammatory outcomes of apoptosis, necrosis and necroptosis. *Biol. Chem.* **395**, 1163–1171 (2014).
151. Rock, K. L. & Kono, H. The inflammatory response to cell death. *Annu Rev Pathol* **3**, 99–126 (2008).

152. Raucci, A., Palumbo, R. & Bianchi, M. E. HMGB1: a signal of necrosis. *Autoimmunity* **40**, 285–289 (2007).
153. Anthony, P. Robbins' Pathologic Basis of Disease. *J Clin Pathol* **43**, 176 (1990).
154. Collier, J. J., Fueger, P. T., Hohmeier, H. E. & Newgard, C. B. Pro- and antiapoptotic proteins regulate apoptosis but do not protect against cytokine-mediated cytotoxicity in rat islets and beta-cell lines. *Diabetes* **55**, 1398–1406 (2006).
155. Collier, J. J. *et al.* Pancreatic  $\beta$ -Cell Death in Response to Pro-Inflammatory Cytokines Is Distinct from Genuine Apoptosis. *PLoS One* **6**, e22485 (2011).
156. Irawaty, W., Kay, T. W. H. & Thomas, H. E. Transmembrane TNF and IFN $\gamma$  Induce Caspase-independent Death of Primary Mouse Pancreatic Beta Cells. *Autoimmunity* **35**, 369–375 (2002).
157. Scarim, A. L. *et al.* Mechanisms of  $\beta$ -Cell Death in Response to Double-Stranded (ds) RNA and Interferon- $\gamma$ : dsRNA-Dependent Protein Kinase Apoptosis and Nitric Oxide-Dependent Necrosis. *The American Journal of Pathology* **159**, 273–283 (2001).
158. Biarnés, M. *et al.*  $\beta$ -Cell Death and Mass in Syngeneically Transplanted Islets Exposed to Short- and Long-Term Hyperglycemia. *Diabetes* **51**, 66–72 (2002).
159. Cheng, Y. *et al.* Hypoxia/reoxygenation-induced HMGB1 translocation and release promotes islet proinflammatory cytokine production and early islet graft failure through TLRs signaling. *Biochim Biophys Acta Mol Basis Dis* **1863**, 354–364 (2017).

160. Gebe, J. A., Preisinger, A., Gooden, M. D., D'Amico, L. A. & Vernon, R. B. Local, Controlled Release In Vivo of Vascular Endothelial Growth Factor Within a Subcutaneous Scaffolded Islet Implant Reduces Early Islet Necrosis and Improves Performance of the Graft. *Cell Transplant* **27**, 531–541 (2018).
161. Alberts, B. *et al.* Programmed Cell Death (Apoptosis). *Molecular Biology of the Cell. 4th edition* (2002).
162. Berghe, T. V., Linkermann, A., Jouan-Lanhouet, S., Walczak, H. & Vandenabeele, P. Regulated necrosis: the expanding network of non-apoptotic cell death pathways. *Nat Rev Mol Cell Biol* **15**, 135–147 (2014).
163. Conrad, M., Angeli, J. P. F., Vandenabeele, P. & Stockwell, B. R. Regulated necrosis: disease relevance and therapeutic opportunities. *Nat Rev Drug Discov* **15**, 348–366 (2016).
164. Linkermann, A. & Green, D. R. Necroptosis. *New England Journal of Medicine* **370**, 455–465 (2014).
165. Proskuryakov, S. Y. a, Konoplyannikov, A. G. & Gabai, V. L. Necrosis: a specific form of programmed cell death? *Experimental Cell Research* **283**, 1–16 (2003).
166. Galluzzi, L. *et al.* Guidelines for the use and interpretation of assays for monitoring cell death in higher eukaryotes. *Cell Death Differ* **16**, 1093–1107 (2009).
167. Tonnus, W. *et al.* The role of regulated necrosis in endocrine diseases. *Nat Rev Endocrinol* **17**, 497–510 (2021).
168. Contreras, C. J. *et al.* RIPK1 and RIPK3 regulate TNF $\alpha$ -induced  $\beta$ -cell death in concert with caspase activity. *Molecular Metabolism* **65**, 101582 (2022).

169. Yang, B. *et al.* RIPK3-mediated inflammation is a conserved  $\beta$  cell response to ER stress. *Science Advances* **6**, eabd7272 (2020).
170. Bruni, A. *et al.* Ferroptosis-inducing agents compromise in vitro human islet viability and function. *Cell Death Dis* **9**, 1–10 (2018).
171. Vercammen, D. *et al.* Inhibition of Caspases Increases the Sensitivity of L929 Cells to Necrosis Mediated by Tumor Necrosis Factor. *Journal of Experimental Medicine* **187**, 1477–1485 (1998).
172. Liu, C.-Y. *et al.* Broad-spectrum caspase inhibition paradoxically augments cell death in TNF- $\alpha$ -stimulated neutrophils. *Blood* **101**, 295–304 (2003).
173. Wilson, N. S., Dixit, V. & Ashkenazi, A. Death receptor signal transducers: nodes of coordination in immune signaling networks. *Nat Immunol* **10**, 348–355 (2009).
174. Li, X. *et al.* Ubiquitination of RIPK1 regulates its activation mediated by TNFR1 and TLRs signaling in distinct manners. *Nat Commun* **11**, 6364 (2020).
175. Brenner, D., Blaser, H. & Mak, T. W. Regulation of tumour necrosis factor signalling: live or let die. *Nat Rev Immunol* **15**, 362–374 (2015).
176. Gerlach, B. *et al.* Linear ubiquitination prevents inflammation and regulates immune signalling. *Nature* **471**, 591–596 (2011).
177. Lin, Y., Devin, A., Rodriguez, Y. & Liu, Z. G. Cleavage of the death domain kinase RIP by caspase-8 prompts TNF-induced apoptosis. *Genes Dev* **13**, 2514–2526 (1999).
178. Feng, S. *et al.* Cleavage of RIP3 inactivates its caspase-independent apoptosis pathway by removal of kinase domain. *Cell Signal* **19**, 2056–2067 (2007).

179. Dondelinger, Y. *et al.* MLKL Compromises Plasma Membrane Integrity by Binding to Phosphatidylinositol Phosphates. *Cell Reports* **7**, 971–981 (2014).
180. Cai, Z. *et al.* Plasma membrane translocation of trimerized MLKL protein is required for TNF-induced necroptosis. *Nat Cell Biol* **16**, 55–65 (2014).
181. Hildebrand, J. M. *et al.* Activation of the pseudokinase MLKL unleashes the four-helix bundle domain to induce membrane localization and necroptotic cell death. *Proc Natl Acad Sci U S A* **111**, 15072–15077 (2014).
182. Kaczmarek, A., Vandenabeele, P. & Krysko, D. V. Necroptosis: The Release of Damage-Associated Molecular Patterns and Its Physiological Relevance. *Immunity* **38**, 209–223 (2013).
183. Murai, S. *et al.* A FRET biosensor for necroptosis uncovers two different modes of the release of DAMPs. *Nat Commun* **9**, 4457 (2018).
184. Holler, N. *et al.* Fas triggers an alternative, caspase-8-independent cell death pathway using the kinase RIP as effector molecule. *Nat Immunol* **1**, 489–495 (2000).
185. Thapa, R. J. *et al.* Interferon-induced RIP1/RIP3-mediated necrosis requires PKR and is licensed by FADD and caspases. *Proceedings of the National Academy of Sciences* **110**, E3109–E3118 (2013).
186. Meurette, O. *et al.* TRAIL (TNF-Related Apoptosis-Inducing Ligand) Induces Necrosis-Like Cell Death in Tumor Cells at Acidic Extracellular pH. *Annals of the New York Academy of Sciences* **1056**, 379–387 (2005).
187. Li, W. & Yuan, J. Targeting RIPK1 kinase for modulating inflammation in human diseases. *Front Immunol* **14**, 1159743 (2023).

188. Kaestner, K. H., Powers, A. C., Najj, A., HPAP Consortium & Atkinson, M. A. NIH Initiative to Improve Understanding of the Pancreas, Islet, and Autoimmunity in Type 1 Diabetes: The Human Pancreas Analysis Program (HPAP). *Diabetes* **68**, 1394–1402 (2019).
189. Paredes-Juarez, G. A. *et al.* DAMP production by human islets under low oxygen and nutrients in the presence or absence of an immunoisolating-capsule and necrostatin-1. *Sci Rep* **5**, 14623 (2015).
190. Tamura, Y. *et al.* NO donor induces Nec-1-inhibitable, but RIP1-independent, necrotic cell death in pancreatic  $\beta$ -cells. *FEBS Lett* **585**, 3058–3064 (2011).
191. Lau, H. *et al.* Dose-dependent effects of necrostatin-1 supplementation to tissue culture media of young porcine islets. *PLoS One* **15**, e0243506 (2020).
192. Takiishi, T. *et al.* Inhibition of RIPK1 kinase does not affect diabetes development:  $\beta$ -Cells survive RIPK1 activation. *Mol Metab* **69**, 101681 (2023).
193. Newton, K. *et al.* Activity of protein kinase RIPK3 determines whether cells die by necroptosis or apoptosis. *Science* **343**, 1357–1360 (2014).
194. Lawlor, K. E. *et al.* RIPK3 promotes cell death and NLRP3 inflammasome activation in the absence of MLKL. *Nat Commun* **6**, (2015).
195. Orozco, S. & Oberst, A. RIPK3 in cell death and inflammation: The Good, the Bad, and the Ugly. *Immunol Rev* **277**, 102–112 (2017).
196. Moriwaki, K. & Chan, F. K.-M. Chapter Seven - The Inflammatory Signal Adaptor RIPK3: Functions Beyond Necroptosis. in *International Review of Cell and Molecular Biology* (ed. Galluzzi, L.) vol. 328 253–275 (Academic Press, 2017).

197. Kim, H. *et al.* Ischemia-reperfusion induces death receptor-independent necroptosis via calpain-STAT3 activation in a lung transplant setting. *Am J Physiol Lung Cell Mol Physiol* **315**, L595–L608 (2018).
198. Lau, A. *et al.* RIPK3-mediated necroptosis promotes donor kidney inflammatory injury and reduces allograft survival. *Am J Transplant* **13**, 2805–2818 (2013).
199. Pavlosky, A. *et al.* RIPK3-mediated necroptosis regulates cardiac allograft rejection. *Am J Transplant* **14**, 1778–1790 (2014).
200. Lau, H. *et al.* Necrostatin-1 Supplementation to Islet Tissue Culture Enhances the In-Vitro Development and Graft Function of Young Porcine Islets. *International Journal of Molecular Sciences* **22**, 8367 (2021).
201. Zhao, Y. *et al.* Autoreactive T cells induce necrosis and not BCL-2-regulated or death receptor-mediated apoptosis or RIPK3-dependent necroptosis of transplanted islets in a mouse model of type 1 diabetes. *Diabetologia* **58**, 140–148 (2015).
202. Xie, Y. *et al.* Ferroptosis: process and function. *Cell Death Differ* **23**, 369–379 (2016).
203. Dixon, S. J. *et al.* Ferroptosis: An Iron-Dependent Form of Nonapoptotic Cell Death. *Cell* **149**, 1060–1072 (2012).
204. Sun, Y., Zheng, Y., Wang, C. & Liu, Y. Glutathione depletion induces ferroptosis, autophagy, and premature cell senescence in retinal pigment epithelial cells. *Cell Death Dis* **9**, 1–15 (2018).
205. Grankvist, K., Marklund, S. L. & Täljedal, I. B. CuZn-superoxide dismutase, Mn-superoxide dismutase, catalase and glutathione peroxidase in pancreatic islets and other tissues in the mouse. *Biochem J* **199**, 393–398 (1981).

206. Lei, X. G. & Vatamaniuk, M. Z. Two tales of antioxidant enzymes on  $\beta$  cells and diabetes. *Antioxid Redox Signal* **14**, 489–503 (2011).
207. Stancic, A. *et al.* Ferroptosis as a Novel Determinant of  $\beta$ -Cell Death in Diabetic Conditions. *Oxid Med Cell Longev* **2022**, 3873420 (2022).
208. Blesia, V., Patel, V. B., Al-Obaidi, H., Renshaw, D. & Zariwala, M. G. Excessive Iron Induces Oxidative Stress Promoting Cellular Perturbations and Insulin Secretory Dysfunction in MIN6 Beta Cells. *Cells* **10**, 1141 (2021).
209. Bradley, B., Prowse, S. J., Bauling, P. & Lafferty, K. J. Desferrioxamine treatment prevents chronic islet allograft damage. *Diabetes* **35**, 550–555 (1986).
210. Bergsbaken, T., Fink, S. L. & Cookson, B. T. Pyroptosis: host cell death and inflammation. *Nat Rev Microbiol* **7**, 99–109 (2009).
211. Cookson, B. T. & Brennan, M. A. Pro-inflammatory programmed cell death. *Trends in Microbiology* **9**, 113–114 (2001).
212. Kuang, S. *et al.* Structure insight of GSDMD reveals the basis of GSDMD autoinhibition in cell pyroptosis. *Proceedings of the National Academy of Sciences* **114**, 10642–10647 (2017).
213. Phulphagar, K. *et al.* Proteomics reveals distinct mechanisms regulating the release of cytokines and alarmins during pyroptosis. *Cell Rep* **34**, 108826 (2021).
214. Volchuk, A., Ye, A., Chi, L., Steinberg, B. E. & Goldenberg, N. M. Indirect regulation of HMGB1 release by gasdermin D. *Nat Commun* **11**, 4561 (2020).
215. Song, H. *et al.* Focus on the Mechanisms and Functions of Pyroptosis, Inflammasomes, and Inflammatory Caspases in Infectious Diseases. *Oxidative Medicine and Cellular Longevity* **2022**, e2501279 (2022).

216. Brennan, M. A. & Cookson, B. T. Salmonella induces macrophage death by caspase-1-dependent necrosis. *Molecular Microbiology* **38**, 31–40 (2000).
217. Russo, H. M. *et al.* Active Caspase-1 Induces Plasma Membrane Pores That Precede Pyroptotic Lysis and Are Blocked by Lanthanides. *The Journal of Immunology* **197**, 1353–1367 (2016).
218. Fink, S. L. & Cookson, B. T. Caspase-1-dependent pore formation during pyroptosis leads to osmotic lysis of infected host macrophages. *Cell Microbiol* **8**, 1812–1825 (2006).
219. Frørup, C., Svane, C. A. S., Henriksen, K., Kaur, S. & Størling, J. Beta-Cell Pyroptosis – A Burning Flame in Type 1 Diabetes? 2024.01.05.574294 Preprint at <https://doi.org/10.1101/2024.01.05.574294> (2024).
220. Liu, S. *et al.* MiR-17-5p Inhibits TXNIP/NLRP3 Inflammasome Pathway and Suppresses Pancreatic  $\beta$ -Cell Pyroptosis in Diabetic Mice. *Frontiers in Cardiovascular Medicine* **8**, (2021).
221. Tan, A., Li, T., Yang, J., Yu, J. & Chen, H. Irisin attenuates pyroptosis in high glucose-induced pancreatic beta cells via the miR-133a-3p/FOXO1 axis. *Endokrynol Pol* **74**, 277–284 (2023).
222. Xing, Y. *et al.* Emodin Alleviates High-Glucose-Induced Pancreatic  $\beta$ -Cell Pyroptosis by Inhibiting NLRP3/GSDMD Signaling. *Evid Based Complement Alternat Med* **2022**, 5276832 (2022).
223. Zhou, J. *et al.* Salidroside protects pancreatic  $\beta$ -cells against pyroptosis by regulating the NLRP3/GSDMD pathway in diabetic conditions. *International Immunopharmacology* **114**, 109543 (2023).

224. Liu, P. *et al.* Empagliflozin protects diabetic pancreatic tissue from damage by inhibiting the activation of the NLRP3/caspase-1/GSDMD pathway in pancreatic  $\beta$  cells: in vitro and in vivo studies. *Bioengineered* **12**, 9356–9366 (2021).
225. Ankarcona, M. *et al.* Glutamate-induced neuronal death: a succession of necrosis or apoptosis depending on mitochondrial function. *Neuron* **15**, 961–973 (1995).
226. Lin, C.-Y. *et al.* Simultaneous induction of apoptosis and necroptosis by Tanshinone IIA in human hepatocellular carcinoma HepG2 cells. *Cell Death Discov* **2**, 16065 (2016).
227. Preedy, M. K., White, M. R. H. & Tergaonkar, V. Cellular heterogeneity in TNF/TNFR1 signalling: live cell imaging of cell fate decisions in single cells. *Cell Death Dis* **15**, 1–12 (2024).
228. Cnop, M., Hannaert, J. C., Hoorens, A., Eizirik, D. L. & Pipeleers, D. G. Inverse Relationship Between Cytotoxicity of Free Fatty Acids in Pancreatic Islet Cells and Cellular Triglyceride Accumulation. *Diabetes* **50**, 1771–1777 (2001).
229. Saldeen, J. Cytokines Induce Both Necrosis and Apoptosis via a Common Bcl-2-Inhibitible Pathway in Rat Insulin-Producing Cells\*. *Endocrinology* **141**, 2003–2010 (2000).
230. Pancreatic Expression and Secretion of Human Islet Amyloid Polypeptide in a Transgenic Mouse | Diabetes | American Diabetes Association.  
<https://diabetesjournals.org/diabetes/article/43/12/1457/8297/Pancreatic-Expression-and-Secretion-of-Human-Islet>.
231. Cai, E. P. *et al.* Genome-scale in vivo CRISPR screen identifies RNLS as a target for beta cell protection in type 1 diabetes. *Nat Metab* **2**, 934–945 (2020).

232. Rahbar Saadat, Y., Saeidi, N., Zununi Vahed, S., Barzegari, A. & Barar, J. An update to DNA ladder assay for apoptosis detection. *Bioimpacts* **5**, 25–28 (2015).
233. Bone, R. N. *et al.* A Computational Approach for Defining a Signature of  $\beta$ -Cell Golgi Stress in Diabetes. *Diabetes* **69**, 2364–2376 (2020).
234. Dobin, A. *et al.* STAR: ultrafast universal RNA-seq aligner. *Bioinformatics* **29**, 15–21 (2013).
235. Robinson, M. D., McCarthy, D. J. & Smyth, G. K. edgeR: a Bioconductor package for differential expression analysis of digital gene expression data. *Bioinformatics* **26**, 139–140 (2010).
236. Duncan, J. S. *et al.* Dynamic Reprogramming of the Kinome In Response to Targeted MEK Inhibition In Triple Negative Breast Cancer. *Cell* **149**, 307–321 (2012).
237. Templin, A. T. *et al.* Low concentration IL-1 $\beta$  promotes islet amyloid formation by increasing hIAPP release from humanised mouse islets in vitro. *Diabetologia* **63**, 2385–2395 (2020).
238. Hull, R. L. *et al.* Increased dietary fat promotes islet amyloid formation and beta-cell secretory dysfunction in a transgenic mouse model of islet amyloid. *Diabetes* **52**, 372–379 (2003).
239. Wang, F., Hull, R. L., Vidal, J., Cnop, M. & Kahn, S. E. Islet Amyloid Develops Diffusely Throughout the Pancreas Before Becoming Severe and Replacing Endocrine Cells. *Diabetes* **50**, 2514–2520 (2001).

240. Meier, D. T. *et al.* Determination of Optimal Sample Size for Quantification of  $\beta$ -Cell Area, Amyloid Area and  $\beta$ -Cell Apoptosis in Isolated Islets. *J. Histochem. Cytochem.* **63**, 663–673 (2015).
241. Mathis, D., Vence, L. & Benoist, C. Beta-cell death during progression to diabetes. *Nature* **414**, 792–798 (2001).
242. Meier, J. J., Bhushan, A., Butler, A. E., Rizza, R. A. & Butler, P. C. Sustained beta cell apoptosis in patients with long-standing type 1 diabetes: indirect evidence for islet regeneration? *Diabetologia* **48**, 2221–2228 (2005).
243. Green, E. A., Eynon, E. E. & Flavell, R. A. Local Expression of TNF $\alpha$  in Neonatal NOD Mice Promotes Diabetes by Enhancing Presentation of Islet Antigens. *Immunity* **9**, 733–743 (1998).
244. Kägi, D. *et al.* TNF receptor 1-dependent beta cell toxicity as an effector pathway in autoimmune diabetes. *J. Immunol.* **162**, 4598–4605 (1999).
245. Quattrin, T. *et al.* Golimumab and Beta-Cell Function in Youth with New-Onset Type 1 Diabetes. *New England Journal of Medicine* **383**, 2007–2017 (2020).
246. Stephens, L. A. *et al.* Tumor necrosis factor-alpha-activated cell death pathways in NIT-1 insulinoma cells and primary pancreatic beta cells. *Endocrinology* **140**, 3219–3227 (1999).
247. Chang, I. *et al.* Nuclear Factor  $\kappa$ B Protects Pancreatic  $\beta$ -Cells From Tumor Necrosis Factor- $\alpha$ -Mediated Apoptosis. *Diabetes* **52**, 1169–1175 (2003).
248. Kim, H.-E. *et al.* Tumour necrosis factor-alpha-induced glucose-stimulated insulin secretion inhibition in INS-1 cells is ascribed to a reduction of the glucose-stimulated Ca<sup>2+</sup> influx. *J Endocrinol* **198**, 549–560 (2008).

249. Ortis, F. *et al.* Induction of nuclear factor-kappaB and its downstream genes by TNF-alpha and IL-1beta has a pro-apoptotic role in pancreatic beta cells. *Diabetologia* **51**, 1213–1225 (2008).
250. Irawaty, W., Kay, T. W. H. & Thomas, H. E. Transmembrane TNF and IFN $\gamma$  Induce Caspase-independent Death of Primary Mouse Pancreatic Beta Cells. *Autoimmunity* **35**, 369–375 (2002).
251. Yang, X. D. *et al.* Effect of tumor necrosis factor alpha on insulin-dependent diabetes mellitus in NOD mice. I. The early development of autoimmunity and the diabetogenic process. *Journal of Experimental Medicine* **180**, 995–1004 (1994).
252. Mastrandrea, L. *et al.* Etanercept Treatment in Children With New-Onset Type 1 Diabetes: Pilot randomized, placebo-controlled, double-blind study. *Diabetes Care* **32**, 1244–1249 (2009).
253. Eizirik, D. L. & Mandrup-Poulsen, T. A choice of death—the signal-transduction of immune-mediated beta-cell apoptosis. *Diabetologia* **44**, 2115–2133 (2001).
254. Linkermann, A. & Green, D. R. Necroptosis. *N Engl J Med* **370**, 455–465 (2014).
255. Newton, K. *et al.* Activity of Protein Kinase RIPK3 Determines Whether Cells Die by Necroptosis or Apoptosis. *Science* **343**, 1357–1360 (2014).
256. Vandenabeele, P., Galluzzi, L., Vanden Berghe, T. & Kroemer, G. Molecular mechanisms of necroptosis: an ordered cellular explosion. *Nat Rev Mol Cell Biol* **11**, 700–714 (2010).
257. Kaczmarek, A., Vandenabeele, P. & Krysko, D. V. Necroptosis: The Release of Damage-Associated Molecular Patterns and Its Physiological Relevance. *Immunity* **38**, 209–223 (2013).

258. Wang, J.-S., Wu, D., Huang, D.-Y. & Lin, W.-W. TAK1 inhibition-induced RIP1-dependent apoptosis in murine macrophages relies on constitutive TNF- $\alpha$  signaling and ROS production. *Journal of Biomedical Science* **22**, 76 (2015).
259. Amin, P. *et al.* Regulation of a distinct activated RIPK1 intermediate bridging complex I and complex II in TNF $\alpha$ -mediated apoptosis. *PNAS* **115**, E5944–E5953 (2018).
260. Dannappel, M. *et al.* RIPK1 maintains epithelial homeostasis by inhibiting apoptosis and necroptosis. *Nature* **513**, 90–94 (2014).
261. Liu, C.-Y. *et al.* Broad-spectrum caspase inhibition paradoxically augments cell death in TNF- $\alpha$  -stimulated neutrophils. *Blood* **101**, 295–304 (2003).
262. Varfolomeev, E. E. *et al.* Targeted disruption of the mouse Caspase 8 gene ablates cell death induction by the TNF receptors, Fas/Apo1, and DR3 and is lethal prenatally. *Immunity* **9**, 267–276 (1998).
263. Fritsch, M. *et al.* Caspase-8 is the molecular switch for apoptosis, necroptosis and pyroptosis. *Nature* **575**, 683–687 (2019).
264. Wang, H. *et al.* Mixed Lineage Kinase Domain-like Protein MLKL Causes Necrotic Membrane Disruption upon Phosphorylation by RIP3. *Molecular Cell* **54**, 133–146 (2014).
265. Tummers, B. & Green, D. R. Caspase-8; regulating life and death. *Immunol Rev* **277**, 76–89 (2017).
266. Tabebi, M. *et al.* Association study of apoptosis gene polymorphisms in mitochondrial diabetes: A potential role in the pathogenicity of MD. *Gene* **639**, 18–26 (2018).

267. Caccamo, A. *et al.* Necroptosis activation in Alzheimer's disease. *Nature Neuroscience* **20**, 1236–1246 (2017).
268. Wang, S., Zhang, C., Hu, L. & Yang, C. Necroptosis in acute kidney injury: a shedding light. *Cell Death Dis* **7**, e2125–e2125 (2016).
269. Riegger, J. & Brenner, R. E. Evidence of necroptosis in osteoarthritic disease: investigation of blunt mechanical impact as possible trigger in regulated necrosis. *Cell Death Dis* **10**, 1–12 (2019).
270. Chen, A.-Q. *et al.* Microglia-derived TNF- $\alpha$  mediates endothelial necroptosis aggravating blood brain–barrier disruption after ischemic stroke. *Cell Death Dis* **10**, 1–18 (2019).
271. Orozco, S. *et al.* RIPK1 both positively and negatively regulates RIPK3 oligomerization and necroptosis. *Cell Death Differ.* **21**, 1511–1521 (2014).
272. Silke, J. & Brink, R. Regulation of TNFRSF and innate immune signalling complexes by TRAFs and cIAPs. *Cell Death Differ* **17**, 35–45 (2010).
273. El-Mesery, M., Shaker, M. E. & Elgaml, A. The SMAC mimetic BV6 induces cell death and sensitizes different cell lines to TNF- $\alpha$  and TRAIL-induced apoptosis. *Exp Biol Med (Maywood)* **241**, 2015–2022 (2016).
274. Li, W. *et al.* BV6, an IAP Antagonist, Activates Apoptosis and Enhances Radiosensitization of Non-small Cell Lung Carcinoma In Vitro. *Journal of Thoracic Oncology* **6**, 1801–1809 (2011).
275. Akara-amornthum, P., Lomphithak, T., Choksi, S., Tohtong, R. & Jitkaew, S. Key necroptotic proteins are required for Smac mimetic-mediated sensitization of

- cholangiocarcinoma cells to TNF- $\alpha$  and chemotherapeutic gemcitabine-induced necroptosis. *PLoS One* **15**, e0227454 (2020).
276. Soldevila, G. *et al.* Cytotoxic effect of IFN-gamma plus TNF-alpha on human islet cells. *J Autoimmun* **4**, 291–306 (1991).
277. Carswell, E. A. *et al.* An endotoxin-induced serum factor that causes necrosis of tumors. *Proc Natl Acad Sci U S A* **72**, 3666–3670 (1975).
278. Yang, B. *et al.* RIPK3-mediated inflammation is a conserved  $\beta$  cell response to ER stress. *Science Advances* **6**, eabd7272.
279. Annibaldi, A. *et al.* Ubiquitin-Mediated Regulation of RIPK1 Kinase Activity Independent of IKK and MK2. *Mol Cell* **69**, 566-580.e5 (2018).
280. Petersen, S. L., Peyton, M., Minna, J. D. & Wang, X. Overcoming cancer cell resistance to Smac mimetic induced apoptosis by modulating cIAP-2 expression. *Proceedings of the National Academy of Sciences* **107**, 11936–11941 (2010).
281. Cho, Y. S. *et al.* Phosphorylation-driven assembly of the RIP1-RIP3 complex regulates programmed necrosis and virus-induced inflammation. *Cell* **137**, 1112–1123 (2009).
282. Jörns, A. *et al.* Immune cell infiltration, cytokine expression, and beta-cell apoptosis during the development of type 1 diabetes in the spontaneously diabetic LEW.1AR1/Ztm-iddm rat. *Diabetes* **54**, 2041–2052 (2005).
283. O’Brien, B. A., Harmon, B. V., Cameron, D. P. & Allan, D. J. Apoptosis is the mode of beta-cell death responsible for the development of IDDM in the nonobese diabetic (NOD) mouse. *Diabetes* **46**, 750–757 (1997).

284. Babon, J. A. B. *et al.* Analysis of self-antigen specificity of islet-infiltrating T cells from human donors with type 1 diabetes. *Nat Med* **22**, 1482–1487 (2016).
285. Eizirik, D. L., Colli, M. L. & Ortis, F. The role of inflammation in insulinitis and beta-cell loss in type 1 diabetes. *Nat Rev Endocrinol* **5**, 219–226 (2009).
286. Mukherjee, N., Lin, L., Contreras, C. J. & Templin, A. T.  $\beta$ -Cell Death in Diabetes: Past Discoveries, Present Understanding, and Potential Future Advances. *Metabolites* **11**, 796 (2021).
287. Mandal, P. *et al.* RIP3 induces apoptosis independent of pro-necrotic kinase activity. *Mol Cell* **56**, 481–495 (2014).
288. Ishizuka, N. *et al.* Tumor necrosis factor alpha signaling pathway and apoptosis in pancreatic  $\beta$  cells. *Metabolism* **48**, 1485–1492 (1999).
289. Barthson, J. *et al.* Cytokines tumor necrosis factor- $\alpha$  and interferon- $\gamma$  induce pancreatic  $\beta$ -cell apoptosis through STAT1-mediated Bim protein activation. *J. Biol. Chem.* **286**, 39632–39643 (2011).
290. Polykratis, A. *et al.* RIPK1 kinase inactive mice are viable and protected from TNF-induced necroptosis in vivo. *J Immunol* **193**, 1539–1543 (2014).
291. Cheng, E. H. *et al.* A Bcl-2 homolog encoded by Kaposi sarcoma-associated virus, human herpesvirus 8, inhibits apoptosis but does not heterodimerize with Bax or Bak. *Proc Natl Acad Sci U S A* **94**, 690–694 (1997).
292. Thome, M. *et al.* Viral FLICE-inhibitory proteins (FLIPs) prevent apoptosis induced by death receptors. *Nature* **386**, 517–521 (1997).
293. Filippi, C. M. & von Herrath, M. G. Viral Trigger for Type 1 Diabetes. *Diabetes* **57**, 2863–2871 (2008).

294. Takita, M. *et al.* Unique Inflammatory Changes in Exocrine and Endocrine Pancreas in Enterovirus-Induced Fulminant Type 1 Diabetes. *J Clin Endocrinol Metab* **104**, 4282–4294 (2019).
295. Jiao, H. *et al.* Z-nucleic-acid sensing triggers ZBP1-dependent necroptosis and inflammation. *Nature* **580**, 391–395 (2020).
296. Yang, D. *et al.* ZBP1 mediates interferon-induced necroptosis. *Cell Mol Immunol* **17**, 356–368 (2020).
297. Thomas, H. E., Parker, J. L., Schreiber, R. D. & Kay, T. W. IFN-gamma action on pancreatic beta cells causes class I MHC upregulation but not diabetes. *J Clin Invest* **102**, 1249–1257 (1998).
298. Durinovic-Bello, I. Autoimmune Diabetes: The Role of T Cells, MHC Molecules and Autoantigens. *Autoimmunity* **27**, 159–177 (1998).
299. Eizirik, D. L., Pasquali, L. & Cnop, M. Pancreatic  $\beta$ -cells in type 1 and type 2 diabetes mellitus: different pathways to failure. *Nat Rev Endocrinol* **16**, 349–362 (2020).
300. Waibel, M. *et al.* Baricitinib and  $\beta$ -Cell Function in Patients with New-Onset Type 1 Diabetes. *New England Journal of Medicine* **389**, 2140–2150 (2023).
301. De George, D. J., Ge, T., Krishnamurthy, B., Kay, T. W. H. & Thomas, H. E. Inflammation versus regulation: how interferon-gamma contributes to type 1 diabetes pathogenesis. *Front. Cell Dev. Biol.* **11**, (2023).
302. Campbell, I. L., Wong, G. H. W., Schrader, J. W. & Harrison, L. C. Interferon- $\gamma$  Enhances the Expression of the Major Histocompatibility Class I Antigens on Mouse Pancreatic Beta Cells. *Diabetes* **34**, 1205–1209 (1985).

303. Kim, S. *et al.* Essential Role for Signal Transducer and Activator of Transcription-1 in Pancreatic  $\beta$ -Cell Death and Autoimmune Type 1 Diabetes of Nonobese Diabetic Mice. *Diabetes* **56**, 2561–2568 (2007).
304. Newton, K. Multitasking Kinase RIPK1 Regulates Cell Death and Inflammation. *Cold Spring Harb Perspect Biol* **12**, a036368 (2020).
305. Kim, W. H., Lee, J. W., Gao, B. & Jung, M. H. Synergistic activation of JNK/SAPK induced by TNF- $\alpha$  and IFN- $\gamma$ : Apoptosis of pancreatic  $\beta$ -cells via the p53 and ROS pathway. *Cellular Signalling* **17**, 1516–1532 (2005).
306. Åkerfeldt, M. C. *et al.* Cytokine-Induced  $\beta$ -Cell Death Is Independent of Endoplasmic Reticulum Stress Signaling. *Diabetes* **57**, 3034–3044 (2008).
307. Li, W. *et al.* Nuclear RIPK1 promotes chromatin remodeling to mediate inflammatory response. *Cell Res* **32**, 621–637 (2022).
308. Thapa, R. J. *et al.* NF- $\kappa$ B Protects Cells from Gamma Interferon-Induced RIP1-Dependent Necroptosis  $\nabla$ . *Mol Cell Biol* **31**, 2934–2946 (2011).
309. Kondylis, V., Kumari, S., Vlantis, K. & Pasparakis, M. The interplay of IKK, NF- $\kappa$ B and RIPK1 signaling in the regulation of cell death, tissue homeostasis and inflammation. *Immunological Reviews* **277**, 113–127 (2017).
310. Yatim, N. *et al.* RIPK1 and NF- $\kappa$ B signaling in dying cells determines cross-priming of CD8<sup>+</sup> T cells. *Science* **350**, 328–334 (2015).
311. Meng, H. *et al.* Death-domain dimerization-mediated activation of RIPK1 controls necroptosis and RIPK1-dependent apoptosis. *Proceedings of the National Academy of Sciences* **115**, E2001–E2009 (2018).

312. Zhang, X., Dowling, J. P. & Zhang, J. RIPK1 can mediate apoptosis in addition to necroptosis during embryonic development. *Cell Death Dis* **10**, 1–11 (2019).
313. Hänninen, A. *et al.* Macrophages, T cell receptor usage, and endothelial cell activation in the pancreas at the onset of insulin-dependent diabetes mellitus. *J Clin Invest* **90**, 1901–1910 (1992).
314. Itoh, N. *et al.* Mononuclear cell infiltration and its relation to the expression of major histocompatibility complex antigens and adhesion molecules in pancreas biopsy specimens from newly diagnosed insulin-dependent diabetes mellitus patients. *J Clin Invest* **92**, 2313–2322 (1993).
315. Somoza, N. *et al.* Pancreas in recent onset insulin-dependent diabetes mellitus. Changes in HLA, adhesion molecules and autoantigens, restricted T cell receptor V beta usage, and cytokine profile. *J Immunol* **153**, 1360–1377 (1994).
316. O'reilly, L. A. *et al.* Characterization of pancreatic islet cell infiltrates in NOD mice: effect of cell transfer and transgene expression. *European Journal of Immunology* **21**, 1171–1180 (1991).
317. Kay, T. W. H., Campbell, I. L., Oxbrow, L. & Harrison, L. C. Overexpression of class I major histocompatibility complex accompanies insulinitis in the non-obese diabetic mouse and is prevented by anti-interferon- $\gamma$  antibody. *Diabetologia* **34**, 779–785 (1991).
318. Ohashi, P. S. *et al.* Induction of diabetes is influenced by the infectious virus and local expression of MHC class I and tumor necrosis factor-alpha. *J Immunol* **150**, 5185–5194 (1993).

319. Thapa, R. J. *et al.* Interferon-induced RIP1/RIP3-mediated necrosis requires PKR and is licensed by FADD and caspases. *Proceedings of the National Academy of Sciences* **110**, E3109–E3118 (2013).
320. Meng, H. *et al.* Death-domain dimerization-mediated activation of RIPK1 controls necroptosis and RIPK1-dependent apoptosis. *Proceedings of the National Academy of Sciences* **115**, E2001–E2009 (2018).
321. Zhang, X., Dowling, J. P. & Zhang, J. RIPK1 can mediate apoptosis in addition to necroptosis during embryonic development. *Cell Death Dis* **10**, 1–11 (2019).
322. Thapa, R. J. *et al.* NF-kappaB protects cells from gamma interferon-induced RIP1-dependent necroptosis. *Mol Cell Biol* **31**, 2934–2946 (2011).
323. Sano, R. & Reed, J. C. ER stress-induced cell death mechanisms. *Biochimica et Biophysica Acta (BBA) - Molecular Cell Research* **1833**, 3460–3470 (2013).
324. Shamas-Din, A., Kale, J., Leber, B. & Andrews, D. W. Mechanisms of Action of Bcl-2 Family Proteins. *Cold Spring Harb Perspect Biol* **5**, a008714 (2013).
325. Hagenlocher, C. *et al.* ER stress-induced cell death proceeds independently of the TRAIL-R2 signaling axis in pancreatic  $\beta$  cells. *Cell Death Discov* **8**, 34 (2022).
326. Saveljeva, S., Mc Laughlin, S. L., Vandenabeele, P., Samali, A. & Bertrand, M. J. M. Endoplasmic reticulum stress induces ligand-independent TNFR1-mediated necroptosis in L929 cells. *Cell Death Dis* **6**, e1587 (2015).
327. Ma, Y.-M. *et al.* Novel CHOP activator LGH00168 induces necroptosis in A549 human lung cancer cells via ROS-mediated ER stress and NF- $\kappa$ B inhibition. *Acta Pharmacol Sin* **37**, 1381–1390 (2016).

328. McGrath, E. P., Centonze, F. G., Chevet, E., Avril, T. & Lafont, E. Death sentence: The tale of a fallen endoplasmic reticulum. *Biochimica et Biophysica Acta (BBA) - Molecular Cell Research* **1868**, 119001 (2021).
329. Mannion, J. *et al.* A RIPK1-specific PROTAC degrader achieves potent antitumor activity by enhancing immunogenic cell death. *Immunity* **57**, 1514-1532.e15 (2024).
330. Mukherjee, N. *et al.* RIPK3 promotes islet amyloid-induced  $\beta$ -cell loss and glucose intolerance in a humanized mouse model of type 2 diabetes. *Mol Metab* **80**, 101877 (2024).
331. Kahn, S. E. The importance of beta-cell failure in the development and progression of type 2 diabetes. *J Clin Endocrinol Metab* **86**, 4047–4058 (2001).
332. Cho, N. H. *et al.* IDF Diabetes Atlas: Global estimates of diabetes prevalence for 2017 and projections for 2045. *Diabetes Research and Clinical Practice* **138**, 271–281 (2018).
333. Westermark, P., Engström, U., Johnson, K. H., Westermark, G. T. & Betsholtz, C. Islet amyloid polypeptide: pinpointing amino acid residues linked to amyloid fibril formation. *Proc. Natl. Acad. Sci. U.S.A.* **87**, 5036–5040 (1990).
334. Verchere, C. B. *et al.* Islet amyloid formation associated with hyperglycemia in transgenic mice with pancreatic beta cell expression of human islet amyloid polypeptide. *Proc. Natl. Acad. Sci. U.S.A.* **93**, 3492–3496 (1996).
335. Janson, J. *et al.* Spontaneous diabetes mellitus in transgenic mice expressing human islet amyloid polypeptide. *Proc. Natl. Acad. Sci. U.S.A.* **93**, 7283–7288 (1996).

336. Birol, M., Kumar, S., Rhoades, E. & Miranker, A. D. Conformational switching within dynamic oligomers underpins toxic gain-of-function by diabetes-associated amyloid. *Nat Commun* **9**, 1312 (2018).
337. Janson, J., Ashley, R. H., Harrison, D., McIntyre, S. & Butler, P. C. The mechanism of islet amyloid polypeptide toxicity is membrane disruption by intermediate-sized toxic amyloid particles. *Diabetes* **48**, 491–498 (1999).
338. Abedini, A., Derk, J. & Schmidt, A. M. The receptor for advanced glycation endproducts is a mediator of toxicity by IAPP and other proteotoxic aggregates: Establishing and exploiting common ground for novel amyloidosis therapies. *Protein Sci* **27**, 1166–1180 (2018).
339. Westwell-Roper, C. Y. *et al.* IL-1 mediates amyloid-associated islet dysfunction and inflammation in human islet amyloid polypeptide transgenic mice. *Diabetologia* **58**, 575–585 (2015).
340. Zou, C. *et al.* Reduction of mNAT1/hNAT2 Contributes to Cerebral Endothelial Necroptosis and A $\beta$  Accumulation in Alzheimer's Disease. *Cell Reports* **33**, 108447 (2020).
341. Kumar, S. *et al.* Role of the Caspase-8/RIPK3 axis in Alzheimer's disease pathogenesis and A $\beta$ -induced NLRP3 inflammasome activation. *JCI Insight* (2023) doi:10.1172/jci.insight.157433.
342. Preston, S. P. *et al.* Epigenetic Silencing of RIPK3 in Hepatocytes Prevents MLKL-mediated Necroptosis From Contributing to Liver Pathologies. *Gastroenterology* **163**, 1643-1657.e14 (2022).

343. Moriwaki, K., Bertin, J., Gough, P. J. & Chan, F. K.-M. A RIPK3-Caspase 8 complex mediates atypical pro-IL-1 $\beta$  processing. *J Immunol* **194**, 1938–1944 (2015).
344. Moriwaki, K. & Chan, F. K.-M. Necroptosis-independent signaling by the RIP kinases in inflammation. *Cell. Mol. Life Sci.* **73**, 2325–2334 (2016).
345. Orozco, S. L. *et al.* RIPK3 Activation Leads to Cytokine Synthesis that Continues after Loss of Cell Membrane Integrity. *Cell Rep* **28**, 2275-2287.e5 (2019).
346. Dondelinger, Y. *et al.* RIPK3 contributes to TNFR1-mediated RIPK1 kinase-dependent apoptosis in conditions of cIAP1/2 depletion or TAK1 kinase inhibition. *Cell Death Differ* **20**, 1381–1392 (2013).
347. Rodriguez, D. A. *et al.* Characterization of RIPK3-mediated phosphorylation of the activation loop of MLKL during necroptosis. *Cell Death Differ* **23**, 76–88 (2016).
348. Zraika, S. *et al.* Glucose- and time-dependence of islet amyloid formation in vitro. *Biochem. Biophys. Res. Commun.* **354**, 234–239 (2007).
349. Templin, A. T. *et al.* Loss of perlecan heparan sulfate glycosaminoglycans lowers body weight and decreases islet amyloid deposition in human islet amyloid polypeptide transgenic mice. *Protein Eng Des Sel* **32**, 95–102 (2019).
350. Templin, A. T. *et al.* Use of the PET ligand florbetapir for in vivo imaging of pancreatic islet amyloid deposits in hIAPP transgenic mice. *Diabetologia* **61**, 2215–2224 (2018).
351. Bussi re, T. *et al.* Morphological Characterization of Thioflavin-S-Positive Amyloid Plaques in Transgenic Alzheimer Mice and Effect of Passive A $\beta$  Immunotherapy on Their Clearance. *Am J Pathol* **165**, 987–995 (2004).

352. Grootjans, S. *et al.* A real-time fluorometric method for the simultaneous detection of cell death type and rate. *Nat Protoc* **11**, 1444–1454 (2016).
353. Park, Y. J. *et al.* The role of caspase-8 in amyloid-induced beta cell death in human and mouse islets. *Diabetologia* **57**, 765–775 (2014).
354. Kaiser, W. J. *et al.* RIP3 mediates the embryonic lethality of caspase-8-deficient mice. *Nature* **471**, 368–372 (2011).
355. Abdelhady, R. *et al.* Cognitive enhancing effects of pazopanib in D-galactose/ovariectomized Alzheimer’s rat model: insights into the role of RIPK1/RIPK3/MLKL necroptosis signaling pathway. *Inflammopharmacol* **31**, 2719–2729 (2023).
356. Wong, W. W.-L. *et al.* cIAPs and XIAP regulate myelopoiesis through cytokine production in an RIPK1- and RIPK3-dependent manner. *Blood* **123**, 2562–2572 (2014).
357. Moriwaki, K. *et al.* The Necroptosis Adaptor RIPK3 Promotes Injury-Induced Cytokine Expression and Tissue Repair. *Immunity* **41**, 567–578 (2014).
358. Masters, S. L. *et al.* Activation of the NLRP3 inflammasome by islet amyloid polypeptide provides a mechanism for enhanced IL-1 $\beta$  in type 2 diabetes. *Nat. Immunol.* **11**, 897–904 (2010).
359. Butcher, M. J. *et al.* Association of proinflammatory cytokines and islet resident leucocytes with islet dysfunction in type 2 diabetes. *Diabetologia* **57**, 491–501 (2014).

360. Wu, L. *et al.* RIPK3 Orchestrates Fatty Acid Metabolism in Tumor-Associated Macrophages and Hepatocarcinogenesis. *Cancer Immunology Research* **8**, 710–721 (2020).
361. Roychowdhury, S. *et al.* Receptor interacting protein 3 protects mice from high-fat diet-induced liver injury. *Hepatology* **64**, 1518–1533 (2016).
362. Newton, K., Sun, X. & Dixit, V. M. Kinase RIP3 is dispensable for normal NF- $\kappa$ Bs, signaling by the B-cell and T-cell receptors, tumor necrosis factor receptor 1, and Toll-like receptors 2 and 4. *Mol Cell Biol* **24**, 1464–1469 (2004).
363. Andrikopoulos, S. *et al.* Differential effect of inbred mouse strain (C57BL/6, DBA/2, 129T2) on insulin secretory function in response to a high fat diet. *J Endocrinol* **187**, 45–53 (2005).
364. Zhang, D.-W. *et al.* RIP3, an Energy Metabolism Regulator That Switches TNF-Induced Cell Death from Apoptosis to Necrosis. *Science* **325**, 332–336 (2009).
365. Cabrera, O. *et al.* The unique cytoarchitecture of human pancreatic islets has implications for islet cell function. *Proceedings of the National Academy of Sciences* **103**, 2334–2339 (2006).
366. Liu, S., Joshi, K., Denning, M. F. & Zhang, J. RIPK3 signaling and its role in the pathogenesis of cancers. *Cell. Mol. Life Sci.* **78**, 7199–7217 (2021).
367. Conev, N. V. *et al.* RIPK3 expression as a potential predictive and prognostic marker in metastatic colon cancer. *Clinical and Investigative Medicine* **42**, E31–E38 (2019).
368. Martin-Sanchez, D. *et al.* Bone Marrow-Derived RIPK3 Mediates Kidney Inflammation in Acute Kidney Injury. *J Am Soc Nephrol* **33**, 357–373 (2022).

369. Sureshababu, A. *et al.* RIPK3 promotes sepsis-induced acute kidney injury via mitochondrial dysfunction. *JCI Insight* **3**, e98411.
370. Oñate, M. *et al.* The necroptosis machinery mediates axonal degeneration in a model of Parkinson disease. *Cell Death Differ* **27**, 1169–1185 (2020).
371. Wirth, F. *et al.* A human antibody against pathologic IAPP aggregates protects beta cells in type 2 diabetes models. *Nat Commun* **14**, 6294 (2023).

## **Curriculum Vitae**

**Noyonika Mukherjee**

### **Education**

PhD August 2019- November 2024

Indiana University, Indianapolis, IN, USA

Department of Biochemistry and Molecular Biology

M.Sc. August 2017- June 2019

St. Xavier's College (University of Calcutta), Kolkata, WB, India

Department of Microbiology

B.Sc. June 2014- July 2017

Asutosh College (University of Calcutta), Kolkata, WB, India

Department of Microbiology

### **Research Experience**

Indiana University

PhD

Department of Biochemistry and Molecular Biology

Indiana University School of Medicine

- Investigated the role of receptor interacting protein kinases in diabetes pathogenesis. Designed and conducted experiments using various  $\beta$ -cell lines, mouse islets, human islets and human iPSCs, including cell culture, caspase

activity assays, immunohistochemistry, immunoblot analysis, and gene expression analysis (RT-qPCR) *in vitro*. Additionally, performed metabolic phenotyping of mice for *in vivo* analysis. Innovatively developed techniques to visualize real-time cell death and islet amyloid formation in mouse and human islets *in vitro*.

- Analyze data and prepare texts, figures, and presentations.
- Performed experiments, wrote, edited, and published research and review manuscripts.
- Prepared and submitted a successfully funded predoctoral fellowship.
- Mentored multiple summer interns and research associates.

#### St. Xavier's College

##### Graduate student

- Conceived and executed an experiment pioneering the formation of *Tilicora racemosa* explants by infecting leaves of this medicinally potent plant with *Agrobacterium* sp

#### Bose Institute

##### Summer intern

- Conducted experiments to observe minimal inhibitory concentration (MIC) of natural antimycobacterial product, plumbagin, in comparison to a standard anti-tubercular antibiotic, rifampicin.
- Prepared figures and co-authored on a published research manuscript.

St. Xavier's College

Graduate student

- Analyzed air quality index (AQI) and determined how air quality can affect interaction of microbes and suspended particulate matter (SPM).
- Conducted experiments, wrote a research article and prepared figures for the same.

University of Calcutta

Summer intern

- Isolated genomic DNA from whole blood samples collected from human subjects.
- Conducted PCR and restriction fragment length polymorphism (RFLP) on genomic DNA to detect single nucleotide polymorphisms (SNPs) suitable as markers for an individual's susceptibility to lung cancer.
- Also involved in in silico analysis of single nucleotide variants of the human orthologues of 171 different murine loci, with the aim to seek novel insights into the genetics of human pigmentation.

## **Publications**

### Published manuscripts

1. Colglazier KA, Mukherjee N, Contreras CJ, Templin AT. "Evidence for novel mechanisms of programmed cell death in diabetogenic  $\beta$ -cell loss." Journal of Endocrinology. 2024 Jul. doi: 10.1530/JOE-23-0378.

2. Mukherjee N, Contreras CJ, Lin L, Colglazier KA, Mather EG, Kalwat MA, Esser N, Kahn SE, Templin AT. RIPK3 promotes islet amyloid-induced  $\beta$ -cell loss and glucose intolerance in a humanized mouse model of type 2 diabetes. *Mol Metab.* 2024 Jan. doi: 10.1016/j.molmet.2024.101877.
3. Contreras CJ, Mukherjee N, Branco RCS, Lin L, Hogan MF, Cai EP, Oberst AA, Kahn SE, Templin AT. RIPK1 and RIPK3 regulate TNF $\alpha$ -induced  $\beta$ -cell death in concert with caspase activity. *Mol Metab.* 2022 Aug. doi: 10.1016/j.molmet.2022.101582.
4. Mukherjee N, Lin L, Contreras CJ, Templin AT.  $\beta$ -Cell Death in Diabetes: Past Discoveries, Present Understanding, and Potential Future Advances. *Metabolites.* 2021 Nov. doi:10.3390/metabo11110796.
5. Sengupta D, Mukhopadhyay P, Banerjee S, Ganguly K, Mascharak P, Mukherjee N, Mitra S, Bhattacharjee S, Mitra R, Sarkar A, Chaudhuri T, Bhattacharjee G, Nath S, Roychoudhury S, Sengupta M. Identifying polymorphic cis-regulatory variants as risk markers for lung carcinogenesis and chemotherapy responses in tobacco smokers from eastern India. *Sci Rep.* 2023 Mar. doi: 10.1038/s41598-023-30962-9.
6. Ganguly, K., Sengupta, D., Sarkar, N., Mukherjee N., Dutta, T., Saha A., Saha T., Ghosh B., Chatterjee S., Brahmachari P., Kundu A., Sengupta M. Comprehensive in Silico Analyses of Single Nucleotide Variants of the Human Orthologues of 171 Murine

Loci to Seek Novel Insights into the Genetics of Human Pigmentation. Proc Zool Soc.  
2022 Aug. doi: 10.1007/s12595-022-00449-y.

7. Sarkar A, Ghosh S, Shaw R, Patra MM, Calcuttawala F, Mukherjee N, Das Gupta SK.  
Mycobacterium tuberculosis thymidylate synthase (ThyX) is a target for plumbagin, a  
natural product with antimycobacterial activity. PLoS One. 2020 Feb. doi:  
10.1371/journal.pone.0228657.

#### Published abstract

1. Mukherjee N, Contreras CJ, Lin L, Cai EP, Kahn SE, Templin AT; 1724-P: Caspase  
3/7 Activation and RIPK3 Are Dispensable for Synthetic hIAPP-Induced  $\beta$ -Cell Death.  
Diabetes 20 June 2023; 72 (Supplement\_1): 1724–P.

2. Mukherjee N, Contreras CJ, Lin L, Cai EP, Templin AT; 1722-P: RIPK1 Promotes  
Thapsigargin-Induced  $\beta$ -Cell Death Independent of Caspase 3/7 Activity In Vitro.  
Diabetes 20 June 2023; 72 (Supplement\_1): 1722–P.

3. Rodrigues dos Santos K, Mukherjee N, Barella LF, Armoo F, Eizirik DL, Templin AT,  
Kalwat MA, SAT069 Targeting Human  $\beta$ -Cell G Protein-coupled Receptors to Alter  
Cytokine-mediated Caspase Activation, Journal of the Endocrine Society, Volume 7,  
(Supplement\_1), October-November 2023.

## **Fellowships and awards**

Rita Levi-Montalcini Fellowship

Postdoctoral fellowship provided by the Center of Regenerative Medicine at Washington University School of Medicine in St. Louis

Erica Daniel Kepner Award

For scientific achievement based upon a graduate student's contributions to a single research manuscript

Jack Davis Award

For best seminar by a graduate student in the Biochemistry and Molecular Biology Department in Fall 2022 academic semester, IU School of Medicine

Oral Presentation Certificate

9<sup>th</sup> Annual Diabetes Symposium, IU School of Medicine

DeVault Fellowship

Predocctoral fellowship provided from T32 DK064466 to Indiana University Diabetes and Obesity Research Training Program

## **Participation in conferences**

Oral Presentations:

*“RIPK1 mediates ER stress-induced  $\beta$ -cell death independent of caspase 3/7 activity in vitro”* Oral presentation at 9<sup>th</sup> Annual Center for Diabetes and Metabolic Diseases (CDMD) Indiana University, Indianapolis, IN, 2023.

*“RIPK3 promotes islet amyloid-induced  $\beta$ -cell death and hyperglycemia.”* Oral presentation at Metabolism and Islet Biology Virtual Seminar, Center for Diabetes and Metabolic Diseases, Indiana University, Indianapolis, IN, 2023.

*“RIPK1 and MLKL promote endoplasmic reticulum stress-induced b-cell death in vitro.”* Oral presentation at Biochemistry Research Day, Department of Biochemistry and Molecular Biology, Indiana University, Indianapolis, IN, 2022.

*“MLKL promotes endoplasmic reticulum stress-induced b-cell death in vitro.”* Oral presentation at 8<sup>th</sup> Annual Diabetes Symposium, Center for Diabetes and Metabolic Diseases (CDMD), Indiana University, Indianapolis, IN, 2022.

*“The role of RIPK3 in amyloid-induced islet inflammation and  $\beta$ -cell death.”* Oral presentation at Metabolism and Islet Biology Virtual Seminar, Center for Diabetes and Metabolic Diseases, Indiana University, Indianapolis, IN, 2022.

*“A Novel Organic Supplementation for Better Crop Productivity.”* 6<sup>th</sup> International Conference of Ecotoxicology and Environmental Sciences, Netaji Subhas Institute of Technology, Sector-3, Dwarka, New Delhi, India, 2018.

*“Genome Editing Reduces Serum Cholesterol in Large Animal Model”* Modern Trends in Microbiology, Chapter 15 St. Xavier’s College (Autonomous), University of Calcutta, Kolkata, WB, India, 2018.

Poster Presentations:

*“Caspase 3/7 Activation and RIPK3 Are Dispensable for Synthetic hIAPP-Induced  $\beta$ -Cell Death”* Poster Presentation at 83<sup>rd</sup> Scientific Session, American Diabetes Association, CA, USA, 2023.

*“ER stress-induced beta-cell death is regulated by RIPK1 independent of caspase 3/7 activity in vitro”* Poster Presentation Islet Study Group Meeting, BC, Canada, 2023.

*“RIPK3 promotes islet amyloid-induced  $\beta$ -cell death in vitro”* Poster Presentation Midwest Islet Club (MIC) Annual Meeting, MN, USA, 2023.

*“RIPK3 promotes islet amyloid-induced  $\beta$ -cell death”* Poster Presentation at Midwest Islet Club (MIC) Annual Virtual Meeting, 2022.

*“Evaluation of Antimicrobial Activity of Alkaloids of Tiliacora racemosa”* National Seminar on Sustainable Utilization of Plants and Microbes, Visva-Bharati University, Shantiniketan, West Bengal, India, 2019.